

Review of synthetic aperture radar with deep learning in agricultural applications

Mahya G.Z. Hashemi^a, Ehsan Jalilvand^{b,c}, Hamed Alemohammad^d, Pang-Ning Tan^e, Narendra N. Das^{a,f,*}

^a Department of Civil and Environmental Engineering, Michigan State University, Michigan, MI 48824, USA

^b Hydrological Science Laboratory, NASA Goddard Space Flight Center, Greenbelt, MD 20771, USA

^c Science Applications International Corporation, Reston, VA 22102, USA

^d Center for Geospatial Analytics, Clark University, Worcester, MA 01610, USA

^e Department of Computer Science & Engineering, Michigan State University, Michigan, MI 48824, USA

^f Department of Biosystems and Agricultural Engineering, Michigan State University, Michigan, MI 48824, USA



ARTICLE INFO

Keywords:

SAR
Deep learning
Crop classification
Phenology
Yield prediction
Agricultural management practice

ABSTRACT

Synthetic Aperture Radar (SAR) observations, valued for their consistent acquisition schedule and not being affected by cloud cover and variations between day and night, have become extensively utilized in a range of agricultural applications. The advent of deep learning allows for the capture of salient features from SAR observations. This is accomplished through discerning both spatial and temporal relationships within SAR data. This study reviews the current state of the art in the use of SAR with deep learning for crop classification/mapping, monitoring and yield estimation applications and the potential of leveraging both for the detection of agricultural management practices.

This review introduces the principles of SAR and its applications in agriculture, highlighting current limitations and challenges. It explores deep learning techniques as a solution to mitigate these issues and enhance the capability of SAR for agricultural applications. The review covers various aspects of SAR observables, methodologies for the fusion of optical and SAR data, common and emerging deep learning architectures, data augmentation techniques, validation and testing methods, and open-source reference datasets, all aimed at enhancing the precision and utility of SAR with deep learning for agricultural applications.

1. Introduction

Satellite-based remote sensing (RS) through optical/thermal sensors and synthetic aperture radar (SAR) (e.g., Sentinel-1A/B (Torres et al., 2012), Sentinel-2A/B (Drusch et al., 2012), and Landsat-8 (Roy et al., 2014)) has revolutionized our ability to collect vast amounts of open-access images at various temporal, spectral, and spatial resolutions. This has led to the creation of Big Data on a wide range of geophysical and biophysical features across the Earth's surface (Adrian et al., 2021; Kussul et al., 2017). However, analyzing extensive time-series RS data and extracting features by understanding sequential relationships for classification applications has consistently presented challenges to scientists (Zhong et al., 2019). The emergence of machine learning (ML) techniques has significantly enhanced scientists' capabilities in refining crop type mapping processes. Nevertheless, these methods often heavily rely on comprehensive feature engineering and the use of external

indices (Zheng and Casari, 2018), and struggle to capture the dynamic temporal behaviors of crop classes, which fluctuate according to seasonal cycles (Wang et al., 2021).

The advent of cloud computing has significantly empowered the RS community to explore new avenues for creating classification maps, particularly by harnessing the sophisticated capabilities of Deep Learning (DL) algorithms (Brown et al., 2022; Ma et al., 2019). Unlike traditional ML methods, DL networks offer an advanced methodology through multiple interconnected layers that facilitate automatic feature extraction and representation learning (Kamilaris and Prenafeta-Boldú, 2018). They also excel at identifying both spatial and temporal relationships within RS data, from the level of individual pixels to broader parcel scales, greatly improving the accuracy of models that depict the complex dynamics of crop phenology (Han et al., 2023).

While DL techniques have been successfully applied with multispectral sensors for various agricultural tasks, such as crop classification

* Corresponding author.

(Dong et al., 2016; Drusch et al., 2012), monitoring (Katal et al., 2022), and yield prediction (Qiao et al., 2021; Wang et al., 2023), the integration of SAR imagery has opened up new possibilities for enhancing these applications by offering a consistent acquisition schedule and remains unaffected by cloud cover and the day-night cycle (Steele-Dunne et al., 2017). SAR data overcome the limitations of multi-spectral sensors, such as susceptibility to cloud cover, background interference, aerosol effects, and saturation in regions of high biomass (Soudani et al., 2008). Furthermore, SAR observations are sensitive to water under the canopy, such as in the stem and ears, which is not detectable by multi-spectral sensors (Judge et al., 2021; Tigliatti et al., 2022).

Despite the significant potential of SAR data for agricultural applications, its usage comes with a multiple of challenges such as speckle effect, the complexity of information due to both amplitude and phase, geometric distortions inherent in the side-looking nature of SAR, and temporal decorrelation (Oveis et al., 2022). SAR data can be complex, noisy, and difficult to interpret, especially in agricultural applications where a wide range of factors can influence the signals received (Alemohammad et al., 2018). In this review paper, we discuss how DL can be instrumental in addressing these challenges and in extracting valuable information from a large stack of SAR images (Ma et al., 2014). To the best of our knowledge, this is the first review that explores the intersection of common and emerging DL techniques, SAR observations, and their classification, and monitoring applications in agriculture. While Desai and Gaikwad. (2021) primarily addressed crop and land cover classification using SAR without venturing into advanced DL architectures like Transformers, Autoencoders, Transfer Learning, and Foundation Models, our review broadens the narrative to include a vast range of DL methodologies across various agricultural applications. Unlike Kamaris and Prenafeta-Boldú, (2018), who limited their focus to Convolutional Neural Networks (CNNs) excluding SAR imagery, and Saleem et al. (2021), whose work on crop disease detection and land cover classification overlooked the potential of SAR, our review comprehensively explores the synergy between SAR and DL. We delve into end- and in-season crop classification, phenology, and biophysical parameters (BPs) estimation, yield prediction, and the agricultural management practices detection through the lens of SAR-enhanced DL approaches. A perspective only partially explored by Parikh et al. (2020) in classification applications, and largely neglected in the agricultural context by Zhu et al. (2021) and Sivasankar et al. (2018). Therefore, unlike other reviews that touch on multi-sensor approaches but offer limited discussion on SAR-specific studies (Kattenborn et al., 2021; Victor et al., 2022; Wang et al., 2022a) and those that focus on hyperspectral imaging in agriculture with DL (Khan et al., 2022; Vali et al., 2020) our work delves deeply into the integration of SAR with DL which recommends guidelines to readers for DL modeling tailored to each above-mentioned application. Moreover, by focusing on the synergy between SAR and DL, we illuminate the significant, yet underexplored, potential of their combination to advance agricultural management practices such as planting and harvest date estimation, grass mowing monitoring, crop residue and tillage detection, presenting a novel perspective not thoroughly examined in existing reviews. We also review the integration of SAR and optical data by focusing on their combined efficacy in agricultural applications that is less explored by other review papers such as Zhu et al. (2021). Our review stands out by offering an in-depth overview of available SAR datasets, open-access reference data for crop types, and labeled data crucial for effective crop monitoring—areas often overlooked in previous literature.

This literature review covers studies from 2015 through the beginning of 2024. We conducted a keyword-driven search to identify relevant conference papers and journal articles using six electronic search engines: IEEE Xplore, ScienceDirect, Web of Science, Google Scholar, ResearchGate, and arXiv. The search results were then screened using a set of exclusion criteria, ultimately leading to the selection of 82 studies for inclusion in this review. Finally, we used a questionnaire to systematically extract and code relevant information, including the

geographic location of the study area, area of application, SAR platform, DL classifier, augmentation method, training, validation and test ratio, reference datasets, evaluation of the DL methods and comparison with ML methods (all data are presented in Table A1 in the supplementary material).

The structure of this review is organized into six main sections. Section 1 is the introduction. Section 2, probes into the prevalent SAR techniques and data sources used in the literature. In Section 3, we discuss the data processing techniques, common and emerging DL algorithms utilized with SAR imagery for agricultural applications, and their implementation considerations. Section 4 identifies the challenges of using SAR and DL in agriculture and explores how the synergy between DL and SAR can help mitigate those obstacles. Section 5 highlights the current gaps in our knowledge and outlines possible directions for future research, and Section 6 summarizes the key insights and findings from the review.

2. SAR in agricultural applications

2.1. Techniques

SAR technology has proven to be a valuable tool for monitoring and assessing agricultural landscapes. This section will delve into the key techniques employed in SAR systems for agricultural applications, namely backscatter, polarimetry, and interferometry. By examining the principles and applications of each technique, we aim to provide a comprehensive understanding of how SAR data are utilized to extract crucial information for crop classification, health, growth (i.e., tracking phenology), and management practices.

2.1.1. Backscatter

Backscatter in SAR refers to the portion of the transmitted radar signal that is reflected back to the sensor by the target surface, providing information about the target's physical properties and structure. Three properties of the SAR imagery make them ideal for agricultural applications: (i) The SAR backscatter's sensitivity to the dielectric properties, size, shape, orientation, roughness, and distribution of canopy (i.e., leaves, stems, and fruits, etc.) (McDonald et al., 2000), (ii) the ability of exact repeat with multi-temporal SAR observations to capture crop growth stages and crop structure variation enabling improved distinction among individual crops (Deschamps et al., 2012; McNairn et al., 2009), and (iii) the high spatial resolution (<=50 m) of backscatter data that is instrumental in tracking crop growth/phenology and health status at a field scale.

The SAR backscatter signal from vegetated surfaces primarily comprises three major first-order components: (i) surface scattering from the soil; (ii) multiple (volume) scattering from the canopy; and (iii) double-bounce scattering from the interaction between the canopy and the soil surface (Lopez-Sanchez and Ballester-Berman, 2009; Ulaby et al., 1996). Several factors influence the interaction between the active microwave signal and canopy structure, including SAR instrument characteristics, microwave frequency, and incidence and azimuth angles (Balenzano et al., 2010). Thus, SAR observations enable the characterization of unique structural attributes and dielectric properties of crop canopies, providing valuable insights for phenology tracking and crop discrimination (McNairn et al., 2009).

When considering the SAR configuration for agricultural applications, the choice of frequency is crucial. This decision is not straightforward and must take into account the canopy characteristics, such as crop type and development stage.

Recent studies have shown that SAR backscatter data at X-band (~9.65 GHz), C-band (~5.6 GHz), and L-band (~1.4 GHz) have the potential for crop classification (Fontanelli et al., 2022; Phan et al., 2018; Skakun et al., 2015; Huang et al., 2021; Whelen and Siqueira, 2017), crop monitoring (Canisius et al., 2018; Mascolo et al., 2015), crop biophysical estimation (Inoue et al., 2014; Kim et al., 2018; Ryu and Lee,

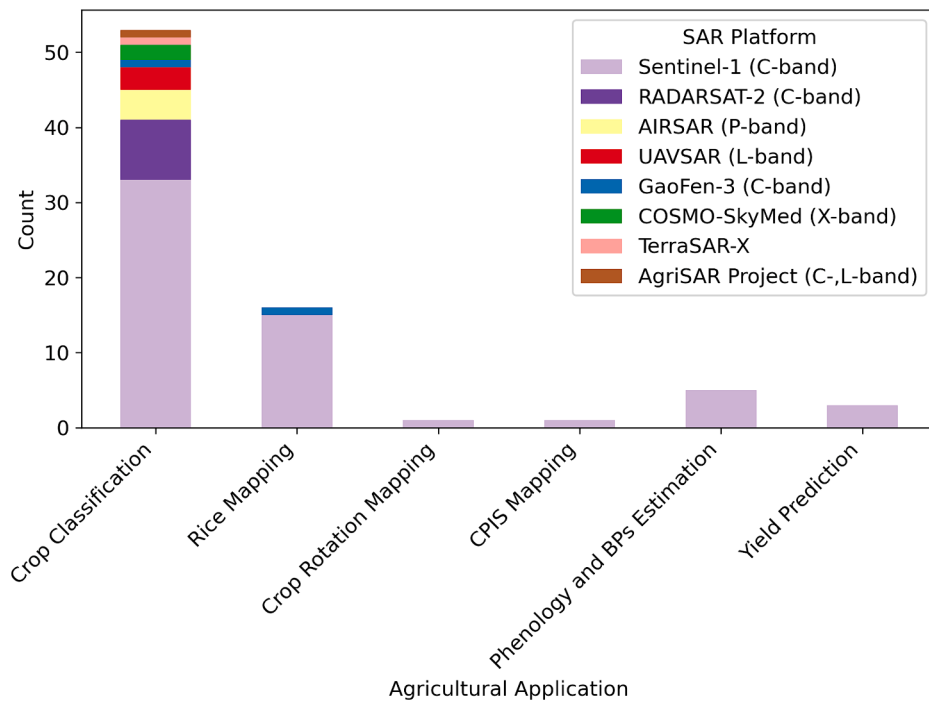


Fig. 1. The stacked bar chart illustrates the distribution of SAR platforms used in conjunction with DL for various agricultural applications. Each bar represents the count for a specific application, and the height of the bar indicates the cumulative count across multiple SAR platforms. On the x-axis, 'CPIS' refers to the Center Pivot Irrigation Systems.

2023) and land use land cover classification (Busquier et al., 2022). Lower-frequency bands, such as the C- and L-band, are capable of penetrating deeper into the canopy, providing insights into the plant structure. Conversely, the higher-frequency X-band, due to its limited penetration ability, is more effective in correlating with surface-level canopy details, such as the weight of rice heads, highlighting its utility for precise measurements. However, while the X-band has shown potential for early growth monitoring and grain yield estimation, it faces challenges in accurately correlating with volumetric properties of the canopy that influence LAI and biomass (Inoue et al., 2002). Building on this understanding, Busquier et al. (2022) further established the comparative advantages of frequency bands for agricultural applications. Specifically, they found that for crop classification tasks, C-band data typically outperform X-band data. This superior performance is attributed to the C-band's optimal sensitivity towards both vegetation and soil moisture (SM) levels, crucial factors that significantly enhance the effectiveness of differentiating various crop types. However, C-band SAR signals, with their shorter wavelengths compared to L-band, interact more with smaller vegetation elements like leaves and small stems, making them suitable for discriminating herbaceous crops such as wheat, alfalfa, and canola, even at moderate growth stages. In contrast, L-band SAR signals, having longer wavelengths, are less affected by the upper canopy layers and interact more with intermediate-sized crop elements like stems and leaf ribs of wide-leaf crops such as corn and sunflower. This L-band characteristics allows for better sensitivity to biomass in crops with low plant density. However, for crops with high plant density, both L-band and C-band provide useful information for biomass estimation, with C-band saturating earlier than L-band due to the significant contribution of leaves to backscatter at C-band. In fact, for broad-leaf crops, the leaf contribution to backscatter at C-band is significant and comparable to that of stems. Conversely, the leaf contribution is minimal at L-band for most crop types, as the longer wavelengths interact more with the larger plant structures (Ferrazzoli et al., 1997). The above-mentioned characteristics make L-band particularly well-suited for assessing vegetation properties such as biomass, structure, density, height, and vegetation water content (VWC), as well

as SM beneath the canopy (Dobson et al., 1985).

Although some studies not using DL techniques have shown that integrating different SAR frequencies can enhance crop classification accuracy significantly—reporting improvements up to 37 % for early-season and 5 % for end-season classifications (McNairn et al., 2014)—most SAR with DL studies (75 out of 82) focusing on crop classification, monitoring, and yield estimation predominantly utilized a single frequency. In cases where frequency integration was used, the comparison results between multi-frequency and single frequency were not reported. Additionally, Busquier et al. (2022) suggested that having a longer time-series of images, even from a single frequency band, can be as beneficial as combining data from multiple frequency bands with fewer images per band.

Fig. 1 illustrates the usage of various SAR platforms and frequency bands along with DL across different agricultural applications. The C-band emerges as the most frequently utilized band, represented in 70 out of 82 studies (85 %), followed by the L and P bands (4 studies each) and the X band (3 studies). The figure indicates a predominant use of the C-band frequency for classification/mapping tasks within agricultural contexts. Despite the L-band's potential advantages for crop monitoring and yield estimation, its application in these areas remains limited, with the C-band, especially images from Sentinel-1, being the favored option. This preference is largely attributed to the cost-free access to C-band Sentinel-1 imagery, making it a more feasible and attractive option for agricultural purposes.

In addition to frequency, the SAR signal's interaction with the crop canopy is influenced by the polarization of the signals transmitted and received by the SAR system. Polarization refers to the orientation of the electric field in the electromagnetic wave. Single-polarization SAR systems measure only one polarization (e.g., HH or VV), while dual-polarization SAR systems measure two polarization combinations (e.g., HH and HV, or VV and VH). A signal with co-polarization, such as Vertical-Vertical (VV), exhibits heightened sensitivity to the vertical alignment of leaves (Le Toan et al., 1997). Conversely, a cross-polarization channel like Vertical-Horizontal (VH) demonstrates a stronger association with the Leaf Area Index (LAI) due to the volume

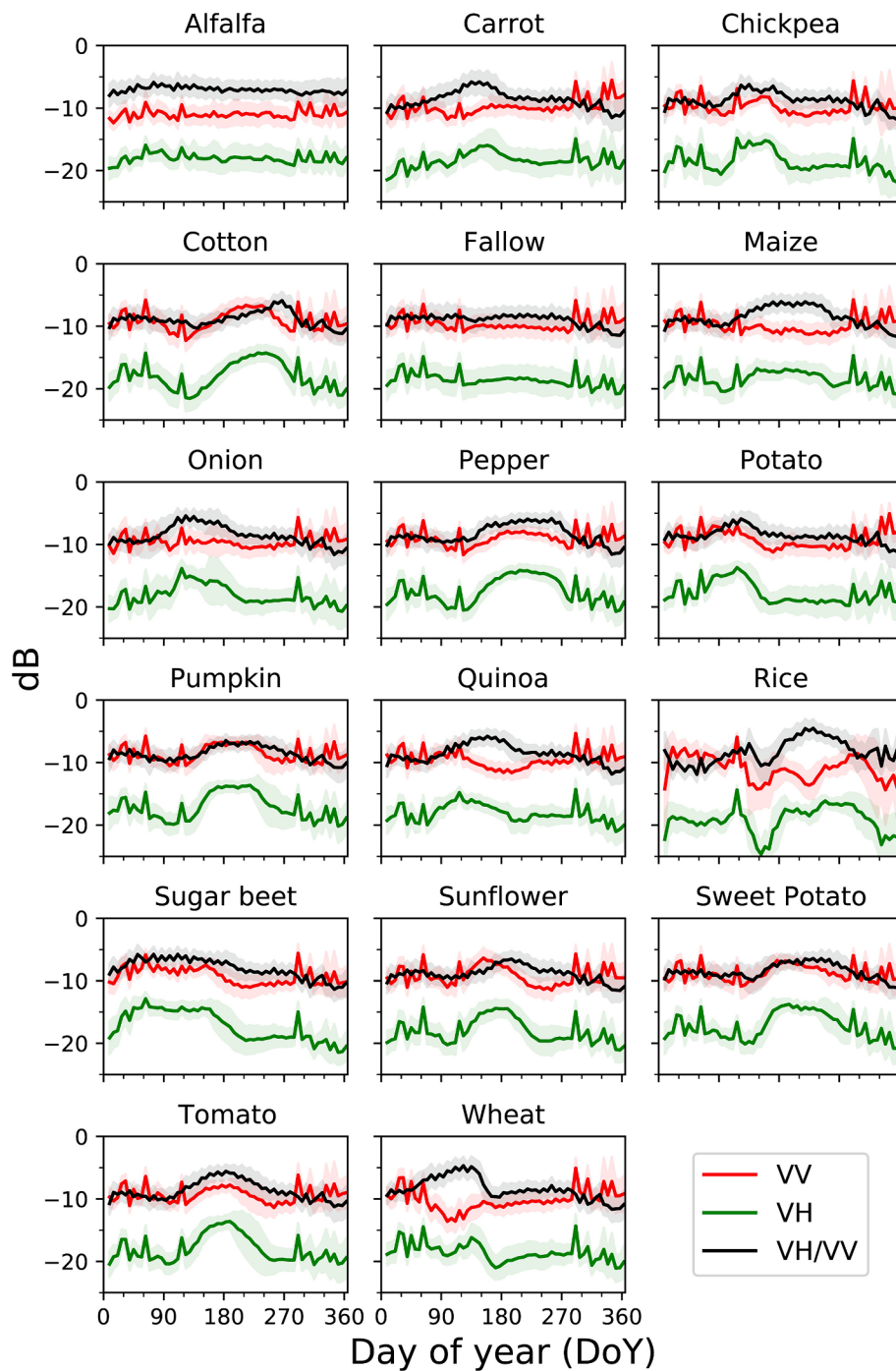


Fig. 2. Time-series data for the backscatter coefficient (σ_0) in both VV and VH channels, along with their ratio—all measured in decibels (dB)—across sixteen crop types. For each date, the mean value is depicted by a solid line, while the standard deviation is illustrated through a shaded region surrounding the mean (Adapted from Villarroya-Carpio et al., 2022).

scattering occurring within the crop canopy (Inoue et al., 2014; McNairn and Brisco, 2004).

In SAR imagery, three principal metrics—Beta-naught (β_0), Sigma-naught (σ_0), and Gamma-naught (γ_0)—quantify the returned radar backscatter. While Beta-naught measures backscatter in slant-range geometry, reflecting surface properties, it is less commonly used in agricultural applications. Sigma-naught and Gamma-naught are more relevant for agricultural studies, as they account for local incidence angle and terrain-induced variations, respectively. Sigma-naught corrects for local incidence angle, presenting backscatter in ground-range geometry as a natural normalization of beta-naught. Gamma-naught,

adjusted for the plane perpendicular to the slant range, excels in areas of significant topographic variation, where beta-naught and sigma-naught may falter (Small, 2011).

While most papers have used sigma-naught (σ_0) as the input feature for their DL algorithms, several studies have highlighted the advantages of gamma-naught over sigma-naught for crop mapping (Lobert et al., 2023) and crop monitoring (Pandžić et al., 2024; Sonobe, 2019) as they are less dependent on incidence angle. Sigma-naught is more commonly used for applications involving flat terrain, while gamma-naught is preferred when dealing with areas of varying topography (Small, 2011).

Fig. 2 presents time-series data of the backscatter coefficient (σ_0) in

both VV and VH channels, as well as their ratio, from Sentinel-1C-band SAR signals for sixteen crop types. At any single point in time, two crops may exhibit similar backscatter values, but as the crop structure evolves, particularly during seed and fruit development stages, the backscatter signature changes accordingly. By acquiring multi-temporal SAR data, these changes can be captured and analyzed to distinguish different crop types and monitor their growth. However, interpreting the sequential relationship in the SAR time-series can be challenging, and DL has been recognized as a valuable tool in addressing these challenges by learning spatial and temporal relationships of crops at the pixel or parcel level (Han et al., 2023).

Preprocessing of SAR images is a critical step in improving their quality and enhancing their interpretability. Out of the 82 papers analyzed, 60 (75 %) have conducted SAR preprocessing, while the remaining papers have used preprocessed SAR data from public or non-public datasets. The majority of these preprocessing efforts were focused on Sentinel-1 data, with only eight papers addressing RADARSAT-2 and AIRSAR. The preprocessing workflow has been presented in Fig. 5 flowchart.

The majority of the papers employed Sentinel Application Platform (SNAP) software for SAR processing, with a few exceptions. Garnot et al. (2022) and Kussul et al. (2018) utilized the Orfeo toolbox and Sentinel-Toolbox (S1TBX), respectively, while Mei et al. (2018) used PolSARpro to generate coherency matrix (Sec 2.1.2) for AirSAR data. Recently, cloud-based platforms such as Google Earth Engine have gained popularity for SAR processing, as demonstrated by Paul et al. (2022), Ngo et al. (2023) and Y. Zhou et al. (2019). Most of the papers utilized Lee and Refined Lee filters for speckle filtering, making them the most commonly employed methods for reducing speckle effect in SAR imagery for agriculture. Similarly, the Shuttle Radar Topography Mission (SRTM) was frequently used as the digital elevation model (DEM) for terrain and geometric corrections.

To summarize, the selection of SAR backscatter observables from specific bands as input features for DL classifiers was strategically tailored to align with the crop types, structural characteristics, and intended agricultural application. This included employing both co-polarization and cross-polarization, or their combinations, standardized into decibel scales.

2.1.2. Polarimetry

In addition to single and dual-polarization SAR systems, fully polarimetric SAR (PolSAR) systems also known as quad-polarization systems, have the capability to transmit and receive electromagnetic waves in all four possible combinations of horizontal (H) and vertical (V) polarizations: HH, HV, VH, and VV. This allows the PolSAR systems to measure the complete scattering matrix of a target, which consists of four complex elements (S_{HH} , S_{HV} , S_{VH} , and S_{VV}) that describe how the target interacts with the incident electromagnetic wave and changes the polarization state of the scattered wave. By measuring the complete scattering matrix, PolSAR systems provide valuable insights into the scattering mechanisms and physical characteristics of agricultural crops and the underlying soil surface (Hajnsek and Desnos, 2021; Lee and Pottier, 2017). However, interpreting the raw scattering matrix directly can be challenging. Therefore, to better understand and interpret the scattering behavior, polarimetric decomposition techniques are employed. Polarimetric decomposition is the process of breaking down the PolSAR scattering matrix into simpler, physically meaningful components that represent different scattering mechanisms such as surface, volume, and double-bounce scattering (Vicente-Guijralba et al., 2014). The temporal evolution of the relative contributions of these scattering mechanisms relates to crop growth stages, and therefore, they are effective features for crop classification application. In the early growth stages, surface scattering typically dominates as the SAR signal primarily interacts with the soil surface, double-bounce scattering can also occur if the crop has vertical structure or residues that facilitate this interaction. In the specific case of rice planting in flooded fields, double-bounce

scattering becomes prominent right after transplanting, due to the radar signal reflecting off both the flat-water surface and the upright rice stalks. As the crop grows and the canopy develops, volume scattering becomes more prominent, since the SAR signal interacts with the leaves, stems, and fruits of the plants. This volume scattering is mainly related to VWC and LAI. Moreover, the combination of both double-bounce and volume scattering can provide valuable information for biomass and yield estimation, as it captures the density and structure of the crop canopy.

To facilitate the interpretation of PolSAR data, various decomposition strategies have been proposed, including those by Cloude and Pottier. (1996), Freeman and Durden. (1998), Yang et al. (1998), Yamaguchi et al. (2005), Cameron and Rais. (2006), and Raney et al. (2012).

Pauli decomposition, based on the Pauli matrices (Cloude and Pottier, 1996), is widely used to break down the backscatter matrix into surface, double-bounce and volume scattering mechanisms. Cloude and Pottier also introduced a method based on eigenvectors and eigenvalues for deriving decomposition parameters from the coherency matrix (a 3x3 hermitian matrix derived from the scattering matrix that characterizes the polarimetric properties of a target), helping to identify entropy (H, indicating the randomness of scattering mechanisms), alpha angle (α , showing the main or average scattering mechanism), and anisotropy (A, evaluating the intensity difference between the second and third scattering mechanisms) (Lee and Pottier, 2017; Xu and Jin, 2005). Additionally, pedestal height, the ratio of the smallest to the largest eigenvalue, has been adopted to indicate the share of unpolarized scattering (Lee and Pottier, 2017).

In addition to the Cloude-Pottier decomposition, model-based decomposition techniques such as Freeman-Durden (Freeman and Durden, 1998) and Yamaguchi (Yamaguchi et al., 2005) decompositions have been widely used for several decades. The Freeman-Durden decomposition conceptualizes the covariance matrix as deriving from three distinct scattering mechanisms, enabling identification of the predominant scattering types (Freeman and Durden, 1998; Lee and Pottier, 2017). Yamaguchi et al. (2005) enhanced this model by incorporating helix scattering power (the co-pol and the cross-pol correlations) as a fourth element. The m-chi decomposition technique, introduced by Raney et al. (2012) for lunar and astronomical studies, offers a valuable approach for analyzing polarimetric SAR data in various terrestrial applications, including agriculture. This decomposition is centered around two parameters: m, which measures the portion of the electromagnetic wave that is polarized, and chi, the Poincaré ellipticity parameter. Different types of crops and their varying conditions (e.g., healthy, stressed, different growth stages) can alter the degree of polarization of the radar signal (m), while the structural characteristics and orientation of crop leaves and stems, as well as the properties of the underlying soil, can influence chi parameter.

While most reviewed studies predominantly input raw linear polarization data (e.g., VV, HH, VH) into their DL classifiers, several have further enhanced classification accuracy in agricultural applications by effectively utilizing polarimetric decomposition parameters along with single and dual polarization measurements for crop mapping (Gu et al., 2019; Li et al., 2021; Li et al., 2022c; Ma et al., 2022), crop biophysical parameters estimation (Han et al., 2022), grassland mowing events detection (Komisarenko et al., 2022), and soil salinity mapping (Zhang et al., 2020).

In addition to decomposition parameters from PolSAR data, various SAR indices have been used, such as Span, calculated as the sum of various polarizations (HH, VV, HV, and VH) and measuring the total backscattering strength from these polarizations (Yahia et al., 2020), cross ratio (CR) $\frac{\sigma_{VH}^0}{\sigma_{VV}^0}$, the quad-pol Radar Vegetation Index (RVI) which measures the randomness of scattering mechanisms $8\sigma_{HV}^0 / (\sigma_{HH}^0 + \sigma_{VV}^0 + 2\sigma_{HV}^0)$ (Zhang et al., 2020), and was modified for dual-pol SAR data as $4\sigma_{HV}^0 / (\sigma_{HV}^0 + \sigma_{HH}^0)$ (Trudel et al., 2012), and Later adopted by

several studies as $4\sigma_{VH}^0/(\sigma_{VH}^0 + \sigma_{VV}^0)$ using Sentinel-1 dual-pol data (VV-VH) (Nasirzadehdizaji et al., 2019), Polarimetric Radar Vegetation Index (PRVI), (1-degree of polarization) $\times \sigma_{HV}$ (Chang et al., 2018), Dual-pol radar vegetation index (DpRVI), (1-degree of polarization \times normalized dominant eigenvalue) Mandal et al., (2020) and Dual Polarization SAR Vegetation Index (DPSVI), $(\sigma_{VV} + \sigma_{VH})/\sigma_{VV}$ (Periasamy, 2018). Furthermore, Nasirzadehdizaji et al. (2019) introduced a new index, $(\sigma_{VV}^0 - \sigma_{VH}^0)/(\sigma_{VV}^0 + \sigma_{VH}^0)$, for estimating crop height and canopy coverage. This index was later utilized by Sun et al. (2022) for rice mapping using Sentinel-1 data. Mei et al. (2018) enhanced crop classification accuracy by combining RVI with eigenvalues from the H/A/Alpha polarimetric decomposition instead of linear polarization, formulated as $4\lambda_3/\lambda_1 + \lambda_2 + \lambda_3$, and from scattered power components derived from the Freeman-Durden decomposition, expressed as $F_v/F_v + F_d + F_s$, where F_v , F_d , and F_s represent the volume, double-bounce, and surface scattering components, respectively.

Texture features extracted from polarimetric SAR images is another measure that capture the structural characteristics of the target surface and its surrounding environment, providing insights into spatial variations in land cover. The Gray-Level Co-occurrence Matrix (GLCM) technique, introduced by Haralick et al. (1973), is widely used for texture analysis in polarimetric SAR images, which is a statistical method used to extract texture features from an image. It analyzes the spatial relationship between pixels by considering the frequency of occurrence of pairs of pixel values at a specified distance and orientation. Hoa et al. (2019) highlighted the importance of GLCM-derived textural features for soil salinity detection using polarimetric SAR imagery.

While various studies have adopted combinations of different decomposition parameters and SAR indices as input features for DL classifiers, future research should focus on feature Selection, as will be detailed in Section 3.1.3. This is crucial for minimizing feature redundancy and selecting the optimal parameters based on the intended application.

2.1.3. Interferometry

In addition to SAR observables derived from measured backscattered intensity and polarimetric decomposition parameters, SAR also provide access to interferometric data. The technique involves the combination of pairs of exact repeat SAR images to produce phase measurements that relate to the vertical dimension of the scene being observed, among other properties (Bamler and Hartl, 1998). A critical element in interferometric SAR (InSAR) is the concept of interferometric coherence, a measure that reflects the quality of the interferometric phase and, by extension, the quality of the products derived from it. This coherence is influenced by a variety of factors, including scene characteristics, sensor specifications, and the configuration of the interferometric pair itself (Zebker and Villasenor, 1992). Repeat-pass InSAR involves capturing SAR images of the same area at different times, allowing for the detection of changes within a scene. This technique has proven effective in measuring decreases in interferometric coherence, which often occur due to the rapid growth of plants or wind-induced movements, leading to temporal decorrelation, particularly over areas with agricultural crops (Rosen et al., 2000). The time gap between the two acquisitions can range from days to weeks or even months, depending on the satellite revisit time and the application requirements. The presence or absence of vegetation, as indicated by changes in coherence over time, provides insights into the agricultural calendar and, consequently, the types of crops present in a given area. This aspect of temporal decorrelation has been extensively explored through the use of time-series data from various SAR satellite sensors, enabling detailed mapping of crop types (Busquier et al., 2022). Villarroya-Carpio et al. (2022) established a strong correlation between the coherence measured in each polarimetric channel (VV and VH) and the NDVI, proposing that data from intensity and interferometry serve as complementary sources, a concept

previously validated by Mestre-Quereda et al. (2020) in crop-type mapping.

In addition to repeat-pass interferometry, single-pass interferometry has also demonstrated potential for crop classification and vegetation height estimation. Single-pass interferometry involves acquiring two SAR images simultaneously or within a very short time interval, eliminating temporal decorrelation effects. This technique is particularly useful for capturing the vertical structure of vegetation. Erten et al. (2016) found that single-pass interferometry provided valuable information about crop height and structure, especially when using large spatial baselines. Building on this, Busquier et al. (2020) showed that single-pass coherence can contribute to improve classification accuracy in both dual-pol and single-pol cases, with more notable improvements observed for taller crops. The sensitivity to vertical structure provided by the physical baseline in single-pass interferometry allows for better discrimination between crop types based on their height and architectural differences.

While both repeat-pass and single-pass interferometry offer valuable insights into crop characteristics, combining interferometric techniques with polarimetric information (PolInSAR) can provide enhanced sensitivity to vegetation structure and height. As reviewed by Romero-Puig and Lopez-Sanchez (2021), PolInSAR techniques have been successfully applied to crop height estimation, offering advantages over single-polarization interferometry or polarimetry alone. By exploiting the varying penetration depths of different polarizations, PolInSAR can more accurately locate the scattering phase centers within the vegetation volume. This allows for improved estimation of crop height, especially for taller or denser crops where single-channel approaches may saturate. While PolInSAR generally requires fully polarimetric data, which limits coverage compared to single-pol acquisitions, it provides a powerful tool for crop monitoring when such data are available. Despite its potential, interferometry coherence has been underutilized in crop mapping and monitoring using DL, being employed in two crop classification studies. Future research should concentrate on harnessing the potential synergies between intensity data and interferometric measurements to enhance crop mapping, monitoring, and the detection of agricultural management practices.

2.2. Applications

The SAR techniques described in the previous section provide valuable insights into the physical properties and temporal dynamics of agricultural landscapes. These SAR-derived features serve as input to DL models, enabling the development of architectures for crop classification/mapping, monitoring, and yield estimation. In this section, we review how SAR observables from linear polarization, PolSAR, and InSAR have been used as input features to DL approaches for the aforementioned applications.

2.2.1. Classification/Mapping

SAR linear polarizations, specifically VH and VV, have been the subject of extensive investigation for their utility in crop mapping. Research, including studies by Asadi and Shamsoddini (2024), Liu et al. (2023), and Zhou et al. (2019) highlights the superior performance of cross polarization (VH or HV) in identifying the majority of crops. However, a synergistic approach combining both VH and VV polarizations has been shown to provide a more detailed insight into crop characteristics, thereby improving model accuracy. This is supported by findings from Jo et al. (2022) and Y. Zhou et al. (2019), which demonstrated the enhanced crop classification accuracy achieved through the integrated use of VH and VV signals, as further evidenced by Magalhães et al. (2022), Paul et al. (2022) and Liu et al. (2023). Their research underscores the advantage of this combined approach over the exclusive use of either VH, VV, or their ratio. Additionally, the integration of various SAR polarimetric parameters from Pauli, Cloude and Pottier (H, A, alpha), Yamaguchi, and Freeman–Durden decomposition,

as explored by K. Li et al. (2022), [Mei et al. \(2018\)](#), [Yin et al. \(2023\)](#), and [Zeyada et al. \(2016\)](#) extended the potential of SAR data for high accuracy crop mapping. These studies highlight the value of leveraging a multi-dimensional dataset to refine crop classification methods. [McNairn et al. \(2009\)](#) found that L-band polarimetric parameters derived from three decomposition approaches—Cloude-Pottier, Freeman-Durden, and Krogager—yielded higher crop classification accuracies relative to those achieved using the single and dual polarization. Further advancing this research, [McNairn et al. \(2014\)](#) showed that employing PolSAR technology over linear polarization could improve Overall Accuracy (OA) of crop classifications by up to 7 %. Extending these insights, [Ma et al. \(2022\)](#) confirmed that polarimetric decomposition parameters specifically enhance rice mapping accuracy by an additional 3 % over traditional VV and VH polarizations.

In addition to PolSAR data, the role of interferometric coherence in crop classification has gained attention. [Busquier et al. \(2022\)](#) further explored the synergistic effects of combining backscatter intensity with repeat-pass interferometric coherence, particularly emphasizing the value of C-band coherence in enhancing classification accuracies. Despite the lower performance of X-band coherence data due to quicker decorrelation, its fusion with C-band data significantly improved classification outcomes. Further, [Ni et al. \(2022\)](#) introduced the asymmetric coherence term or polarimetric ratio, which focuses on variations in polarimetric properties and radiometric changes between observations, whereas traditional coherence measures the temporal correlation and stability of scattering properties in SAR data. They illustrated that using asymmetric coherence can improve classification accuracy by 20 % to 50 % compared to traditional coherence-based methods. Consequently, given InSAR's potential to enhance crop classification accuracy, further research should focus on utilizing this SAR technique in conjunction with intensity measurements and polarimetry.

2.2.2. Crop monitoring: phenology and biophysical parameters estimation

In the domain of crop phenology and BPs estimation, SAR data have proven to be a powerful tool, providing detailed insights into agricultural crop dynamics. Among the extensive set of linear and dual polarization SAR data, particularly VH, emerges as a critical feature due to its heightened sensitivity to volumetric scattering within crop canopies. This characteristic makes VH polarization particularly effective in distinguishing between different crop growth stages, as it adeptly captures the complex scattering interactions among canopy components, such as leaves, stems, and branches. The superiority of VH polarization over VV polarization lies in its reduced sensitivity to factors like water, topography, and the canopy's morphological structure, as demonstrated in studies focusing on rice phenology estimation ([Yang et al., 2021](#)).

In addition to linear polarization, SAR polarimetric decompositions and radar indices have established their significance by revealing key physical attributes closely associated with various crop BPs ([Mandal et al., 2021](#)). Notably, features like the RVI, Entropy, and the Alpha angle have been instrumental in delineating growth patterns across various crops, including soybeans and onions ([Kim et al., 2011](#); [Mascolo et al., 2015](#)). However, there are varied findings on the effectiveness of the cross ratio (VH/VV). [Blaes et al. \(2006\)](#) highlighted a diminished sensitivity of cross ratio to maize growth beyond certain LAI and VWC thresholds, and [Hosseini et al. \(2019\)](#) emphasized the significance of VH and VV backscatter over cross ratio for accurate winter wheat LAI and Canopy Chlorophyll Content (CCC) estimation. Conversely, studies like [Mercier et al. \(2020\)](#) demonstrated cross ratio's correlation with wheat LAI and the adept application of entropy in assessing wheat's VWC.

Moreover, the comprehensive analysis by [Canisius et al. \(2018\)](#) employing a wide array of SAR features from RADARSAT-2, including both VV and VH backscatter coefficients alongside several decomposition parameters, highlighted the significant role of VH cross-polarization and the Alpha angle from Cloude-Pottier decomposition in tracking the growth stages of canola and spring wheat. Further, [Mandal et al. \(2020\)](#), presented a strong correlation between DpRVI and essential BPs such as

Plant Area Index (PAI), VWC, and dry biomass (DB) across various crops, notably outperforming other indices in terms of performance. This approach's efficacy was further validated by [Ge et al. \(2023\)](#), who leveraged a combination of polarimetric decomposition techniques to discern characteristics crucial to rice phenology.

Collectively, these studies affirm the strategic importance of integrating multiple SAR features, particularly polarimetric parameters and VH polarization, in enhancing the accuracy and reliability of crop phenology and BPs estimations.

2.2.3. Yield prediction

Recent research has revealed the intricate relationship between SAR polarizations, frequencies, and their applications in crop yield predictions. The sensitivity of SAR backscatter to crop biomass and LAI, which directly correlates with crop yield, can be valuable for yield estimation. However, the relationship between SAR backscatter and crop biomass is not uniform and varies based on factors such as crop type, growth stage, and SAR sensor characteristics, including wavelength and polarization ([Bouman and Hoekman, 1993](#)). The structural differences among crops significantly influence how SAR signals interact with vegetation, which can affect the selection of SAR frequency, as discussed in [Section 2.2.1](#). Optimizing the timing and frequency of SAR acquisitions based on crop growth stages is crucial for accurate yield prediction. Studies have shown that SAR data acquired during the reproductive and ripening stages are most effective for estimating rice yield ([Nguyen et al., 2016](#)), while for soybean, data from the pod development and seed filling stages are more informative ([Navarro et al., 2016](#)). In the case of corn, SAR data from the late vegetative and early reproductive stages, such as tasseling and silking, have demonstrated potential for yield estimation ([Fieuza et al., 2017](#)).

SAR polarization is another critical factor affecting the sensitivity of backscatter to crop biomass and yield. Studies by [Tesfaye et al. \(2022\)](#), [Tripathi et al. \(2022\)](#), and [Sharma et al. \(2022\)](#) have demonstrated the superiority of VH polarization in predicting rice and wheat, respectively. Conversely, VV polarization has exhibited better performance for sugarcane stalk development, which serves as a critical reservoir for sucrose accumulation ([den Besten et al., 2023](#)). However, the synergistic use of both VV and VH polarizations has been shown to enhance the robustness and precision of yield estimation models ([Yu et al., 2023](#)). Besides linear polarization, the highest correlations with LAI and biomass have been found for volume scattering components from polarimetric parameters indicative of multiple scattering events, pedestal height and RVI ([Steele-Dunne et al., 2017](#)). This suggests that incorporating these parameters into DL classifiers for yield prediction could improve their performance.

However, for DL-based studies, only VH and VV SAR observables have been used as input features. This reliance is due to the inherent capability of DL models to automatically learn and extract relevant features from raw input data, such as VH and VV signals in SAR imagery. This capability negates the need for manually crafted SAR indices like the RVI, which depends on the ratio of VH to VV signals. By directly processing raw SAR observables, DL models can uncover complex patterns and relationships that predefined indices may not capture, potentially leading to more precise and efficient analysis of agricultural scenes.

2.3. Data sources

Out of the 82 papers reviewed, 11 % (9 papers) utilized airborne SAR data, such as multi-temporal AirSAR, UAVSAR, and PolSAR images from the AgriSAR project ([Fig. 1](#)). These airborne SAR systems offer high spatial resolution and flexibility in data acquisition, making them valuable for small-scale studies and algorithm development. However, the majority of the papers (89 %) employed spaceborne SAR data, with Sentinel-1 (C-band) being the most commonly used in 80 % (66 papers) of the cases. The widespread use of Sentinel-1 data can be attributed to

Table 1

Overview of SAR Spaceborne Satellites: Specifications, Operators, and Data Accessibility.

Name	Operated by	Mission	Spatial coverage	Spatial Resolution (meter)	Temporal Resolution (days)	Band/Frequency (GHz)	Incidence Angle (°)	Polarization	Data Accessibility	Acquisition Method
ERS-1	ESA	1991 to 2000	global	10–30	35 in IM	C-5.2	5–45	VV	Paid	Tasked
JERS-1	NASDA	1992–1998	global	18	44	L- 1.275	32–38	HH	Paid	Tasked
ERS-2	ESA	1995 to 2011	global	10–30	35 in IM	C-5.3	5–45	VV	Paid	Tasked
RADARSAT-1	CSA	1995 to 2013	Regional*	10(FM),25 (SM),10–50 (SWM), 30 (SNM)	24 (FM), 12 (SM), 72 (SWM)	C-5.3	20–35(FM), 20–45(SM) 10–60 (SWM), 30(SNM)	HH	Paid	Tasked
ENVISAT-ASAR	ESA	2002 to 2012	global	30	35 in APM and IM modes	C-5.6	15–45(WSM, IM, APM),17–43 (GMM),23 (WM),20–44 (SNSM)	HH, VV, HH/VH, VV/VH	Paid	Tasked
RADARSAT-2	CSA and MDA	2007 to now	global	10(FM), 25 (SM) 10–50 (SWM), 30 (SNM), 3 (UFM)	24 (SM), 3 (FM)	C-5.405	20–35(FM), 20–45 (SM),10–60 (SWM), 30 (SNM), 3 (UFM)	HH, VV, HV, VH	Paid	Tasked
COSMO-SkyMed	ASI	v1-2(2007), v3(2008), v4 (2010) to now	global	1(Spotlight)	16	X-9.65	20–59	VV, HH	Paid	Tasked
TerraSAR-X/TanDEM-X	Airbus and DLR	TerraSAR –2007 to now, TanDEM-2010 to now	global	1–3 (SL and SM), 16 (SC)	11	X-9.65	20–55	HH, VV, HH/VV, HH/HV, VV/VH	Paid	Tasked
RISAT-1	ISRO	2012–2017	global	1–50	25	C-5.35	12–55	HH, VV, HH/HV, VV/VH, Quad-pol	Open	Always Acquired
Gaofen-3 (GF-3)	CNSA	2014 to now	Swath of 10–650 km	1–10	1.5–3	C-5.405	20–50	HH, VV, HH/HV, VV/VH	Open	Always Acquired
ALOS-2	JAXA	2014 to now	global	10–100	46	L-1.27	20–40	HH, HV, VH, VV	Paid	Tasked
Sentinel-1A, C	ESA	A-2014 to now, C-2024	global	3–10	12	C-5.405	20–45	VV-VH (IW), VV-VH, VV or HH (strip mode), VV (WM)	Open	Always Acquired
Sentinel-1B	ESA	2016–2021	global	3–10	12	C-5.405	20–45	VV-VH (IW), VV-VH, VV or HH (strip mode), VV (WM)	Open	Always Acquired
NovaSAR-1	SSTL	2018 to now	global	6 (SM), 20 (SC), 30–50 (SC wide)	16	S-3.1 – 3.3	16–31.2 (SM), 11.29–32.01 (SC), 11.82 – 31.18 (SC wide)	HH or VV (SM), HH, VV and HV (SC and SC wide)	Paid	Tasked
PAZ	Hisdesat	2018 to now	global	1–3 (SL and SM), 16 (SC)	11	X-9.65	20–55	VV, HH, HV, and VH	Paid	Tasked
SAOCOM-1A, B	CONAE	A-2018 and B-2020 to now	global	10 (SM)	16	L-1.215	18–50	HH, VV, HH/HV, VV/VH, Quad-pol	Open	Always Acquired
RCM	CSA	2019 to now	global	1–3 (SL), 50–100 (SC)	4	C-5.405	33.63–35.93	HH, VV, HV, VH, Compact-pol	Paid	Tasked
Capella2-10	Capella Space	2020–2023	global	0.5	<= 2 h	X-9.3–9.9	45–53	VV, VH	Paid	Tasked
Umbra	Umbra Lab	2023-now	global	0.25	6–12 h	X-9.2 – 10.4	10–75	VV, VV+VH	Open	Always Acquired
Iceye	Iceye	2023	Regional	0.5–3	1–22	X-9.65	15–35	HH, VV, HH/HV, VV/VH, Quad-pol	Open	Always Acquired
NISAR	NASA& ISRO	2024	global	3–10	12	L- (1.215–1.3) and S-3.2	33–47	HH, VV	Open	Always Acquired

(continued on next page)

Table 1 (continued)

Name	Operated by	Mission	Spatial coverage	Spatial Resolution (meter)	Temporal Resolution (days)	Band/Frequency (GHz)	Incidence Angle (°)	Polarization	Data Accessibility	Acquisition Method
BIOMASS	ESA	2024	global	50–200	365	P-0.435	23–34	Quad-pol	Open	Always Acquired
Sentinel-1 NG	ESA	2029	global	1–5	4–12	C-5.405	17–45	HH, VV, HH/ HV, VV/VH, Quad-pol	Open	Always Acquired
ROSE-L	ESA	2028	global	<=5	3–6	L-1.2575	15–45	HH/HV, VV/ VH, Quad-pol	Open	Always Acquired
Tandem-L	DLR	2028	global	1 for spot image	16	L-1.215–1.3	20–45	HH, VV, Quad-pol	Paid	Tasked

* Canada, the Arctic, and areas of the United States, South America, Europe, and Asia.

The European Remote Sensing Satellite (ERS), National Space Development Agency of Japan (NASDA), RADARSAT Constellation Mission (RCM), German Aerospace Center (DLR), Comisión Nacional de Actividades Espaciales, Argentina (CONAE), China National Space Administration (CNSA), Italian Space Agency (ASI), Canadian Space Agency (CSA), MacDonald, Dettwiler and Associates Ltd (MDA), Surrey Satellite Technologies (SSTL), SAAtélite Argentino de Observación COn Microondas (SAOCOM), National Aeronautics and Space Administration (NASA), Indian Space Research Organization (ISRO), Image Mode (IM), Wide Swath Mode (WSM), Global Monitoring Mode (GMM), Alternating Polarization Mode (APM), Wave Mode (WM), ScanSAR Narrow Swath Mode (SNSM), Fine mode (FM), Standard mode (ST), Strip Map (SM), Wave Mode (WV), Spotlight (SL), ScanSAR(SC).

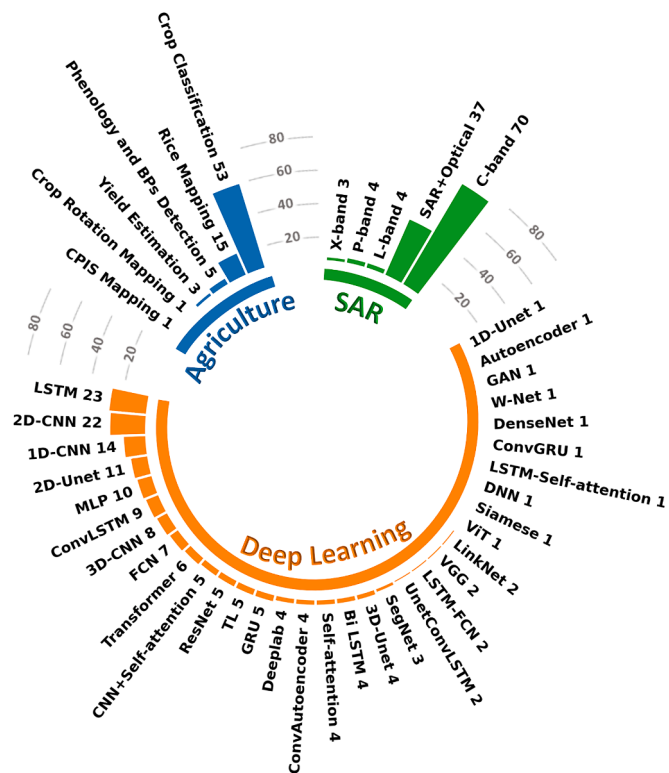


Fig. 3. Distribution of studies across SAR bands, agricultural applications, and DL architectures. Emphasis on C-band SAR for crop classification using LSTM and 2D-CNNs. CPIS: Mapping of Center Pivot Irrigation Systems.

its open access policy, systematic acquisition strategy, and global coverage. The Sentinel-1 mission, comprising two satellites (Sentinel-1A and Sentinel-1B, which was decommissioned on 23 December 2021), provides C-band SAR data with a revisit time of 6–12 days, making it an invaluable resource for agricultural monitoring applications. Given the widespread use of spaceborne SAR data in conjunction with DL for agriculture, Table 1 offers a comprehensive overview of all the spaceborne SAR satellites.

3. Use of deep learning in agricultural applications of SAR

DL and SAR technologies have been widely utilized in the agricultural sector, with numerous studies conducted in various countries.

Europe, the USA, Brazil, and China have emerged as key regions with a significant number of research efforts in this field. This trend highlights the widespread adoption of DL applications in diverse ecosystems, showcasing their adaptability for different vegetation types and agricultural applications.

Upon a detailed review of the existing literature, it's clear that a substantial number of studies emphasize the use of SAR and DL techniques for classification/mapping application, particularly targeting the end-of-season crop mapping, most notably for rice (Fig. 3 and Fig. 4). Despite the potential for wider applications, it appears that there is a surprisingly limited utilization of contemporary DL techniques for crop monitoring (5 studies) and crop yield estimation (3 studies).

A probable factor could be the relative scarcity of training datasets for these applications, which are critical for the optimal performance of DL algorithms.

In this section, we delve into the potential of DL algorithms to mitigate the speckle effect in SAR images. Furthermore, we investigate the fusion of SAR and optical data, as research has shown that combining these two data sources can yield superior results compared to using SAR and optical data alone in various agricultural applications, such as crop classification, monitoring, and yield estimation. This underscores the potential benefits of integrating multiple remote sensing data sources within DL frameworks for agricultural purposes. Additionally, we explore feature selection methods, which enhance DL model efficiency and generalization by reducing data dimensionality and eliminating redundant features. We also examine both established and emerging DL architectures to gain a deeper understanding of their contributions to SAR applications in mapping/classification, including early- and end-season crop classification, crop rotation, mapping of center pivot irrigation systems, and soil salinity mapping, as well as crop monitoring and yield prediction. Moreover, we discuss crucial implementation considerations, such as data collection and augmentation techniques, along with training and validation ratios, which play a vital role in the successful deployment of DL models for agricultural applications.

3.1. Data processing techniques

3.1.1. Speckle filtering

Speckle effect is a common phenomenon in SAR imagery that degrades image quality and hinders the accurate interpretation of dynamic crop phenology. Traditional speckle filtering methods often struggle to achieve a balance between noise reduction and preservation of fine details. However, DL approaches, particularly Convolutional Neural Networks (CNNs), have shown remarkable success in addressing this challenge. CNNs can learn hierarchical features from SAR data, enabling them to effectively distinguish between noise and actual ground

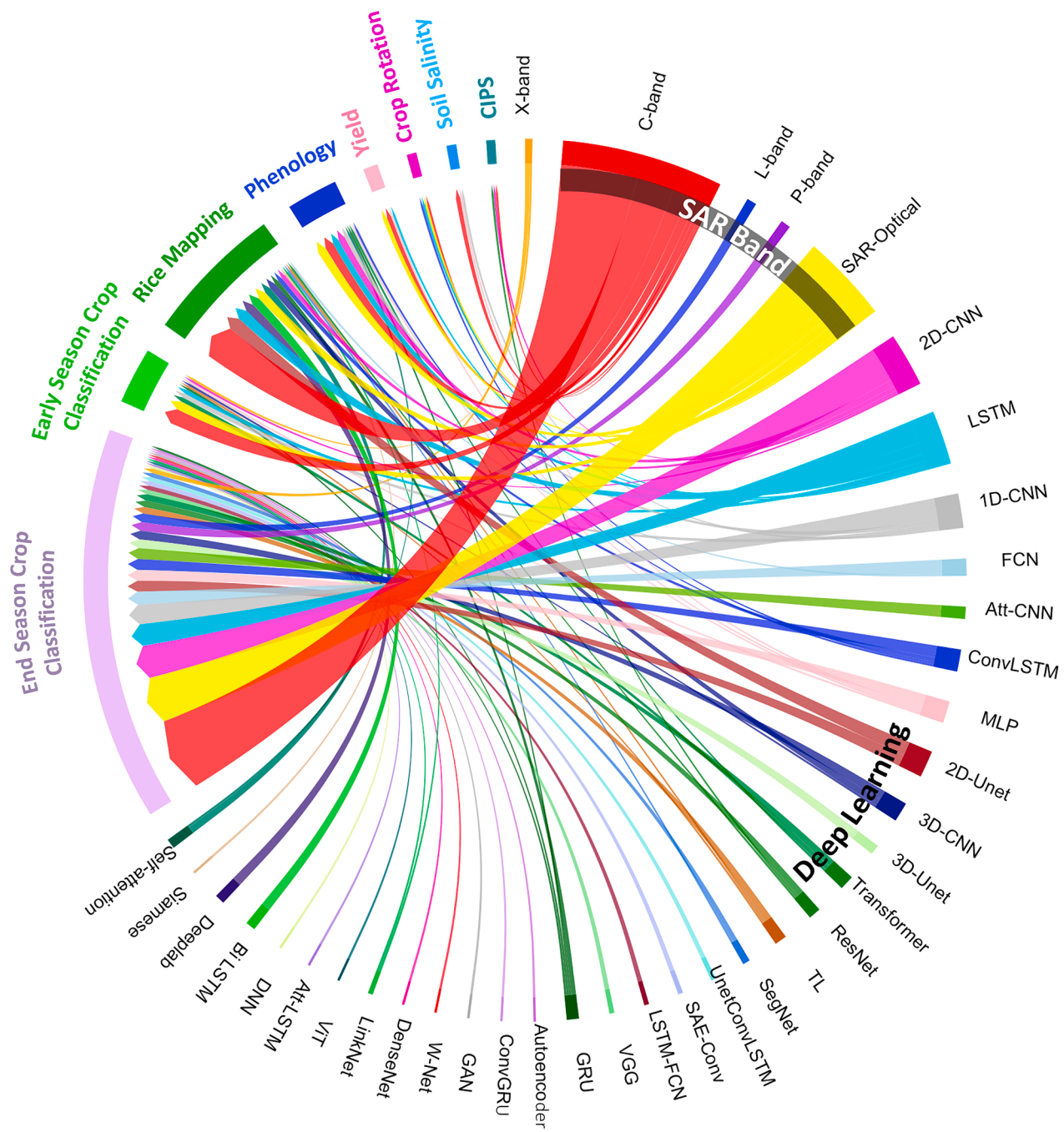


Fig. 4. Network analysis of interconnections between agricultural applications, SAR frequencies, and DL architectures in reviewed studies. Node size indicates number of studies. Att: self-attention mechanism; TL: transfer learning; CPIS: mapping of Center Pivot Irrigation Systems.

features. By training on large datasets of SAR images with varying levels of speckle effect, CNNs can learn to suppress speckle while retaining important spatial and textural information. This capability has led to significant improvements in SAR image quality, facilitating more accurate crop classification, monitoring, and yield estimation.

Several studies in this review have explored the application of DL techniques for speckle filtering in SAR data. [Mei et al. \(2018\)](#) employed Simple Linear Iterative Clustering (SLIC) superpixel segmentation to reduce speckle effect by dividing the SAR image into smaller superpixel blocks. Similarly, [Sonobe et al. \(2019\)](#) utilized linear discriminant analysis (LDA) to remove noisy data from TerraSAR-X images ([Phalke and Özdogan, 2018](#)). Furthermore, [Adrian et al. \(2021\)](#) introduced Denoising Convolutional Neural Networks (DnCNNs), which adapt to the specific noise characteristics within SAR images, preserving essential

details while eliminating noise.

Interestingly, some studies have highlighted the potential of DL algorithms to obviate the need for preprocessing SAR data. [Garnot et al. \(2022\)](#) demonstrated that the U-Net architecture, combined with temporal attention-based networks (will be discussed in Sec 3.2.1), could effectively learn features and patterns from vast raw datasets without requiring radiometric terrain correction or speckle filtering. This approach enhanced crop mapping models without the need for extensive SAR preprocessing. Similarly, [Gargiulo et al. \(2020\)](#) showed that the W-net architecture (will be discussed in Sec 3.2.1) could produce reliable segmentation maps without speckle filtering, reducing computational complexity.

These findings underscore the potential of DL methods to not only effectively mitigate speckle effect in SAR data but also to potentially

eliminate the need for certain preprocessing steps. Further research into the capabilities of DL in handling raw SAR data could lead to more efficient and streamlined workflows for agricultural applications.

3.1.2. SAR and optical fusion techniques

Integrating SAR with optical data represents a pivotal advancement in agricultural monitoring, optimizing the strengths and mitigating the limitations of each sensor type (Ofori-Ampofo et al., 2021). This fusion approach confronts challenges such as integrating multi-band spectral reflectance with SAR backscatter intensity and overcoming differences in spatial resolutions and temporal characteristics. Evidence of the successful application of SAR and optical data fusion is abundant, with notable examples including the combination of Sentinel-1 with Landsat-8 (Kussul et al., 2018, 2017; Cué La Rosa et al., 2023), and Sentinel-2 datasets (Asadi and Shamsoddini, 2024; Komisarenko et al., 2022; Liu et al., 2021; Ngo et al., 2023; Saadat et al., 2022; Sun et al., 2019a; Thorp and Drajat, 2021; Tripathi et al., 2022; Wang et al., 2020; Yu et al., 2023; Zhao et al., 2020; Zhao et al., 2022). A comprehensive review of 82 studies in this field revealed that 45 % (37 papers) utilized a combination of optical and SAR data, primarily for crop classification, while encompassing all studies related to yield and BPs estimation. This review also highlighted the wide array of optical data sources employed beyond Sentinel-2 and Landsat-8, such as VENµS, RapidEye, ZY-3, Planet satellite imagery, Very High Resolution orthophotos, AVIRIS, ROSIS, and RGB data from the CNES/Airbus Pleiades satellite. For comprehensive insights into the specific optical and SAR data utilized in each study, readers are referred to Table A1 in the supplementary material.

The superiority of combining SAR and optical data over approaches relying on a single modality has been consistently validated across research, particularly for crop classification (de Albuquerque et al., 2021; Giordano et al., 2020; Ofori-Ampofo et al., 2021), crop monitoring (Lobert et al., 2023; Thorp and Drajat, 2021), and yield prediction (Yu et al., 2023). This fusion technique benefits from combining SAR's detailed textural insights with the spectral richness of optical imagery, offering a broader spectrum of data for analysis.

Data fusion strategies can be broadly categorized into three approaches: Early fusion (input/pixel level), Mid fusion (feature/layer level), and Late fusion (decision-level). Early fusion combines SAR and optical data at the input level using specific methods to address gaps in optical images, such as interpolation. Mid fusion merges features from each source at an intermediate stage, facilitating the use of a single temporal model and reducing preprocessing efforts. Late fusion, on the other hand, focuses on combining the outputs from independently processed modalities, emphasizing class confidence scores for final decision-making. For a deeper understanding of various fusion methods, readers are encouraged to read the papers by Garnot et al. (2022), Ofori-Ampofo et al. (2021) and Weilandt et al. (2023).

The choice between these fusion strategies largely depends on the desired outcomes, the specific characteristics of the datasets involved, and computational constraints. While most studies have shown a preference for early fusion due to its straightforward implementation, other studies compared all the three fusion methods to find the best one. Ofori-Ampofo et al. (2021) demonstrated the effectiveness of early fusion, especially under cloudy conditions, and proposed Layer-Level Fusion at Pixel Set Encoders (PSE) and Temporal Attention Encoder (TAE) (will be detailed in Section 3.2.1) for better identification of minor classes. Garnot et al. (2022) explored late fusion with the same classifier PSE-TAE, augmented with auxiliary supervision and temporal dropout, finding it generally superior but noted that mid-fusion offers a pragmatic balance between accuracy and computational efficiency, being 20 % faster than late fusion. This makes mid-fusion appealing for scenarios with computational constraints. Yuan et al. (2023) effectively tackle the high computational costs associated with late fusion by introducing a shared temporal encoder and a 'feature stacking' technique to the PSE-TAE classifier. This method consolidates temporal variation metrics from separately processed optical and SAR data, achieving a 60 %

reduction in trainable parameters without compromising performance. This innovation retains the effectiveness of the DL classifiers used by Ofori-Ampofo et al. (2021) and Garnot et al. (2022), streamlining late fusion processes in RS applications. Ienco et al. (2019) also demonstrated that late fusion, involving features extracted separately from SAR and optical streams using two ConvGRU networks, outperformed other fusion techniques. However, Saadat et al. (2022) further confirmed the advantages of mid-fusion in rice mapping using CNNs. Consequently, the choice between mid- and late fusion becomes a strategic decision, influenced by the specific application and the DL classifier utilized, for optimal SAR and optical data integration.

Common and emerging DL further confirmed the advantages of mid-fusion in rice mapping using CNNs. Consequently, the choice between mid- and late fusion becomes a strategic decision, influenced by the specific application and the DL classifier utilized, for optimal SAR and optical data integration.

3.1.3. Feature selection

Although DL models possess the ability to learn features automatically, providing them with a carefully selected subset of relevant features can help reduce the computational complexity and training time of the model. This is particularly important when dealing with large, high-dimensional datasets, such as multi-temporal SAR data. Consequently, to enhance classification accuracy, it is essential to minimize feature redundancy and avoid overfitting—a challenge noted by Zhang et al. (2020), yet addressed in only a limited number of studies concerning optimal SAR feature selection. Additionally, Zhang et al. (2021) observed that even with similar crop types, the most effective features for crop identification vary across different regions. To address this, Zhang et al. (2020) advocated for a tree structure-based feature selection algorithm that prioritizes features based on their calculated significance. Mei et al. (2018) improved classification accuracy by optimizing the feature set through a quantitative index that evaluates the separability of crop types. Zeyada et al. (2016) enhanced classification accuracy by identifying the superior performance of polarimetric parameters from Pauli, Cloude-Pottier, and Freeman-Durden decompositions, in conjunction with fundamental backscatter coefficients. They determined that expanding the parameter set from three to twelve could minimize training errors and prevent overfitting. Similarly, Yu et al. (2023) and Lobert et al. (2023) evaluated the performance of different sets of features to select the optimal features for yield prediction and phenology stages estimation, respectively. The results indicated that the combination of SAR with optical and meteorological data was the most effective combination for both studies. Delving further into SAR features, Hashemi et al. (2024) recently investigated the impact of different SAR observable combinations on crop yield estimation. Their findings revealed that the fusion of VH polarization with climate data outperformed other feature sets, which included VV polarization, cross ratio, RVI, and incidence angle for corn, soybeans, and winter wheat yield estimation.

The aforementioned studies collectively emphasize the crucial role of feature selection in enhancing the performance and efficiency of DL models when applied to SAR data in agricultural applications. By carefully choosing the most informative SAR observables and ancillary data prior to training DL models, researchers can optimize the models' ability to achieve reliable results in tasks such as crop classification, yield prediction, and phenology stage estimation.

3.2. Common and emerging deep learning modeling

3.2.1. Classification/mapping

a. End-season crop classification

The integration of SAR imagery with ML approaches has revolutionized the field of agricultural technology, particularly in the realm of precise crop classification at the pixel and parcel level. Traditionally, these methods relied on stacking time-series SAR imagery as a composite

of features and employing data mining techniques to differentiate various crop types (Han et al., 2023). This reliance on handcrafted features, however, has necessitated expert knowledge and often overlooked the nuanced spatio-temporal relationships inherent in time-series SAR data. Techniques such as Random Forest (RF) have shown proficiency in identifying predominant crop types but struggle when distinguishing less prevalent ones, attributed to their tendency for overfitting as the decision trees expand, particularly in multi-class scenarios (Jin et al., 2018).

Moreover, traditional ML models face inherent limitations, such as their inability to effectively process sequences or time-dependent data due to their auto-regressive nature, which hinders their ability to generalize and adapt to new data (Katharopoulos et al., 2020). In contrast, DL models have emerged as a superior alternative, showcasing their capacity for multiscale feature learning and demonstrating a remarkable ability to generalize across diverse datasets (Olimov et al., 2023). The launch of the C-band-equipped Sentinel-1A and Sentinel-1B satellites in 2014 and 2016, respectively, has significantly accelerated the adoption of DL techniques alongside SAR data by providing widespread access to high-quality, freely accessible SAR data from these satellites. This development has enabled more comprehensive studies, specifically in crop classification, harnessing the power of SAR data and DL techniques for this application. The investigation commenced with the exploration of Multilayer Perceptrons (MLP), a class of artificial neural networks (ANNs) in which each neuron in one layer is connected to every neuron in the next layer. It generally consists of two or more layers that can separate nonlinear data (Mas and Flores, 2008). Sonobe et al. (2017) and Skakun et al. (2015) illustrated the efficacy of MLP for crop classification, achieving an OA exceeding 90 %. Conversely, Zeyada et al. (2016) highlighted that shallow ML methods, when applied to C-band SAR data, outperformed MLP in crop classification tasks. This insight underscored the limitations of MLP, particularly its less optimal performance in handling complex spatial and channel information inherent in SAR imagery. Consequently, the year 2017 witnessed a strategic shift towards Convolutional Neural Networks (CNNs) and Recurrent Neural Networks (RNNs) to better capture the spatial and temporal dynamics of multi-temporal SAR imagery. CNNs, in particular, are known for their hierarchical structure, enabling high-accuracy classification and prediction tasks by learning spatial contextual representations through convolutional filters to realize end-to-end classification in large-scale SAR imagery (Oquab et al., 2014). Carranza-García et al. (2019) highlighted the unparalleled ability of CNNs to excel at processing minority classes in their research, distinguishing them from other ML methods. Notably, CNNs can be utilized in 1D for analyzing the channel or temporal dimension, in 2D for spatial dimension, or in 3D across channel, spatial and temporal dimension. Although 3D convolution has demonstrated a high accuracy in crop classification (Kussul et al., 2017), CNNs are rarely used as feature extractors for the temporal domain of remotely sensed time-series (Zhong et al., 2019). However, highlighting the effectiveness of CNNs in temporal analysis, Asadi & Shamsoddini. (2024) demonstrated the superiority of 1D-CNNs over shallow ML methods by using the backscatter and polarimetric features from SAR time-series for crop mapping. Further supporting the advancements in CNNs application, Teimouri et al. (2022) corroborated earlier findings, demonstrating the superior performance of 3D-CNNs over 2D-CNNs and MLP. Their study underscored the importance of fine-tuning the kernel depth in 3D-CNNs to optimize classification accuracy which facilitated the successful learning of crop growth cycles and consequently, boosted the classification accuracy. To address the “curse of dimensionality” issue plaguing CNNs in handling high-dimensional SAR data, stacked auto-encoder (SAE) was combined with 1D-CNNs to design a convolutional-autoencoder neural network (C-AENN) by Luo et al. (2022) and Guo et al. (2022). This model is taking advantage of dimension reduction capabilities of the SAE (Guo et al., 2020; Hinton and Salakhutdinov, 2006), and achieves a superior classification ability that surpasses standalone 1D-CNNs and SAE

approaches, as well as traditional ML methods. Autoencoders are primarily linked with unsupervised learning, as they are designed to compress input data into a condensed representation and subsequently reconstruct it without requiring labeled data during the training process. Di Martino et al. (2021) successfully employed C-AENN to classify crops in an unsupervised manner, proving its effectiveness in extracting detailed agricultural classes from temporal SAR signatures. Furthermore, when incorporated into supervised learning frameworks, autoencoders can enhance classifier performance providing richer and more relevant data representation (Goodfellow et al., 2016). Di Martino et al. (2022) also demonstrated the utility of C-AENN in a semi-supervised context to identify and rectify labeling errors in crop type datasets. Unlike CNNs, fully convolutional network (FCN) avoids fully connected layers in favor of convolutional and pooling operations that facilitate pixel level crop classification by learning spatial relationships and generating predictions for each individual pixel in the input image (Long et al., 2015). While Cué La Rosa et al. (2018) and Mullissa et al. (2018) highlighted the superiority of FCN over patch-based 2D-CNNs, Cué La Rosa et al. (2019) have confirmed the superior performance of 3D-CNNs compared to 3D-FCN and traditional ML methods. Classifying pixels independently using FCNs, while considering their spatial pattern, is particularly effective when dealing with high-resolution SAR data where pixel-level classification is critical. In contrast, patch-based 2D-CNNs, which classify patches of pixels, can result in a loss of spatial detail and potentially lower classification accuracy. However, for 3D data, 3D-CNNs, which are capable of learning hierarchical features across both temporal and spatial dimensions, appear to perform better than 3D-FCNs, despite the latter’s ability to model spatio-temporal information. This could be attributed to 3D-CNN’s ability to capture complex temporal patterns and dependencies in time series SAR data, which is crucial for distinguishing crops with similar backscatter characteristics but different temporal behaviors.

The U-Net architecture, a variant of CNNs, has revolutionized the field of semantic segmentation by providing an innovative approach to preserving spatial integrity, which is crucial for accurate crop classification (Ronneberger et al., 2015). U-Net’s unique structure allows it to effectively capture and integrate spatial information and contextual features across different scales. During the contracting/encoding phase, U-Net reduces the spatial dimensions while increasing the number of feature channels. In the expansive/decoding phase, it combines the feature information with the spatial information from the contracting path through skip connections, enabling precise localization of classified pixels (Wenger et al., 2022). This architecture also demonstrates robustness in handling imbalanced datasets, a common challenge in crop classification tasks (L. Ma et al., 2019). Recent advancements in U-Net have further enhanced its performance in crop mapping. Adrian et al. (2021) introduced a 3D U-Net method that learns local spatial and temporal features simultaneously by applying 3D convolution kernels throughout the crop growing season. This approach outperformed 2D U-Net, Squeeze-and-Excitation Residual Network (SegNet) (Badrinarayanan et al., 2017), and Random Forest (RF) models in terms of overall crop mapping accuracy. Following the validation of U-Net’s effectiveness in rice mapping by Wei et al. (2021), Xu et al. (2021) integrated a Conditional Random Field (CRF) with U-Net, significantly improving the accuracy of field boundaries and plot compactness on a large scale.

Attention mechanisms have also been incorporated into U-Net to boost its performance. Ma et al. (2022) proposed an attention-gated U-Net architecture (Oktay et al., 2018) that outperformed DeepLab v3 (Chen et al., 2017), and traditional ML methods in rice mapping accuracy. Furthermore, Wang et al. (2022c) augmented the U-Net model with a SegNet backbone and incorporated Object-Based Image Analysis (OBIA), resulting in high-resolution rice field mapping that surpassed the performance of a U-Net model based on a Residual Networks (ResNet) (Szegedy et al., 2017) backbone. However, in a recent comparative study by Ngo et al. (2023), U-Net with ResNet backbone

surpassed DeepLab-V3 + utilized the Xception network (Chollet, 2017) by 1–3 % in accuracy. Ngo et al. (2023) also evaluated the performance of two widely used ML methods in crop classification, XGBoost (Chen and Guestrin, 2016) and LightGBM (Ke et al., 2017), which employ gradient boosting algorithms. Interestingly, both ML methods achieved an accuracy of 92 %, matching the performance of Linknet (Chaurasia & Culurciello, 2017), a CNN-based model that utilizes ResNet for feature extraction. However, U-Net demonstrated superior performance, surpassing XGBoost, LightGBM, and Linknet in rice mapping accuracy using SAR imagery.

This supremacy of U-Net was challenged by Gargiulo et al. (2020), who demonstrated a 3 % improvement in crop classification using W-Net over U-Net, LinkNet, Feature Pyramid Network (FPN) (T.-Y. Lin et al., 2017), and SegNet (Badrinarayanan et al., 2017) using Sentinel-1. Moreover, W-Net offers advantages in processing time, memory usage, and performance while mitigating the multiplicative speckle effect more efficiently and maintaining fewer parameters despite its additional convolution layers.

The exploration of DL models in crop classification using SAR imagery continues to evolve, with RNNs marking a significant advancement in processing sequential data. Specialized for analyzing multitemporal SAR data, RNNs, particularly Long Short-Term Memory (LSTM) networks and their bidirectional counterparts (Bi-LSTM), have been widely adopted for crop mapping. These models have shown remarkable accuracy in capturing temporal correlations and extracting multi-temporal features from time-series SAR data, significantly outperforming traditional ML approaches in mapping rice crops (de Castro et al., 2020; Wang et al., 2020). The inherent gating mechanism of LSTM allows for selective information retention or discarding within the hidden state layer, effectively addressing long-term dependencies and the challenge of vanishing gradients in input sequences—a common obstacle in traditional RNNs training (Graves, 2012). Building on this foundation, Y. Zhou et al. (2019) leveraged LSTM with GLCM feature extraction to achieve a 5 % boost in OA over traditional ML methods. Despite these advancements, Qu et al. (2020) highlighted the superiority of 1D-CNNs over LSTM in crop classification. Furthermore, Lin et al. (2022) advanced the application of LSTM through Multi-Task Learning for extensive rice mapping, leveraging time-series SAR data from Sentinel-1. Further, scientists started to use a simpler and computationally more efficient variant of RNNs, Gated Recurrent Unit (GRU) that outperformed LSTM in crop classification (Ndikumana et al., 2018; Ni et al., 2022). GRU can effectively model sequential data with fewer gates and parameters compared to LSTM (Cho et al., 2014). Ni et al. (2022) demonstrated that GRU outperformed LSTM and 1D-CNNs in processing temporal data, as well as FCN in modeling spatial polarimetric data. Bidirectional form of LSTM and GRU models process data in both directions—forward and backward—allowing them to incorporate information from both earlier and later data points in the sequence when making prediction. In contrast, Unidirectional-RNNs, process sequential data in a single direction, typically from the beginning of the sequence to the end. Therefore, Bi-LSTM and Bi-GRU surpassed LSTM and GRU in crop classification using SAR imagery (de Castro et al., 2020; Ge et al., 2023; Sun et al., 2022). Additionally, Sun et al. (2022) highlighted the effectiveness of dual-branch BiLSTM (DB-BiLSTM) networks, which demonstrated marked superiority in large-scale rice mapping compared to conventional BiLSTM and RF methods. Ultimately, in a comparative analysis between CNNs and RNNs, Ni et al. (2022) demonstrated the superiority of FCN and 2D-CNNs over RNNs, with GRU outperforming LSTM slightly, and 2D-CNNs excelling beyond FCN. Therefore, scientists started to use hybrid architecture of CNN and RNN variants, e.g., ConvGRU and ConvLSTM, addressing an inherent limitation of LSTM and GRU—the loss of spatial context information when handling images – (Shi et al., 2015). Martinez et al. (2021) and Rogozinski et al. (2022) improved the accuracy of these models by adding Atrous Spatial Pyramid Pooling (ASPP) module to ConvLSTM. Moreover, the integration of the Bi-Tempered Logistic Loss (BiTLL) function during the ConvLSTM

model's training phase enhances its robustness to noise in the training data, making the model less sensitive to outliers or incorrect labels by using temperature settings to modulate logistic loss, thus mitigating the impact of noise. This model achieved high accuracy in rice mapping using Sentinel-1 imagery and surpassed methods like GRU, 3D-CNNs, and basic ConvLSTM (Chang et al., 2022).

Additionally, Rustowicz et al. (2019) demonstrated that a combination of 2D-Unet and ConvLSTM can surpass the performance of 3D-Unet. In this approach, SAR images are initially processed through a U-Net, which enriches the data with detailed spatial context before it is fed into the ConvLSTM. This preprocessing step enhances and structures the spatial features, emphasizing the most relevant information for the task. As a result, the ConvLSTM can more effectively detect and interpret temporal changes, leveraging the improved spatial detail provided by the U-Net.

Since the introduction of the attention mechanism in DL in 2014, its incorporation into various models has markedly enhanced their effectiveness. By enabling models to selectively concentrate on the most pertinent aspects of the input data for a specific task, this dynamic allocation of input features facilitated a more efficient learning of complex patterns and relationships (Bahdanau et al., 2014). Such improvements have been particularly beneficial in advancing the accuracy of crop classification. Notably, the integration of the attention mechanism into LSTM networks has significantly boosted temporal modeling capabilities, leading to state-of-the-art classification performance (Rußwurm & Körner, 2018). Chang et al. (2022) investigated the integration of attention mechanisms into ConvLSTM blocks to focus on specific parts of Sentinel-1 SAR images more relevant for rice field detection. Furthermore, Garnot et al. (2022), Ofori-Ampofo et al. (2021) and Weilandt et al. (2023) proposed a multi-modal crop mapping framework utilizing dense time-series of optical and radar data, combining pixel-set encoder and temporal self-attention (PSE-TAE) to achieve multi-source feature fusion and improve crop mapping accuracy. Similarly, the U-TAE architecture introduced by Garnot and Landrieu, (2021) incorporated the spatial UNet-based architecture into TAE to achieve pixel-level crop mapping from a semantic segmentation perspective.

Further Z. Han et al. (2023) developed spatio-temporal Multi-level Attention (STMA) model for crop mapping that surpassed conventional convolutional models for accurate and generalized crop mapping across various datasets. While 3D U-Net excelled in handling spatial and temporal information with its 3D convolutional kernels, outperforming ConvLSTM, U-TAE, LSTM, and RF, it was surpassed by the STMA. The STMA method, with its multi-level attention mechanism consisting of cascaded spatio-temporal self-attention (STSA) and multi-scale cross-attention (MCA) modules for effective spatio-temporal data processing, especially in noisy datasets, and a novel learnable spatial attention position encoding, demonstrated superior performance in capturing the complex dynamics of crop phenology.

The transformative impact of attention was further amplified with the introduction of the Transformer model in 2017 (Vaswani et al., 2017). The Transformer's novel “self-attention” mechanism marked a significant advancement in DL, particularly beneficial for tasks like crop classification. Unlike previous attention mechanisms that relied on sequential processing, the self-attention mechanism computes attention weights by comparing each element of the input sequence with every other element, allowing the model to determine the relative importance of each data point in the context of the entire sequence. This enables the Transformer to capture long-range dependencies more effectively. Moreover, the Transformer relies solely on the self-attention mechanism, dispensing with recurrent and convolutional layers, allowing for parallel processing of input data and making it more computationally efficient. These features make the Transformer particularly suited for analyzing temporal patterns in crop classification from time-series SAR imagery. However, the Transformer's dependency on large datasets for training poses challenges for its application in scenarios with limited

data availability.

Building upon the success of the Transformer model in natural language processing tasks, researchers have adapted this architecture for visual tasks, giving rise to the Vision Transformer (ViT). ViT interprets images as sequences of patches, offering a more natural approach to handling multiple channels than traditional CNNs. Li et al. (2022c) demonstrated ViT's superior performance in crop classification compared to various models, including 2D-CNNs with Attention (CNN-Att), 2D-CNNs-LSTM (C-LSTM), and LSTM with Attention (LSTM-Att). To further enhance ViT's effectiveness in crop classification tasks, Li et al. (2022c) introduced a hybrid ViT (H-ViT) that incorporates a temporal dimension. This innovative strategy harnesses the spatial feature extraction capabilities of CNNs in the preliminary layers, coupled with the global attention mechanism of Transformers in subsequent stages, enabling comprehensive spatio-temporal analysis. Moreover, Li et al. (2022c) proposed a multi-branch architecture that utilizes self-supervised contrastive learning with ViT to process and integrate data from various sources, outperforming H-ViT in crop classification.

In conclusion, the incorporation of spatio-temporal DL methods has revolutionized crop classification using multi-temporal SAR images, leading to significant improvements in accuracy. Models such as 3D-CNNs and 3D-UNet have showcased their ability to effectively capture both spatial and temporal dependencies, surpassing the performance of traditional 2D approaches. Hybrid CNN-RNN architectures, like ConvLSTM, and the integration of 2D U-Net with ConvLSTM has proven to further boost their performance, enabling them to focus on the most relevant features for the classification task at hand. The introduction of ViT, especially when combined with self-supervised learning techniques, has demonstrated promising results in crop classification by efficiently integrating multi-source data. Moreover, the STMA model, with its innovative attention mechanisms, has excelled in capturing crop phenology dynamics and achieving accurate, generalized crop mapping across various datasets. Despite the demonstrated superiority of these advanced spatio-temporal models, our review reveals that they have been employed in a relatively small number of studies compared to more traditional DL architectures. As illustrated in Fig. 3, LSTM, 2D-CNNs, 1D-CNNs, and 2D-UNet have been utilized in 23, 22, 14 and 11 papers respectively, while ConvLSTM and self-attention mechanisms have been applied in 9 papers each. Transformers and 3D-UNet have been used in 6 and 4 papers, respectively, and the ViT has been explored in only one paper. This disparity in the application of these cutting-edge models highlights the need for future research to further investigate and leverage the potential of spatio-temporal methods for crop classification using SAR imagery.

b. Early-season crop classification

Although a significant volume of research—totaling 60 studies—has thoroughly investigated the use of multiple SAR images for classifying crops at the end of their growing season, the potential for identifying crops during the early stages of growth has received comparatively less attention. Platforms such as Sentinel-1, known for their high temporal resolution (ranging from 6 to 12 days) and minimal delay in data acquisition, present promising opportunities for assessments at the initial stages of crop development. However, the task of identifying crops early in the season presents distinct challenges. The similar appearance of different crops in their early growth phases complicate the task of distinguishing between them. Moreover, variables like surface roughness and SM can influence the backscatter signals in early-season imagery, particularly when the crops have not reached full maturity, thus affecting the precision of early-season mapping across various crop types. As a result, the efficacy of early-season classification varies from one crop to another, highlighting the need for tailored approaches in this application. For instance, Kussul et al. (2018) demonstrated that winter rapeseed, along with spring and summer crops, could be distinguished with high accuracy (>85 %) at least 2 months before harvest. In contrast, crops like winter barley and grassland could not be

reliably discriminated before harvest. Despite these challenges, SAR imaging offers a more viable option for early-season analysis compared to optical imagery. This advantage is particularly evident in regions prone to cloud coverage during this period, which can significantly compromise the quality and usability of optical data. According to Kussul et al. (2018), employing SAR imagery over optical can improve the precision of early-season crop identification by as much as 5 %. Additionally, studies by Weilandt et al. (2023) and Ofori-Ampofo et al. (2021) confirmed that the fusion of SAR and optical datasets surpasses the performance of using either type of data individually for early-season crop classification. Further research by Zhao et al. (2019) revealed that a 1D-CNNs model surpassed LSTM and GRU in early classification while GRU displayed high accuracy earlier than other classifiers for end-season classification. Contrarily, Rußwurm et al. (2023) enhanced LSTM models' capability for early season classification by adding a decision head to evaluate prediction uncertainty. This approach enabled precise classifications of Barley, Wheat, Rapeseed, Orchards, and Corn up to 3 months before harvest, leveraging combined data from Sentinel-1, -2, and Planet satellites for superior accuracy. Further, 2D-CNNs was examined with combination of VH and VV SAR backscatter for early-season classification that let classify Soybean, Fallow, Cotton, Jowar, and Sugarcane 45 days before harvest, albeit with a 3.5 % reduction in accuracy (Paul et al., 2022). Nonetheless, Fontanelli et al. (2022) showcased the superiority of 3D-CNNs compared to 1D- and 2D-CNNs using X-band VV and HH SAR data composition for early-season classification with 98.5 % accuracy one month before harvest. However, they also noted a significant decrease in classification accuracy, by approximately 20 %, when predictions were made three months before the harvest. A recent study by Weilandt et al. (2023) demonstrated that spatio-temporal transfer learning (Sec 4.2) using Transformers alongside a fusion of SAR and optical can classify crops 1 to 3 month prior to harvest. Notably, their model outperformed Heupel et al. (2018) by identifying Barley and Rye at least two months earlier in an unseen year. Their results, consistent with Kondmann et al. (2022), showed that using a CNN-based classification method, Rapeseed and Sugar Beet could be identified at least one month earlier, and Maize three months before harvest, similar to Rußwurm et al. (2023)'s findings.

Moreover, their model detected Wheat two months before harvest, a slight deviation from Heupel et al. (2018) who detected it 3 months prior using optical data. In recent study, Liu et al. (2023) managed to classify tobacco during the mid-growing period with over 85 % accuracy using a combination of VH and VV features alongside an Attention LSTM FCN model.

In conclusion, Simpler DL methods such as 1D-CNNs, GRU, and LSTM have proven effective for early season classification of major crops like corn and rice. For minor crops, however, more complex models like Transformers have showcased its efficacy.

c. Crop rotation mapping

Crop rotation mapping is a complex task that involves predicting the sequence of crops planted in a field over multiple growing seasons. This practice is crucial for sustainable agriculture, as it helps maintain soil health, reduce pest and disease pressure, and optimize nutrient management. Given the sequential nature of crop rotations, DL architectures that can capture temporal patterns and dependencies in time-series data are particularly well-suited for this task.

Among the reviewed literature, Dupuis et al. (2023) employed a Sequence-to-Sequence LSTM (Seq2Seq-LSTM) model alongside SAR data for forecasting field-level crop rotation over multiple years. This Seq2Seq-LSTM model, distinct from traditional LSTM models by its encoder-decoder structure, is specifically designed to handle complex sequence-to-sequence transformations, offering enhanced capability in predicting the sequence of crops over successive periods. It forecasts the likely crops to be planted in future cycles, with predictions further refined through a Conditioned Probability model, showcasing the model's advanced ability to capture temporal patterns and transitions in

crop cultivation practices.

While the application of DL in crop rotation mapping using SAR data is still in its early stages, the potential for temporal and spatio-temporal DL architectures to advance this field is significant.

As discussed in Section 3.2.1a, several temporal and spatio-temporal DL architectures, including LSTM, GRU, ConvLSTM, their combination with attention mechanisms, and Transformers, have shown promising results in crop classification. These architectures have the ability to process and learn from sequential data, making them potential candidates for future research in crop rotation mapping.

d. Mapping of center pivot irrigation system (CPIS)

The study of the temporal dynamics of CPIS, which are influenced by factors such as cropping systems, irrigation practices, and tillage protocols, reveals significant challenges for their detection at a single point in time. However, leveraging multi-temporal SAR images effectively addresses these challenges by facilitating the tracking of changes in shape over time. Three key characteristics of SAR imagery underscore its suitability for CPIS detection. Its ability to penetrate cloud cover, the distinct backscatter signatures reflective of variations in SM, crop types, and growth stages within and outside of the designated areas, and its consistent and comprehensive temporal coverage.

While previous research has investigated the utility of the U-net architecture at the pixel level with optical data for CPIS identification (de Albuquerque et al., 2020; Saraiva et al., 2020), advanced object detection models such as Faster R-CNN and Mask R-CNN were applied to optimal number of SAR observations to detect CPIS (de Albuquerque et al., 2021).

Faster R-CNN introduces a Region Proposal Network (RPN) that streamlines the object detection process by generating region proposals directly from image features. Building on this, Mask R-CNN adds a segmentation mask prediction branch for each Region of Interest, enabling detailed object localization through precise pixel-level segmentation in addition to bounding box identification and object classification. This makes it exceptionally suitable for tasks that require intricate object detailing and effective background differentiation.

Future work in this domain should focus on expanding the methodologies and technologies applied to CPIS detection, leveraging the advancements in SAR imaging with DL models to enhance the accuracy of CPIS mapping.

e. Soil salinity mapping

Given the critical global issue of soil salinization, impacting an estimated 230 million hectares of irrigated land (Metternicht and Zinck, 2003), the need for efficient and accurate monitoring methods is crucial. This is particularly the case in dry seasons when salinity intrusion tends to worsen as river systems undergo significant reductions in water discharges. Such conditions underscore the necessity of meticulous monitoring and management of soil salinity to mitigate its adverse environmental effects (Hoa et al., 2019). RS technology, particularly SAR, offers a cost-effective and promising solution for the acquisition of soil salinity data (Huang et al., 2019). The effectiveness of SAR in soil salinity mapping is particularly attributed to its sensitivity to the soil's dielectric constant, a measure significantly influenced by the soil's moisture content and salinity levels. The dielectric constant, represented as a complex number, comprises real and imaginary components. The imaginary component, crucial for its association with the soil's ability to absorb energy, becomes a pivotal factor in soil salinity detection (Chandrasekaran et al., 2012). This sensitivity has enabled the accurate mapping of soil salinity across varied landscapes, as demonstrated by the correlation of in-field salinity measurements with Radarsat-2 data in semi-arid regions by Barbouchi et al. (2014). While the intersection of SAR and DL in soil salinity detection, is a relatively growing field with few foundational studies such as those by Nurmemet et al. (2018) and Zhang et al. (2020), the potential for future research is vast. These studies, employing quad-polarization and dual-polarization decomposition analyzed through 2D-CNNs and 1D-CNNs respectively, underscore the promise of combining SAR and DL for soil salinity detection.

Future research can build upon the existing groundwork by exploring different SAR data features, incorporating additional SAR frequencies, and examining spatio-temporal DL architectures for more precise detection of soil salinity on a large-scale or worldwide.

3.2.2. Crop monitoring: phenology and biophysical parameters estimation

Crop phenology, which tracks the growth stages of crops from planting to harvest, plays a pivotal role in dynamic crop monitoring (Richardson et al., 2013), precision agriculture (Gao et al., 2017; Jentsch et al., 2009), yield prediction (Yuan et al., 2016), and enhancing agricultural productivity (Jung et al., 2021; Weiss et al., 2020). Moreover, as highlighted in Section 2, the characteristics of SAR data, which include its sensitivity to vegetation biomass, make it a valuable tool for correlating with and indicating the phenological stages of crops (McNairn and Brisco, 2004).

Despite the joint utilization of SAR and optical to estimate BPs and crop growth monitoring (Mercier et al., 2020; Veloso et al., 2017) direct feature stacking has not been successful in exploring the nonlinear complementary relationship between the two data types. This failure is primarily due to the complex nonlinear response exhibited by SAR and optical data in the temporal domain, influenced by crop phenology. ML methods, despite their formidable power across various classification tasks, inherently struggle with temporal sequence data. This limitation can hinder their ability to precisely predict the timing of phenological stages (Lobert et al., 2023). Conversely, DL methods, specifically RNNs, can effectively capture temporal dependencies and dynamics in SAR and optical data. Utilizing LSTM layers within a 1D U-Net has proven effective in estimating different phenology stages of winter wheat by capturing the dynamics in the SAR gamma naught and optical time-series (Lobert et al., 2023).

Recently multi-head attention mechanism employed in RNNs, particularly Transformers, has exhibited superior capabilities in capturing long-range contextual features. The integration of CNNs for features extraction and the fusion of SAR with optical data along with the use of a Transformer model for temporal analysis was explored by Zhao et al. (2022) to enhance the start and end of the growing season detection. Similarly, Thorp and Drajat. (2021) demonstrated the superiority of spatio-temporal DL model, ConvLSTM over Conv2D, LSTM and GRU in detecting/identifying tillering, heading and harvesting stages of paddy rice using SAR and optical fusion. While models integrating spatial and temporal analyses have demonstrated superior accuracy, other studies such as Han et al. (2022) and Hosseini et al. (2019) have applied 2D-CNNs and 1D-CNNs, respectively, for estimating LAI and Canopy Chlorophyll Content (CCC) in winter wheat. These approaches utilize a combination of SAR backscatter data, polarimetric features, and radar vegetation indices to achieve their results.

3.2.3. Yield prediction

Crop yield prediction is of great importance in ensuring food security and meeting the growing demand for crop production (Battude et al., 2016). This is a complex task due to various factors that affect crop yield, such as soil type, weather condition, cultivation practices (e.g., date of sowing, amount of irrigation and fertilizer, etc.), and biotic stress (Dadhwal, 2003). DL-based models are a powerful tool for extracting useful information from raw satellite imagery, enabling accurate crop growth monitoring and yield prediction. These models uniquely bypass the need for directly measuring challenging parameters such as planting schedules, irrigation, fertilizer supply and soil characteristics, traditionally crucial to crop models. Using DL with SAR to predict crop yields represents an emerging area of research, currently evidenced by three published studies. Simple DL methods such as MLP (Tripathi et al., 2022), LSTM (Yu et al., 2023) and DNN with 3–6 hidden layers (Tesfaye et al., 2022) have been used with SAR imagery to predict rice and wheat yield. While Tesfaye et al. (2022) advocated for a fusion of SAR, optical, and meteorological data as the optimal approach for rice yield prediction. In contrast, Tripathi et al. (2022) emphasized the importance of soil

health parameters—SM, Soil Salinity, and Soil Organic Carbon (SOC)—for enhancing wheat yield estimation. While other research indicated LSTM's superiority over ML methods in county-level yield prediction using RS and meteorological data (Barriguinha et al., 2022; Cao et al., 2021), Yu et al. (2023) found that Meta-Learning Ensemble Regression (MLER), an ensemble learning algorithm that integrates predictions from various ML models (Vanschoren, 2018), outperformed LSTM for small datasets and equaled its accuracy for larger ones. Complementing this, Tripathi et al. (2022) underscored the significance of dataset size for MLP's success in yield estimation. They observed that simple regression techniques outperformed MLP for smaller datasets, but an enhanced MLP with additional hidden layers surpassed other ML methods, including OLS, KNN, RF, DT, Ridge regression, and SVR, for larger datasets. Likewise, Tesfaye et al. (2022) illustrated that increasing DNN's hidden layers boosted wheat yield prediction accuracy. This indicates that carefully adding complexity through more hidden layers can uncover more detailed data patterns crucial for yield prediction, thereby enhancing the model's performance.

A recent systematic literature review by Muruganantham et al. (2022) focused on the use of DL and RS for crop yield prediction reported CNNs, LSTM, and ConvLSTM as the most commonly used DL that were used with optical data for yield prediction. 3D-CNNs model was optimal for predicting soybean yield using optical imagery from sources like MODIS (Abbaszadeh et al., 2022; Fernandez-Beltran et al., 2021; Gavahi et al., 2021; Qiao et al., 2021; Russello, 2018; Terliksiz and Altýlar, 2019) and ConvLSTM was superior compared to 2D-CNNs and LSTM in predicting soybean yield using MODIS data, weather information, land surface temperature (LST), and surface reflectance data (Sun et al., 2019b). In a recent study, Hashemi et al. (2024) demonstrated that with a small dataset, 3D-CNNs and XGBoost (a traditional ML method) had comparable performance in maize, soybeans and winter wheat yield estimation.

For future research leveraging advanced DL models such as 3D-CNNs, ConvLSTM, and attention mechanism using Transformers or in combination with the other DL models (was discussed in Mapping/Classification Section, 3.2.1) holds promise for enhancing yield predictions across different crop varieties. However, given the complexity of these models, it is crucial to collect substantial reference data to serve as training datasets.

3.3. Implementation consideration

3.3.1. Data collection and augmentation techniques

Methods for field data collection, such as point observations or plot-based data, frequently encounter difficulties in forming a direct spatial and temporal association with SAR data. This presents a significant challenge when producing adequate reference data for agricultural applications. Most DL studies in classification/mapping applications typically resort to visual interpretation of primary or secondary RS data for reference, or for delineating target classes in a GIS environment. Such interpretations may include identifying individual targets for agricultural object detection (Freudenberg et al., 2019), or demarcating vegetation elements as polygons for semantic or instance segmentation (Kattenborn et al., 2021).

According to our review, several studies utilized visual interpretation using various resources. These included Landsat-8, (de Albuquerque et al., 2021; Wei et al., 2019) fine-resolution RGB images and Pléiades satellite imagery (M. Wang et al., 2022), high-resolution Google Earth images (de Castro et al., 2020), Korea Multi-Purpose Satellite-2 (KOMPSAT-2), IKONOS images, and orthorectified aerial photos (Jo et al., 2020), optical data and physical characteristics (Ge et al., 2023).

Data augmentation, used in 12 % of the studies, enhances the size and diversity of training datasets. By introducing minor alterations or generating synthetic data, this technique improves the network's robustness in classifying unseen data. The literature employed various data augmentation strategies. Rotation and flipping techniques, such as

horizontal, vertical, and 90-degree rotations, were used in studies by (Li et al., 2022c; Rogozinski et al., 2022; Teimouri et al., 2019; Wang et al., 2022c). The addition of noise, specifically Gaussian noise, was a strategy applied in the research by K. Li et al. (2022). Other strategies included solarization, as used by Li et al. (2022c), and scaling or zooming, as employed in the study by Teimouri et al. (2019).

3.3.2. Training and validation

To ensure robustness, transferability, and prevention of overfitting, it's crucial to independently validate DL models before deployment. This ensures that they can effectively generalize beyond specific instances. To this end, supervised DL models require three distinct datasets: training, validation, and testing. The validation dataset is used during model training to tune model parameters, optimize hyperparameters, and implement early stopping mechanisms to mitigating the risk of overfitting, while the test dataset is used post-training to assess the final model's performance. It's essential that this validation doesn't solely depend on iterative shuffling of training and validation data, but rather, is based on entirely independent data unseen by the model. Usually, 20 to 30 % of the reference data is set aside for independent validation and testing. Table A1 in the supplementary material presents the ratios of training, validation, and testing data used in the reviewed papers for various agricultural applications.

4. Challenges

4.1. Challenges in the use of SAR in agriculture

Several challenges must be addressed before SAR observations can be effectively used for feature extraction in DL models:

a) Dynamic Range Management

This involves dealing with the large dynamic range of SAR observations, which could be as high as 90 dB depending on the spatial resolution (Steele-Dunne et al., 2017). Dynamic Range Management in SAR observations is crucial for the stability of DL models like CNNs. These models are designed for data within a certain range (0 and 1 or -1 and 1), and large dynamic ranges can lead to numerical instability, causing issues like exploding or vanishing gradients. This can lead to slower convergence during training or even cause the model to fail to learn from the data. To mitigate this, dynamic compression techniques such as normalization and amplitude value thresholding are employed. Normalization scales data to a standard range, ensuring balanced input features, while amplitude value thresholding clips extreme values, effectively reducing the dynamic range (Metzler et al., 2020; Shi et al., 2022).

b) Speckle Filtering

Speckle effect presents a unique challenge in the analysis of SAR images. Unlike additive noise, speckle is a form of multiplicative interference, which can significantly complicate the extraction of meaningful features from SAR images. Traditional edge and low-level feature detectors, which are typically designed to handle additive noise, may not be optimal for dealing with speckle effect. As such, specific techniques and adaptations are often required to effectively process SAR images. While enhanced speckle filtering techniques can help to mitigate some of the effects of speckle effect, the presence of scatter noise in SAR data remains a significant issue. This can lead to poor model performance, particularly at finer resolutions (e.g., 10 m) (Li et al., 2022b). One common approach to mitigate the impact of speckle effect is to aggregate SAR images to a coarser resolution, such as 30–50 m (typical agricultural plot size). This can help to reduce the impact of speckle effect and improve the performance of subsequent analysis. Incorporating plot-scale data can also help to reduce noise interference and

further improve prediction results (Garioud et al., 2021). In addition to these preprocessing techniques, recent research has also explored the development of robust DL methods that are specifically designed to handle noise and other imperfections in data. One notable example is the combination of CNNs and LSTMs, which has been shown to effectively mitigate the speckle effect in SAR images (Mohan et al., 2021). CNN layers excel in spatially filtering out speckle effect by identifying and preserving essential structural details like edges, while LSTM layers enhance this process by ensuring temporal consistency and coherence across image sequences. This dual approach significantly improves SAR image quality by effectively removing noise while safeguarding critical image features.

Further advancements have been introduced by Dalsasso et al. (2020) initially explored the use of transfer learning from pre-trained denoising models, as well as end-to-end training strategies specifically tailored for SAR despeckling. Building on this foundation, they introduced the SAR2SAR algorithm in 2021, which employs a semi-supervised strategy—starting with training on simulated speckle and then fine-tuning on real SAR image pairs with a change compensation mechanism.

Further innovations include the self-supervised learning approach developed by Dalsasso et al. (2021), which uses a convolutional U-Net architecture to process single-look complex SAR data by exploiting the statistical independence between real and imaginary components. Meraoumia et al. (2023) extended this concept to leverage multiple SAR acquisitions, learning an effective despeckling model without requiring clean ground truth images. Imaging Geometry: The unique range and azimuth coordinates, inherent to the SAR image generation process, pose challenges in terms of processing and data augmentation. The use of rotation as a data augmentation technique could result in distorted imagery due to these unique coordinates. Therefore, careful consideration is required when applying such techniques to SAR data.

c) Phase Component Analysis

The phase component contains valuable information for training the DL model for crop classification and monitoring applications, and careful consideration is necessary when selecting nonlinear activation functions and loss functions. Activation functions introduce nonlinearity into the model, allowing it to learn complex patterns. For processing phase information, the suitability of certain activation functions, such as ReLU, which only handles positive inputs, is limited. They risk ignoring critical phase information that falls below zero. However, normalization application ensures that all phase information is adjusted into a positive range, making it compatible with activation functions like ReLU and safeguarding against the loss of vital data. Loss functions, on the other hand, measure the discrepancy between the model's predictions and the actual values. When dealing with phase information, it's crucial to choose a loss function that can handle the cyclical nature of phase data. Mean Squared Error, for instance, might not be the best choice as it doesn't account for the cyclical nature of phase data, which can lead to inaccuracies. Therefore, the choice of activation functions and loss functions should be made carefully, considering the nature of phase information in SAR data.

d) Orbit Variation

The use of SAR images from both ascending and descending orbits or combination of different sensors can introduce challenges due to varying incidence angles and azimuths between orbits. These differences can cause a periodic “orbit-bias”, requiring extra processing e. g., incidence angle correction algorithm for correcting such orbit effects (Navacchi et al., 2022; Quast et al., 2023). It is worth noting that adding the incidence angle as a feature to the DL algorithm can help reduce the orbit effects. For instance, Han et al. (2022) used local incidence angle as a feature to 2D-CNN to reduce the orbit-bias effect of Sentinel-1 and

Sentinel-3 combination to estimate BPs.

Additionally, the unique imaging principles of SAR introduce complexities in capturing the dynamic scattering characteristics of crops, significantly influenced by factors like irrigation schedules and planting times. These variables can disrupt the temporal consistency of SAR data, posing further challenges to spatio-temporal generalization efforts critical for accurate BPs, yield and agricultural management practices. A promising mitigation strategy involves the fusion of SAR with optical data, leveraging the complementary strengths of both data types to enhance model robustness against these variations.

4.2. Challenges in the use of deep learning in agriculture

DL practitioners in agriculture face a multitude of challenges that can significantly impact the effectiveness of their models. These challenges can be broadly categorized into two main areas: data quality and availability and model design and implementation challenges.

a) Data Quality and Availability Challenges

DL models' success in agriculture depends on the availability of high-quality, well-curated datasets (Zhu et al., 2021). While data augmentation can expand the volume of datasets, publicly available agricultural datasets frequently face limitations, requiring extensive, labor-intensive ground-based data collection efforts. In response to the challenge of scarce labeled data, research has delved into a wide range of strategies. Within this context, numerous studies have investigated how the limited size of reference datasets influences the accuracy of DL models. Advancements in DL methodologies, such as weakly supervised LSTM networks (Wang et al., 2020), Self-Attention Mechanisms (Transformers) (Li et al., 2022b), and Stacked Auto-Encoders (SAE) (Zhang et al., 2023), have demonstrated significant resilience in maintaining model accuracy with substantially reduced dataset size. For instance, innovative approaches have shown that reductions in labeled data by up to 90 % may result in only minimal decreases in accuracy metrics (Wang et al., 2020). For example, employing Transformers has shown good performance maintenance with only 30 % of the training dataset for NDVI construction from SAR data, relevant to crop classification improvements (Li et al., 2022b). Remarkably, SAE-based methods have achieved classification accuracy of 98.6 % with only 2 % of the training dataset, and 94 % accuracy with just 0.5 %, illustrating a critical advancement in the efficient and effective training of DL models (Zhang et al., 2023).

Some other studies have assessed the effectiveness of their developed DL methods for generalization across datasets from various regions and times, spanning both small and large sizes. The Geodesic Distance Spectral Similarity Model (GDSSM) was utilized alongside 1D-CNN to efficiently extract and utilize training samples from a limited dataset (Li et al., 2022a). GDSSM identifies pixels with high similarity to labeled samples, effectively augmenting the amount of training data available.

Furthermore, a Spatial Feature-based Convolutional Neural Network (SF-CNN) incorporating a dual-branch CNN structure was able to process groups of samples rather than individual samples that could expand the training set by combining different samples (Shang et al., 2022). Z. Han et al. (2023) demonstrated the generalization capability of CNNs and Transformers integration handling of multi-scale spatio-temporal features that maintained high accuracy even in regions or where data might be sparse or highly variable.

Another popular technique to mitigate the limitation of scarce labeled data is transfer learning (TL), which enhances the adaptability of DL models to new domains or tasks by utilizing pre-trained models, often referred to as ‘pre-trained backbones’. This method starts with training a model on a vast and varied dataset, known as the source, followed by fine-tuning it for a specific, different domain, termed the target. Studies dealing with transferability of crop mapping models using SAR imagery can be divided roughly into three categories, those dealing with transferability in the temporal domain (Hu et al., 2022; Pandžić et al., 2024), those dealing with transferability in the spatial

domain (Jo et al., 2022) and those dealing with transitioning to a different task (Jo et al., 2022). The combination of these categories, i.e., spatiotemporal transferability as a simultaneous method, is a particularly complex task and thus rarely seen in the literatures (Hao et al., 2020; Weilandt et al., 2023). This technique conserves resources by minimizing the need for extensive training datasets and computational power for the target task. Moreover, it boosts model performance through the strategic use of pre-acquired knowledge. The literature reviewed identified two primary strategies for TL. The 'shallow strategy' uses pre-trained low-level image features, fine-tuning only the final layers of the DL network for task-specific features using relevant imagery. On the other hand, the 'deep strategy' fine-tunes the entire network by back-propagating through all layers of the pre-trained network (Pires de Lima and Marfurt, 2019). However, the choice of layers to fine-tune depends on various factors, including the similarity between the source and target tasks, the complexity of the new task, the amount of available data for the new task, and computational resources. CNNs, known for their ability to identify and utilize hierarchical visual features, are especially adept at this form of learning, making TL a powerful tool for adapting models to new tasks with remarkable efficiency and effectiveness (Kattenborn et al., 2021). Numerous pre-trained backbones are available for popular CNN architectures (Tuia et al., 2016) such as Visual Geometry Group (VGG) (Simonyan and Zisserman, 2014), ResNet (Szegedy et al., 2017), AlexNet (Krizhevsky et al., 2012), Densely Connected Convolutional Networks (DenseNet) (Huang et al., 2017), Inception (Szegedy et al., 2015), and Extreme Inception (Xception) (Chollet, 2017). However, a significant challenge arises when applying these backbones to SAR data. Unlike the 3-channel (RGB) images typically used for training these architectures, SAR datasets are rich in a greater number of features, including backscatter intensity, polarimetric decomposition parameters, coherence measures, radar indices, and observations across different bands. Some potential solutions to this challenge include the use of band selection or feature reduction algorithms (Rezaee et al., 2018). However, these approaches could lead to loss of potentially valuable information, which may affect the model's performance.

Addressing the specific challenges posed by limited labeled data, 3D U-Net was evaluated by Jo et al. (2022) using fine-tuning encoder, decoder, and full model for paddy rice identification across different geographical regions. Among these, fine-tuning the encoder surpassed the other methods in both spatial and task-related TL. Further, Capability of Transformers for spatio-temporal TL for early-season crop classification was explored by Weilandt et al. (2023) using a Pixel-Set Encoder-Temporal Attention Encoder (PSE-TAE) DL model (Garnot et al., 2020). Their conclusion suggests that enhancing the model's adaptability to diverse weather conditions may be attained by including temporal TL and extending the training duration, rather than relying on the integration of weather data. However, Pandžić et al. (2024) showcased the superior performance of CNNs over Transformers and RF models in the context of temporal TL for crop classification, utilizing Sentinel-1 satellite imagery. The application of TL across all three models significantly enhanced classification accuracy within a new domain, with CNNs combined with TL exhibiting the most notable improvement. This outcome highlights the distinct advantage of CNNs in leveraging TL to optimize crop classification results. Consequently, the successful application of temporal TL suggests that it may not be necessary to collect ground truth data annually. The interannual applicability of these trained models holds promise for both predicting future crop type distributions and reconstructing historical ones, as affirmed by Hu et al. (2022).

b) Class Imbalance Challenges

Class imbalance in crop classification is another limitation that needs to be addressed before DL modeling. Yuan et al. (2023) introduced k-positive contrastive loss (KCL) (Kang et al., 2020) to handle imbalanced datasets in crop classification tasks. Specifically, the KCL approach works by randomly selecting K instances of the same crop within a batch

of data to create a set of positive samples, illustrating its practical application in enhancing model performance under class imbalance conditions. If there are fewer than K instances of the same crop in the batch, all instances of that crop are used instead. This approach helps ensure that the model receives enough examples of each class to learn effectively, even when some classes are underrepresented in the dataset. Further, Cué La Rosa et al. (2023) asserted their solution to the class imbalance issue with the introduction of an inventive online deep clustering technique called Learning from Label Proportions with Prototypical Contrastive Clustering (LLP-Co). This approach effectively utilizes government-provided crop proportion data as priors, seamlessly integrating them into a contrastive learning framework. Generative Adversarial Networks (GANs) are a DL method recently applied to generate data for minority classes in crop classification (Mirzaei et al., 2023). A GAN consists of two components: a generator that produces synthetic data and a discriminator that differentiates between synthetic and real data. The generator aims to create data that the discriminator cannot distinguish from real data, improving through adversarial training. However, GANs may struggle with non-Gaussian distributions in tabular data. To address this, Mirzaei et al. (2023) introduced the Conditional Tabular GAN (CTGAN), specifically designed for tabular data. CTGAN supports conditional generation and employs categorical embeddings, making it effective for both continuous and categorical variables. Despite needing substantial training data and being more time-consuming than traditional methods, CTGAN's ability to accurately mirror complex data distributions marks a significant advancement over conventional data generation techniques like Random Under-Sampling (RUS), Random Over-Sampling (ROS), and Synthetic Minority Over-sampling Technique (SMOTE), improving classification performance by 5 % and offering tailored synthetic data creation to better represent minority classes. Resampling and cost-sensitive learning are other techniques that have been used to overcome the issue of imbalanced labeled datasets in the studies by Johnson and Khoshgoftaar. (2019) and Khan et al. (2017).

c) Model Design and Implementation Challenges

Beyond dataset constraints, selecting the optimal network architecture emerges as a pivotal challenge. The decision not only influences a model's ability to discern complex patterns but also its generalization capabilities. This is a delicate balancing act; too complex an architecture risks overfitting with smaller datasets, while too simple a model may underperform with larger or high-dimensional datasets. For example, Crop phenology detection, which involves measuring BPs such as LAI and VWC, generally suffers from limited reference data due to the requirement for destructive in-situ measurements. Consequently, the DL architectures that are appropriate for crop classification may not be optimal for crop phenology detection. Additionally, the impact of hyperparameters on model performance cannot be overstated, yet the practice often defaults to using standard settings, potentially overlooking opportunities to fine-tune models for optimal results.

Training DL models effectively encompasses navigating through a myriad of challenges, such as overfitting, the vanishing or exploding gradient problem, each presenting unique hurdles to model accuracy and generalizability. Overfitting, a common issue with deep architectures, arises from a model's capacity to learn not just the underlying patterns but also the noise within the training data, thereby diminishing its performance on unseen data. This challenge is intricately linked to the structural complexity of DL models and the dimensionality of the input data (Carranza-García et al., 2019).

Parallel to the issue of overfitting is the vanishing and exploding gradient problems, which directly impact the learning process. The vanishing gradient problem slows or halts learning as gradients diminish through layers, while the exploding gradient problem destabilizes learning with excessively large gradients. These issues highlight the delicate balance required in designing and training DL models to ensure stable and effective learning.

Addressing these challenges, a suite of techniques such as

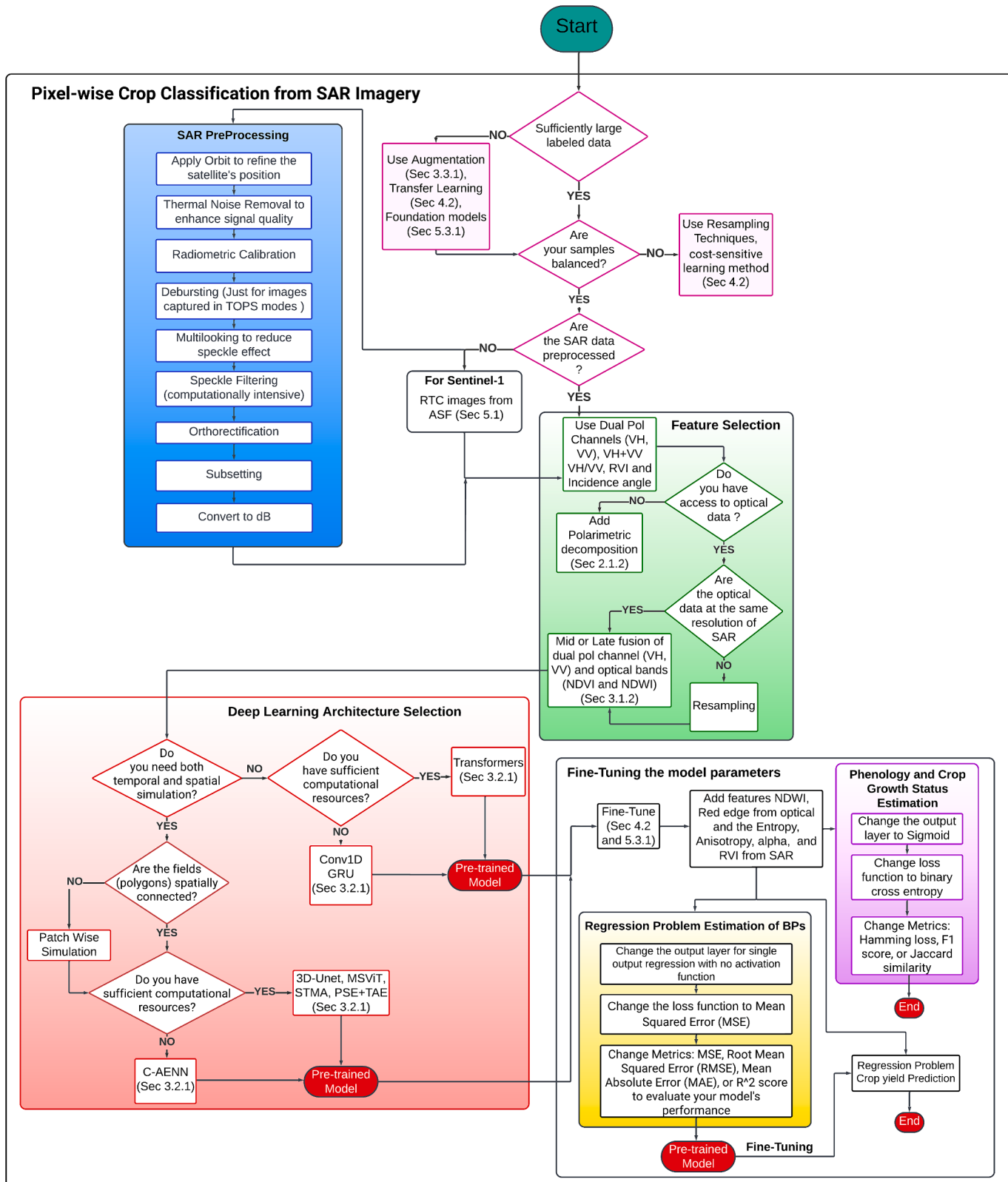


Fig. 5. A flowchart illustrating the integration of SAR and DL for agricultural applications. The flowchart highlights three major components: (1) pixel-wise crop classification from SAR imagery, (2) feature selection, multi-modal fusion, and selection and implementation of appropriate DL architectures, and (3) fine-tuning the crop classification model parameters for robust crop phenology estimation, BPs retrieval, and yield prediction.

regularization, dropout, early stopping, and batch normalization (BN) have been developed to enhance model robustness and prevent overfitting. Regularization adds a penalty to the loss function based on the complexity of the model, encouraging simpler solutions. Dropout randomly “drops out” a number of output features of the layer during training, making the network less reliant on any single feature and more robust to noise in the input data. Early stopping is a form of regularization that halts training when performance on a validation set stops improving, preventing the model from learning noise in the training data. BN is a technique that normalizes the inputs of each layer in a mini batch, reducing internal covariate shift and helping the model generalize better (Mikolajczyk and Grochowski, 2019). Similarly, to combat the vanishing and exploding gradient problems, several techniques have been employed. Activation functions such as Rectified Linear Unit (ReLU), which outputs the input directly if it is positive and zero otherwise, help ensure gradients neither vanish nor explode (Hu et al., 2021). Additionally, gradient clipping is used to prevent gradients from becoming excessively large. Furthermore, the introduction of residual connections, or skip connections, allows gradients to bypass certain layers directly, thus mitigating the vanishing gradient problem (Yahya et al., 2023).

However, the integration of these techniques demands careful consideration to avoid potential adverse interactions, exemplifying the complexity of optimizing DL models. This optimization extends beyond technique selection to encompass implementation costs and the practicalities of model training, which may be hindered by computational or hardware limitations (Chen et al., 2014; Christiansen et al., 2016). Despite these challenges, DL has gained significant popularity owing to various technological advancements. These include efficient data processing techniques, high-performance graphics cards, cloud-computing capabilities, and open data initiatives that offer annotated data. Such developments enable the efficient computation of numerous non-linear transformations of input data, thereby establishing the fundamental strength of DL: its capacity to learn end-to-end (Kattenborn et al., 2021).

5. Opportunities

Despite the advancements in SAR and DL methods for agricultural applications, there are still several gaps and areas that require further exploration. Here are some potential gaps and directions for future work:

5.1. SAR data preprocessing

The Alaska Satellite Facility (ASF) offers Sentinel-1A and Sentinel-1B Radiometrically Terrain Corrected (RTC) products at no cost, developed using the GAMMA software. These products provide a 10-to-30-meter spatial resolution in different scales (decibel, power, and amplitude) and radiometric units (gamma naught and sigma naught) (ASF, 2023).

Additionally, ASF incorporates speckle filtering for these products. Intriguingly, despite the availability of preprocessed Sentinel-1 RTC images, none of the reviewed papers have integrated them with DL techniques in agricultural applications.

5.2. Availability of multi-frequency data from future missions

Notably, spaceborne L-band SAR data availability has been constrained, predominantly sourced from airborne and Advanced Land Observing Satellite (ALOS) PALSAR platforms. These platforms provide data with coarse temporal resolutions, and unlike open-access datasets, they often require specific task submissions for access (Table 1). Our review indicates that, to date, no study has utilized ALOS PALSAR data in conjunction with DL for agricultural applications. Another source, the SMAP mission L-band SAR data, was only accessible for approximately 2.5 months during the summer of 2015. However, the launch of the NASA-ISRO Synthetic Aperture Radar (NISAR) satellite in 2024 and

Radar Observing System for Europe – L-band (ROSE-L) in 2028 brings promising opportunities for utilizing SAR L-band observations (Table 1). With a temporal resolution of 12 days (exact repeat) and a spatial resolution of 10 m, Sentinel-1, NISAR, and ROSE-L enabling the utilization of both C- and L-band data, offering similar spatial and temporal resolutions. The combination of C- and L-band SAR observations may offer significant advantages in crop analysis. Firstly, it can enhance the discrimination and classification of different crop types, particularly during early-season classification when image availability is limited, and the crops’ structures are similar to each other. Integrating C- and L-band SAR data can also improve crop residue and tillage detection. C-band SAR data is sensitive to structural characteristics such as canopy height and biomass, while L-band SAR data responds to moisture content and vegetation water content. Thus, combining these two bands provides a comprehensive understanding of these agricultural management practices. Secondly, the fusion of C- and L-band SAR data can prove to be highly beneficial for phenology and BPs estimation. Each phenological stages exhibits unique radar signatures due to changes in vegetation structure, biomass, and moisture content. By incorporating both C- and L-band SAR data, researchers can more precisely capture these phenological changes, leading to a more accurate representation of crop phenology, yield estimation.

5.3. Emerging applications

5.3.1. Phenology, biophysical parameters, and yield estimation

While SAR has shown promise for crop growth monitoring, BPs estimation, and yield prediction, there is a limited number of studies that have explored the integration of SAR and DL in these areas. The challenge often lies in the DL models’ requirement for extensive training datasets, which are particularly difficult to compile for such specialized applications.

To address this challenge, future research could explore various strategies to enhance the effectiveness of DL models for these applications, even when dealing with limited datasets. Among these strategies are data augmentation (was discussed in Section 3.3.1), transfer learning (was discussed in Section 4.2), and foundation models. Foundation models, which leverage self-supervised learning (SSL) techniques, can be particularly valuable as they do not rely on labeled datasets. Instead, they are pretrained using SSL methods and subsequently fine-tuned for specific tasks with smaller, labeled datasets. Recent advancements have seen the application of foundation models across a range of tasks, utilizing methods like contrastive learning, Masked Autoencoders (MAE), Masked Image Modeling (MIM), DINO, Bootstrap Your Own Latent (BYOL), Momentum Contrast (MoCo), and CACo Loss; along with Seasonal Contrast (SeCo) as SSL methods combined with Transformers or ViT (Wang et al., 2022b) and various RS data types, including SAR, optical, and LiDAR. These applications encompass a wide range of domains, including forest monitoring (Bountos et al., 2023), image segmentation (Fuller et al., 2023), crop mapping (Xu et al., 2024), and land cover classification (Prexl and Schmitt, 2023). Employing these techniques can significantly boost the accuracy and generalizability of models dedicated to yield prediction and BPs estimation, promising substantial progress in the integration of SAR and DL in agricultural monitoring and assessment. Fig. 5 illustrates a comprehensive workflow that integrates SAR data and DL techniques for various agricultural applications, including crop classification, phenology, BPs retrieval, and yield estimation. Since the availability of reference data varies among these applications, with crop type data being more abundant compared to BPs, growth stages, and yield data, the workflow incorporates a fine-tuning step, where the parameters of a pre-trained crop mapping model are adapted to the BPs and yield estimation application. This TL approach leverages the knowledge gained from the crop classification task to improve the performance of the DL models in applications with limited reference data, thereby enhancing the overall effectiveness of the SAR-based DL framework in agricultural

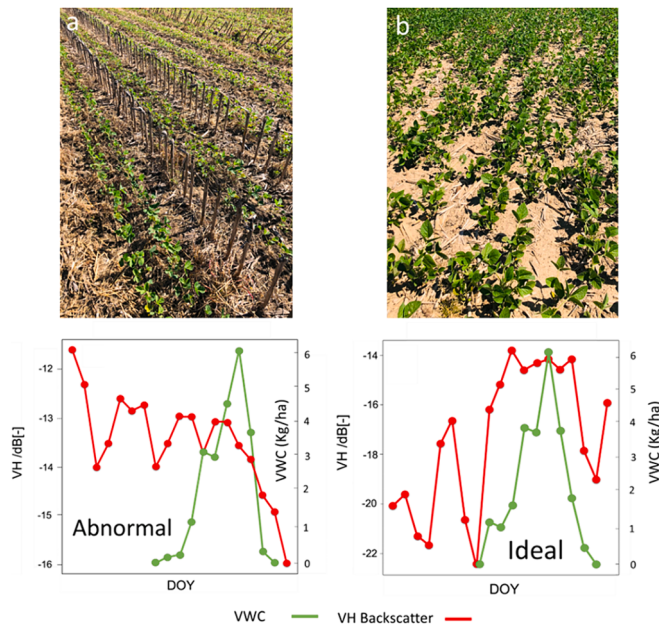


Fig. 6. Impact of crop residues on cross-polarized Sentinel-1 backscatter from a soybean farm and its influence on crop growth cycle monitoring using SAR backscatter time-series. (a) Soybean farm with corn residue. (b) Soybean farm without corn residue (well plowed).

management.

5.3.2. Agricultural management practices detection

a. Planting and harvest dates estimation

Accurate planting and harvest dates estimation is crucial for optimizing crop yields, resource allocation, and adaptation to climate variations. However, traditional crop calendars may not account for dynamic field conditions (Hashemi et al., 2022), highlighting the need for robust, real-time estimation methods using RS data to improve agricultural planning and productivity. Several studies have used the potential of SAR in planting dates estimation (Phan et al., 2018; Shang et al., 2020) and the impact of SAR-based planting dates on estimated crop yield using crop growth models (Hashemi et al., 2022). By integrating DL with SAR data, the estimation of planting and harvest dates becomes more precise and reliable. DL techniques effectively reduce noise and mitigate the effects of varying orbit combinations, enabling the utilization of high temporal resolution SAR data with revisit times of 6 days or less. This enhanced temporal resolution allows for the capture of subtle changes in crop growth and development, leading to more accurate detection of key phenological events such as planting and harvesting.

b. Crop residue and tillage mapping

Crop residue management plays a vital role in maintaining soil health, reducing erosion, increasing fertility, and ensuring agricultural sustainability (Zheng et al., 2014). The determination of timing and variability of tillage across landscapes relies on utilizing multi-temporal imagery to provide a full picture of tillage patterns for a region (Zhang et al., 2012). The cloud-penetrating capabilities of SAR significantly enhance the potential for acquiring sequential imagery. Its sensitivity to surface roughness and moisture makes SAR ideal for mapping crop residue and tillage. Fig. 6 illustrates the impact of corn residues on Sentinel-1 VH backscatter from both a plowed and non-plowed soybean farm. The green line represents the VWC measured every 12 days based on the Sentinel-1 overpass in the summer of 2022 in two different soybean farms in Michigan. In the well-plowed field, the backscatter is consistent with the VWC pattern, indicating the soybean growth cycle. However, the presence of crop residue in the other field has caused abnormal behavior in the VH backscatter. Despite the impact of crop

residue on SAR backscatter, there has been a lack of research investigating its effect on the performance of crop classification/mapping, monitoring, and BPs estimation. Since 2010, only TerraSAR-X (X-band) and Sentinel-1 (C-band) data have been used for conservation tillage monitoring (Zhang et al., 2024). Although the dual-polarization (HH and HV) backscattering coefficients of TerraSAR-X images have been employed to distinguish soil roughness differences due to tillage methods, these SAR observables have shown weak correlations with surface roughness (Pacheco et al., 2010).

In a study by Cai et al. (2019), indices $\sigma_{VV}^0/\sigma_{VH}^0$, and $(\sigma_{VV}^0-\sigma_{VH}^0)/(\sigma_{VV}^0+\sigma_{VH}^0)$ were found to be effective in winter wheat crop residue detection using regression methods. However, with the maximum R^2 value reaching only 0.4, there is a clear need for the application of DL and ML methods to improve accuracy.

To address these limitations and effectively detect and analyze crop residue and tillage practices, future research should focus on developing robust DL algorithms that leverage the potential of SAR data. These algorithms should incorporate ancillary data, such as surface roughness and SM, to enhance the accuracy and reliability of the results. Furthermore, combining different SAR frequencies, such as C and L bands, can provide complementary information and improve the overall performance of crop residue and tillage mapping. By integrating advanced DL techniques, multi-source data fusion, and multi-frequency SAR data, researchers can develop more comprehensive and accurate methods for monitoring and understanding the complex dynamics of crop residue management and tillage practices in agricultural systems.

c. Cover crop mapping

Cover cropping is an essential agricultural practice that plays a vital role in promoting soil health and fertility (Reicosky and Forcella, 1998). By reducing nutrient leaching, cover crops contribute to long-term soil fertility and minimize nitrate losses (De Notaris et al., 2018). Minh et al. (2018) demonstrated the effectiveness of Sentinel-1 σ_{VV}^0 and σ_{VH}^0 in detecting winter cover crop using LSTM and GRU, which outperformed the RF method. Additionally, Najem et al. (2023) highlighted the superiority of multi-level decision trees over RF in both cover crop mapping and the analysis of temporal patterns. While these studies provide valuable insights, there is a pressing need for further research to fully explore the potential of SAR and DL technologies in understanding the complex dynamics of cover cropping, ultimately leading to improved soil health, reduced environmental impact, and increased agricultural sustainability.

d. Grassland mowing

The accurate detection of grassland mowing events holds significant ecological and economic implications, given the multifaceted roles of grasslands (Reinermann et al., 2022). Beyond serving as a primary source of fodder for livestock (Holgrave et al., 2023), grasslands are crucial in delivering a range of ecosystem services, encompassing carbon sequestration (Soussana et al., 2004), water filtration (Jankowska-Huflejt, 2006), and provision of habitats for a myriad of species. A salient challenge in monitoring grassland mowing pertains to the swift regrowth dynamics of grasses, necessitating a high-resolution satellite time-series for precise event identification. In this context, SAR emerges as a valuable tool, adeptly augmenting optical time-series by mitigating observational gaps attributed to cloud interferences. This integration, when synergized with meteorological data, can markedly amplify the precision in detecting mowing events, especially considering the intrinsic association between mowing patterns and specific weather conditions. Several studies have explored the SAR and its fusion with optical data for grassland mowing detection (De Vroey et al., 2021; Holgrave et al., 2023; Reinermann et al., 2022; Schuster et al., 2011; Tamm et al., 2016; Voormansik et al., 2015). Komisarenko et al. (2022) demonstrated the efficacy of employing CNN and LSTM models with an innovative reject region mechanism for the reliable detection of mowing events throughout the growing season, utilizing a blend of optical, InSAR, and PolSAR satellite time-series data. The study highlighted the

Table 2

Open-access Ground reference datasets for crop classification/Mapping.

Product name	Spatial coverage	Time period	Crop type	link	Research Article
EuroCrops (combination of all publicly available self-declared crop reporting datasets)	European countries: Austria, Belgium, Germany, Denmark, Estonia, Spain, France, Croatia, Lithuania, Latvia, Netherlands, Portugal, Romania, Sweden, Slovenia, Slovakia	2015–2022	Meadow, Vineyards, Winter Barley, Barely, Potato, Winter Rye, Summer Barely, Fallow, Vegetables, summer oats, sunflower, soya, Millet, winter Durum, Hops, Berries, Rapeseed, Fodder Roots, Oil seed crops, Maize, wheat, Sorghum	https://github.com/maja601/EuroCrops	(Schneider et al., 2023)
TimeSen2Crop	Austria	2017–2019	16 crop types, Barley, Wheat, Rapeseed, Corn, Sunflower, Orchards, Nuts, Permanent meadows, Temporary meadows, Grassland, Spring cereals, Legumes, Permanent plantations (includes Vineyards, Cherry Plantation, Apricots, Nectarines, Peach, Apples, Pears, and Plums)	https://rslab.disi.unitn.it/timesen2crop/	(Weikmann et al., 2021)
Annual Crop Inventory	Canada	2010–now	More than 16 crop types: Wheat, Barley, Canola, Corn, Soybeans, Oats, Peas, Lentils, Flaxseed, Rye, Potatoes, Beans, Mustard, Sunflowers, Fallow, and Pasture.	https://open.canada.ca/data/en/dataset/ba2645d5-4458-414d-b196-6303ac06c1c9	—
CAWA Crop type dataset	Uzbekistan and Tajikistan	2008, 2011, 2015, 2018	40 crop types and is dominated by “cotton” (40 %) and “wheat”, (25 %). Other crops: rice, maize, orchards, vineyards, alfalfa, potatoes and onions.	https://wuemoca.net/app/	(Remelgado et al., 2020)
Mali Crop Type Training Data-ground	Mali	2019	Maize, Millet, Rice, and Sorghum	https://coldpress.ai/product_page/1671233439301x391910135737130600	(Nakalembe et al., 2021)
Great African Food Company Crop Type	Tanzania	2018	field boundaries and crop types	https://github.com/nasaharvest/cropharvest/blob/main/datasets.md	(Great African Food Company, 2019)
Eyes on the Ground Image Data	Kenya	2019	Georeferenced crop images along with labels on input use, crop management, phenology, crop damage, and yields	https://doi.org/10.34911/rnt.1bs2jw	(Waithaka et al., 2022)
Drone Imagery Classification Training Dataset for Crop Types	Rwanda	2018–2019	19 different land cover types. These land cover types were reduced to three crop types (Banana, Maize, and Legume), two additional non-crop land cover types (Forest and Structure)	https://doi.org/10.34911/rnt.r4p1fr	(Chew et al., 2020; Rineer et al., 2021)
DENETHOR Dataset	Northern Germany	2018–2019	Wheat, Rye, Barley, Oats, Corn, Oil Seeds, Root Crops, Meadows, Forage Crops	https://github.com/lukaskondmann/DENETHOR	(Kondmann et al., 2021)
ZueriCrop	an area of 50 km × 48 km in the Swiss cantons of Zurich and Thurgau	2019	116,000 individual fields spanning 48 crop classes, and 28,000 (multi-temporal) image patches from Sentinel-2	https://polybox.ethz.ch/index.php/s/uXfdr2AcXE3QNB6	(Turkoglu et al., 2021)
BreizhCrops	Brittany region of France	2017	Barley, Wheat, Corn, Fodder, Fallow, Miscellaneous, Orchards, Cereals, Permanent Meadows, Protein Crops, Rapeseed, Temporary Meadows, Vegetables	https://github.com/tum-lmf/BreizhCrops	(Rußwurm et al., 2019)
PlantVillage	Kenya	2020–2023	Cassava, Maize, Potato, Sweet potato, Tomato	https://cmr.earthdata.nasa.gov/search/concepts/C2781412418-MLHUB.html	(PlantVillage, 2019)
CV4A Kenya Crop Type Competition	Kenya	2019	Maize, Cassava, Soybean	https://beta.source.coop/radiantearth/african-crops-kenya-02/	(Kerner et al., 2020)
AgriFieldNet Competition Dataset	Uttar Pradesh, Rajasthan, Odisha and Bihar in northern India	—	13 classes in the dataset including Fallow land and 12 crop types of Wheat, Mustard, Lentil, Green pea, Sugarcane, Garlic, Maize, Gram, Coriander, Potato, Berseem and Rice.	https://beta.source.coop/radiantearth/agrifieldnet-competition/	(Radiant Earth Foundation, 2022)
A Fusion Dataset for Crop Type Classification in Germany	Germany and South Africa	2017(South Africa) 2018–2019 (Germany)	Nine crop types: Wheat, Rye, Barley, Oats, Corn, Oil Seeds, Root Crops, Meadows, Forage Crops	https://cmr.earthdata.nasa.gov/search/concepts/C2781412697-MLHUB.html	(Team, 2022)
World Cereal Project	107 in situ datasets around the world: USA, Canada, Brazil, Sri Lanka, Northern India, Central Asia, Sweden, Estonia, Latvia, Lucas, Europe, Lebanon, Egypt, Senegal, Niger, Mali,	2017–2021	Maize and Cereal including wheat, barley, and rye	https://doi.org/10.5281/zenodo.7875104/	(Van Tricht et al., 2023)

(continued on next page)

Table 2 (continued)

Product name	Spatial coverage	Time period	Crop type	link	Research Article
Burkina Faso, Brazil, Ethiopia, Rwanda, Sudan, Africa, Nigeria, Cameroon, Kenya, Tanzania, Mozambique, Zimbabwe, South Africa, Madagascar					
Crop land USGS. Ground reference	Vietnam, India, USA, Indonesia, Thailand.	2016–2017	Rice, Maize, Barely, Alfalfa, fallow, Sugarcane, Cassava, Soybean, Palm, Cotton	https://www.usgs.gov/apps/croplands/gfsa_dce30info	—
Cropland Data Layer (CDL)-USDA-NASS Campo Verde	US	Annual 1997–now	106 unique crop types	https://nassgeodata.gmu.edu/CropScape/	(Boryan et al., 2011)
Campo Verde	Campo Verde municipality, Mato Grosso state, Brazil.	2015–2016	14 land use classes were detected: soybean, maize, cotton, beans, sorghum, NCC-millet, NCC-crotalaria, NCC-brachiaria, NCC-grasses, pasture, turf grass, eucalyptus, Cerrado	https://dx.doi.org/10.21227/H2804B	(Sanchez et al., 2018)

Table 3

Field campaign vegetation sampling datasets.

Name	SAR Sensor	Time period	SpatialCoverage	SAR Freq	Crop type	Measurements	Reference
Eagle campaign	ESAR	8–18 June 2006	Three sites in the Netherlands (Cabauw, Loobos, Speulderbos)	L, C X	one grass land and two forest area	Land cover type	(Su et al., 2009)
AgriSAR Campaign	ESAR	16 flights in 2006	Northeastern of Germany (DEMMIN test site)	X, C, L	winter wheat, winter raps, winter barley, maize, and sugar beet	Crop type, SM, and in situ measurements of BPs	(Skriver et al., 2011)
SMEX02	PSR and PALS and AIRSAR and GBMR	2002 (fly on 5–8 days)	walnut creek watershed area in Iowa (N: 42.389, S: 41.308, E: -93.017, W: -93.913), Southern Great Plains (SGP) site	C, S, L, P	Soybean and corn, walnut Creek	Vegetation and Land Cover (Plant height, Ground cover, Stand density, Phenology, LAI, Green and dry biomass) Soil Moisture, Surface Temperature, Surface Roughness	(Jackson et al., 2004)
SMEX03	AIRSAR	July 2003 (fly on 6 days)	southern and northern part of Oklahoma around Stillwater and Chickasha (N: 37.02, S: 34.37, E: -97.43, W: -98.39)	C, L and P	Soybean, alfalfa, and corn	Crop height, density, number of leaves, LAI, VWC and soil moisture	(Jackson and McKee, 2007)
SMAPVEX08	PALS	Fall 2008 (fly for 7 days every 1–3 days)	Maryland and Delaware (N: 39.09, S: 38.93, E: -75.55, W: -76.25)	L	Soybean	VWC, LAI and crop type, soil moisture	(Park et al., 2011; NASA, 2008)
SMAPVEX12	PALS and UAVSAR	June to July 2012 (6 days)	Manitoba (N: 50.01, S: 49.32, E: -97.62, W: -98.67)	L	55 Ag-land fields, 5 forested sites, Corn and Soybean, Landcover: cereals (32 %), canola (13 %), corn (7 %), soybean (7 %), grassland & pasture (16 %)	Crop height, stem diameter, number of leaves, VWC, soil moisture, surface roughness	(Fang and Lakshmi, 2014)
SMAPVEX15	AirMOSS and UAVSAR and PALS	August 2015 (every 2–3 days)	Arizona (N: 31.87, S: 31.51, E: -109.84, W: -110.96)–walnut gulch experimental watershed	L	Walnut	Soil moisture, precipitation, vegetation and roughness sampling	(Colliander et al., 2017)
SMAPVEX16	PALS	Summer 2016	Iowa (N: 42.66, S: 42.28, E: 93.21, W: -93.58) and Manitoba (N: 49.79, S: 49.36, E: -97.75, W: -98.12)	L	Corn and Soybean	Crop density, height, and biomass Soil moisture and soil temperature	(NASA, 2016 a,b)

Passive Active L-band System (PALS), The Uninhabited Aerial Vehicle Synthetic Aperture Radar (UAVSAR), Airborne Microwave Observatory of Subcanopy and Subsurface (AirMOSS), National Aeronautics and Space Administration (NASA).

superior performance of CNN and LSTM models over traditional shallow ML methods. Moreover, the study emphasized the critical role of weather data, particularly precipitation, in the successful detection of mowing events. Despite these advancements, there is a notable gap in research that exploits DL in conjunction with SAR data for grassland mowing event detection.

5.4. Training data

The development of DL models for agricultural applications relies heavily on the acquisition of comprehensive and diverse training datasets. To effectively estimate crop phenology, BPs, yield, and detect

agricultural management practices, these datasets must include a wide range of measurements, such as VWC, LAI, canopy surface water, yield metrics, and soil characteristics (e.g., moisture and roughness). However, compiling such datasets is a time-consuming and costly endeavor, presenting significant challenges to researchers and practitioners.

To overcome these challenges, several methodologies have been proposed, including data augmentation, transfer learning, and self-supervised, unsupervised, or weakly supervised learning techniques. While these approaches offer potential solutions, the reliance on pre-trained models that may not be entirely suited for specific agricultural tasks can hamper model performance and limit advancements in the field.

Addressing this issue requires the creation of publicly accessible, extensive, and diverse reference datasets that encompass a variety of agricultural scenarios. Such datasets would greatly facilitate research and development efforts in the application of DL models to agricultural problems. Some European countries have already taken steps towards creating these datasets by mandating farmers to report their cultivar types as a requirement for receiving financial support (Arias et al., 2020). This has led to the development of datasets like EuroCrops (Schneider et al., 2021), ZueriCrop (Turkoglu et al., 2021), BreizhCrops (Rußwurm et al., 2019), and others, which contain hundreds of thousands of labeled parcels and are invaluable for training high-quality ML and DL models. However, assembling a comprehensive, large-scale ground truth database requires involvement from higher public authorities to set guidelines on data collection, storage, usage, and access rights. Establishing these datasets not only aids in developing more precise and efficient models but also supports their evaluation and enhancement. Moreover, access to standardized datasets driven by the community would encourage advancements and innovation in the use of DL with SAR based agricultural applications. Emphasizing this need, we encourage research institutions, academia, and industry stakeholders to collaborate and contribute towards the creation of these reference datasets. Following is a comprehensive overview of all the open-access ground reference datasets for crop classification that is provided in Table 2. Additionally, Table 3 is outlining the field campaign datasets for vegetation sampling, which can be instrumental in collecting training datasets for crop monitoring applications.

6. Conclusion

This comprehensive review has highlighted the transformative impact of SAR with DL on different aspect of agricultural applications. The Sentinel-1 satellite has been the most widely used SAR sensor in agriculture due to its open-access data with continuous temporal coverage. The combination of VH and VV backscatter, along with the inclusion of polarimetric parameters, and SAR indices has significantly enhanced the accuracy of crop classification and monitoring. However, feature selection remains crucial to prevent data redundancy and overfitting problems.

The review revealed that L-band SAR, has not been widely used for monitoring and yield estimation due to the lack of freely accessible data of this sensor. However, the upcoming launches of the NISAR and ROSE-L satellites are expected to bridge this gap by providing L-band SAR data with high temporal and spatial resolution.

End-season crop classification has been extensively covered, and numerous emerging DL methods such as ViT have been developed, leading to improved performance in this application. However, the scarcity of labeled data has hindered the application of DL in crop monitoring and yield prediction. Techniques such as Transfer Learning and self-supervised learning using foundation models can potentially address this issue by enabling the use of smaller datasets. Moreover, future research should focus on exploring the potential of these techniques in early-season crop classification, CPIS, and soil salinity detection, which have received less attention compared to end-season crop classification.

Despite the challenges posed by the limited availability of reference data for training and validation, the integration of SAR with DL continues to revolutionize agricultural applications. Emerging applications, such as mapping crop residue, tillage, and cover crop, as well as detecting grassland mowing and estimating planting and harvest dates, highlight the tremendous potential of SAR with DL in agriculture.

However, to fully harness this potential, the availability of comprehensive training datasets remains a critical bottleneck. Therefore, a concerted effort from the research community is needed to gather and share high-quality, annotated datasets that can support the development of robust DL models for agricultural applications.

CRediT authorship contribution statement

Mahya G.Z. Hashemi: Writing – original draft, Methodology, Investigation, Formal analysis, Data curation, Conceptualization. **Ehsan Jalilvand:** Writing – review & editing, Investigation. **Hamed Aleommahamad:** Writing – review & editing, Methodology, Investigation, Data curation. **Pang-Ning Tan:** Writing – review & editing, Methodology, Investigation. **Narendra N. Das:** Writing – review & editing, Supervision, Investigation, Funding acquisition, Conceptualization.

Declaration of competing interest

The authors declare that they have no known competing financial interests or personal relationships that could have appeared to influence the work reported in this paper.

Acknowledgements

We acknowledge the NASA SERVIR Grant NASA-80NSSC21K0403 and NASA NISAR Science Team Grant NASA-80NSSC21K1181 for this research and review work.

Appendix A. Supplementary material

Supplementary data to this article can be found online at <https://doi.org/10.1016/j.isprsjprs.2024.08.018>.

References

- Abbaszadeh, P., Gavahi, K., Alipour, A., Deb, P., Moradkhani, H., 2022. Bayesian multi-modeling of deep neural nets for probabilistic crop yield prediction. *Agric. Meteorol.* 314, 108773. <https://doi.org/10.1016/j.agrmet.2021.108773>.
- Adrian, J., Sagan, V., Maimaitijiang, M., 2021. Sentinel SAR-optical fusion for crop type mapping using deep learning and Google Earth Engine. *ISPRS J. Photogramm. Remote Sens.* 175, 215–235. <https://doi.org/10.1016/j.isprsjprs.2021.02.018>.
- Alaska Satellite Facility (ASF), 2023. Copernicus Sentinel data. <https://search.asf.alaska.edu/> (accessed 4.6.24).
- Alemohammad, S.H., Konings, A.G., Jagdhuber, T., Moghaddam, M., Entekhabi, D., 2018. Characterization of vegetation and soil scattering mechanisms across different biomes using P-band SAR polarimetry. *Remote Sens Environ* 209, 107–117. <https://doi.org/10.1016/j.rse.2018.02.032>.
- Arias, M., Campo-Bescós, M.Á., Álvarez-Mozos, J., 2020. Crop classification based on temporal signatures of Sentinel-1 observations over Navarre province. Spain. *Remote Sens* 12, 278. <https://doi.org/10.3390/rs12020278>.
- Asadi, B., Shamsoddini, A., 2024. Crop mapping through a hybrid machine learning and deep learning method. *Remote Sens Appl* 33, 101090. <https://doi.org/10.1016/j.rsase.2023.101090>.
- Badrinarayanan, V., Kendall, A., Cipolla, R., 2017. Segnet: a deep convolutional encoder-decoder architecture for image segmentation. *IEEE Trans Pattern Anal Mach Intell* 39, 2481–2495. <https://doi.org/10.1109/TPAMI.2016.2644615>.
- Bahdanau, D., Cho, K., Bengio, Y., 2014. Neural machine translation by jointly learning to align and translate. *arXiv preprint arXiv:1409.0473*. Doi: 10.48550/arXiv.1409.0473.
- Balenzano, A., Mattia, F., Satalino, G., Davidson, M.W.J., 2010. Dense temporal series of C-and L-band SAR data for soil moisture retrieval over agricultural crops. *IEEE J Sel Top Appl Earth Obs Remote Sens* 4, 439–450. <https://doi.org/10.1109/JSTARS.2010.2052916>.
- Bamler, R., Hartl, P., 1998. Synthetic aperture radar interferometry. *Inverse Probl* 14, R1. <https://doi.org/10.1088/0266-5611/14/4/001>.
- Barbouchi, M., Abdelfattah, R., Chokmani, K., Aissa, N.B., Lhissou, R., El Harti, A., 2014. Soil salinity characterization using polarimetric InSAR coherence: case studies in Tunisia and Morocco. *IEEE J. Sel. Top. Appl. Earth Obs. Remote Sens.* 8, 3823–3832. <https://doi.org/10.1109/JSTARS.2014.2333535>.
- Barriguiña, A., Jardim, B., de Castro Neto, M., Gil, A., 2022. Using NDVI, climate data and machine learning to estimate yield in the Douro wine region. *Int. J. Appl. Earth Obs. Geoinf.* 114, 103069. <https://doi.org/10.1016/j.jag.2022.103069>.
- Battude, M., Al Bitar, A., Morin, D., Cros, J., Huc, M., Sicre, C.M., Le Dantec, V., Demarez, V., 2016. Estimating maize biomass and yield over large areas using high spatial and temporal resolution Sentinel-2 like remote sensing data. *Remote Sens Environ* 184, 668–681. <https://doi.org/10.1016/j.rse.2016.07.030>.
- Blaes, X., Defourny, P., Wegmüller, U., Della Vecchia, A., Guerriero, L., Ferrazzoli, P., 2006. C-band polarimetric indexes for maize monitoring based on a validated radiative transfer model. *IEEE Trans. Geosci. Remote Sens.* 44, 791–800. <https://doi.org/10.1109/TGRS.2005.860969>.
- Boryan, C., Yang, Z., Mueller, R., Craig, M., 2011. Monitoring US agriculture: the US department of agriculture, national agricultural statistics service, cropland data layer

- program. *Geocarto Int.* 26, 341–358. <https://doi.org/10.1080/10106049.2011.562309>.
- Bouman, B.A.M., Hoekman, D.H., 1993. Multi-temporal, multi-frequency radar measurements of agricultural crops during the Agriscatt-88 campaign in The Netherlands. *Int. J. Remote Sens.* 14 (8), 1595–1614. <https://doi.org/10.1080/01431169308953988>.
- Boutous, N.I., Quaknine, A., Rolnick, D., 2023. FoMo-Bench: a multi-modal, multi-scale and multi-task Forest Monitoring Benchmark for remote sensing foundation models. arXiv preprint arXiv:2312.10114. Doi: 10.48550/arXiv.2312.10114.
- Brown, C.F., Brumby, S.P., Guzder-Williams, B., Birch, T., Hyde, S.B., Mazzariello, J., Czerwinski, W., Pasquarella, V.J., Haertel, R., Ilyushchenko, S., 2022. Dynamic World, Near real-time global 10 m land use land cover mapping. *Sci Data* 9, 251. <https://doi.org/10.1038/s41597-022-01307-4>.
- Busquier, M., Lopez-Sanchez, J.M., Mestre-Quereda, A., Navarro, E., González-Dugo, M.P., Mateos, L., 2020. Exploring TanDEM-X interferometric products for crop-type mapping. *Remote Sens. (Basel)* 12 (11), 1774. <https://doi.org/10.3390/rs12111774>.
- Busquier, M., Lopez-Sanchez, J.M., Ticconi, F., Floury, N., 2022. Combination of time series of L-, C-, and X-Band SAR images for land cover and crop classification. *IEEE J. Sel. Top. Appl. Earth Obs. Remote Sens.* 15, 8266–8286. <https://doi.org/10.1109/JSTARS.2022.3207574>.
- Cai, W., Zhao, S., Wang, Y., Peng, F., Heo, J., Duan, Z., 2019. Estimation of winter wheat residue coverage using optical and SAR remote sensing images. *Remote Sens.* 11, 1163. <https://doi.org/10.3390/rs11101163>.
- Cameron, W.L., Rais, H., 2006. Conservative polarimetric scatterers and their role in incorrect extensions of the Cameron decomposition. *IEEE Trans. Geosci. Remote Sens.* 44, 3506–3516. <https://doi.org/10.1109/TGRS.2006.879115>.
- Canisius, F., Shang, J., Liu, J., Huang, X., Ma, B., Jiao, X., Geng, X., Kovacs, J.M., Walters, D., 2018. Tracking crop phenological development using multi-temporal polarimetric Radarsat-2 data. *Remote Sens. Environ.* 210, 508–518. <https://doi.org/10.1016/j.rse.2017.07.031>.
- Cao, J., Zhang, Z., Tao, F., Zhang, L., Luo, Y., Zhang, J., Han, J., Xie, J., 2021. Integrating multi-source data for rice yield prediction across China using machine learning and deep learning approaches. *Agric. Meteorol.* 297, 108275 <https://doi.org/10.1016/j.agrmet.2020.108275>.
- Caranza-Garcia, M., García-Gutiérrez, J., Riquelme, J.C., 2019. A framework for evaluating land use and land cover classification using convolutional neural networks. *Remote Sens.* 11, 274. <https://doi.org/10.3390/rs11030274>.
- Chandrasekaran, S., Ramanathan, S., Basak, T., 2012. Microwave material processing—a review. *AIChE J.* 58, 330–363. <https://doi.org/10.1002/aic.12766>.
- Chang, J.G., Shoshany, M., Oh, Y., 2018. Polarimetric radar vegetation index for biomass estimation in desert fringe ecosystems. *IEEE Trans. Geosci. Remote Sens.* 56, 7102–7108. <https://doi.org/10.1109/TGRS.2018.2848285>.
- Chang, Y.-L., Tan, T.-H., Chen, T.-H., Chuah, J.H., Chang, L., Wu, M.-C., Tatini, N.B., Ma, S.-C., Alkhaleefah, M., 2022. Spatial-temporal neural network for rice field classification from SAR images. *Remote Sens.* 14, 1929. <https://doi.org/10.3390/rs14081929>.
- Chaurasia, A., Culurciello, E., 2017. Linknet: Exploiting encoder representations for efficient semantic segmentation. In: 2017 IEEE Visual Communications and Image Processing (VCIP). IEEE, pp. 1–4. Doi: 10.1109/VCIP.2017.8305148.
- Chen, T., Guestrin, C., 2016. Xgboost: A scalable tree boosting system, in: Proceedings of the 22nd ACM SIGKDD International Conference on Knowledge Discovery and Data Mining. pp. 785–794. Doi: 10.1145/2939672.2939785.
- Chen, J.-L., Kuo, C.-C., Chen, L.-G., 2014. Region-of-unpredictable determination for accelerated full-frame feature generation in video sequences. In: 2014 IEEE Visual Communications and Image Processing Conference. pp. 434–437. Doi: 10.1109/VCIP.2014.7051599.
- Chen, L.-C., Papandreou, G., Schroff, F., Adam, H., 2017. Rethinking atrous convolution for semantic image segmentation. Doi: 10.48550/arXiv.1706.05587.
- Chew, R., Rineer, J., Beach, R., O’Neil, M., Ujeneza, N., Lapidus, D., Miano, T., Hegarty-Craver, M., Polly, J., Temple, D.S., 2020. Deep neural networks and transfer learning for food crop identification in UAV images. *Drones* 4, 7. <https://doi.org/10.3390/drones4010007>.
- Cho, K., Van Merriënboer, B., Gulcehre, C., Bahdanau, D., Bougares, F., Schwenk, H., Bengio, Y., 2014. Learning phrase representations using RNN encoder-decoder for statistical machine translation. Doi: 10.48550/arXiv.1406.1078.
- Chollet, F., 2017. Xception: Deep learning with depthwise separable convolutions, in: Proceedings of the IEEE Conference on Computer Vision and Pattern Recognition. pp. 1251–1258. Doi: 10.48550/arXiv.1610.02357.
- Christiansen, P., Nielsen, L.N., Steen, K.A., Jørgensen, R.N., Karstoft, H., 2016. DeepAnomaly: combining background subtraction and deep learning for detecting obstacles and anomalies in an agricultural field. *Sensors* 16, 1904. <https://doi.org/10.3390/s16111904>.
- Cloude, S.R., Pottier, E., 1996. A review of target decomposition theorems in radar polarimetry. *IEEE Trans. Geosci. Remote Sens.* 34, 498–518. <https://doi.org/10.1109/36.485127>.
- Colliander, A., Cosh, M.H., Misra, S., Jackson, T.J., Crow, W.T., Chan, S., Bindlish, R., Chae, C., Collins, C.H., Yueh, S.H., 2017. Validation and scaling of soil moisture in a semi-arid environment: SMAP validation experiment 2015 (SMAPVEX15). *Remote Sens. Environ.* 196, 101–112. <https://doi.org/10.1016/j.rse.2017.04.022>.
- Cué La Rosa, L.E., Happ, P.N., Feitosa, R.Q., 2018. Dense fully convolutional networks for crop recognition from multitemporal SAR image sequences, in: IGARSS 2018–2018 IEEE International Geoscience and Remote Sensing Symposium. IEEE, pp. 7460–7463. Doi: 10.1109/IGARSS.2018.8517995.
- Cué La Rosa, L.E., Queiroz Feitosa, R., Nigri Happ, P., Del’Arco Sanches, I., Ostwald Pedro da Costa, G.A., 2019. Combining deep learning and prior knowledge for crop mapping in tropical regions from multitemporal SAR image sequences. *Remote Sens.* 11, 2029. Doi: 10.3390/rs11172029.
- Cué La Rosa, L.E., Oliveira, D.A.B., Ghamisi, P., 2023. Learning crop type mapping from regional label proportions in large-scale SAR and optical imagery. *IEEE Trans. Geosci. Remote Sens.* <https://doi.org/10.1109/TGRS.2023.3321156>.
- Dadhwal, V.K., 2003. Crop growth and productivity monitoring and simulation using remote sensing and GIS. Satellite remote sensing and GIS applications in agricultural meteorology 263–289. https://www.preventionweb.net/files/1682_9970.pdf#page=263.
- Dalsasso, E., Yang, X., Denis, L., Tupin, F., Yang, W., 2020. SAR image despeckling by deep neural networks: from a pre-trained model to an end-to-end training strategy. *Remote Sens. (Basel)* 12 (16), 2636. <https://doi.org/10.3390/rs12162636>.
- Dalsasso, E., Denis, L., Tupin, F., 2021. As if by magic: self-supervised training of deep despeckling networks with MERLIN. *IEEE Trans. Geosci. Remote Sens.* 60, 1–13. <https://doi.org/10.1109/TGRS.2021.3128621>.
- de Albuquerque, A.O., de Carvalho Júnior, O.A., Carvalho, O.L.F. de, de Bem, P.P., Ferreira, P.H.G., de Moura, R. dos S., Silva, C.R., Trancoso Gomes, R.A., Fontes Guimarães, R., 2020. Deep semantic segmentation of center pivot irrigation systems from remotely sensed data. *Remote Sens.* 12, 2159. Doi: 10.3390/rs12132159.
- de Albuquerque, A.O., de Carvalho, O.L.F., de Bem, P.P., Gomes, R.A.T., Borges, D.L., Guimarães, R.F., Pimentel, C.M.M., de Carvalho Júnior, O.A., 2021. Instance segmentation of center pivot irrigation systems using multi-temporal SENTINEL-1 SAR images. *Remote Sens. Appl.* 23, 100537. Doi: 10.1016/j.rsase.2021.100537.
- Crisóstomo de Castro Filho, H., Abílio de Carvalho Júnior, O., Ferreira de Carvalho, O.L., Pozzobon de Bem, P., dos Santos de Moura, R., Olino de Albuquerque, A., Rosa Silva, C., Guimarães Ferreira, P.H., Fontes Guimarães, R., Trancoso Gomes, R.A., 2020. Rice crop detection using LSTM, Bi-LSTM, and machine learning models from Sentinel-1 time series. *Remote Sens.* 12, 2655. Doi: 10.3390/rs12162655.
- De Notaris, C., Rasmussen, J., Sørensen, P., Olesen, J.E., 2018. Nitrogen leaching: A crop rotation perspective on the effect of N surplus, field management and use of catch crops. *Agric. Ecosyst. Environ.* 255, 1–11. <https://doi.org/10.1016/j.agee.2017.12.009>.
- De Vroeij, M., Radoux, J., Defourny, P., 2021. Grassland mowing detection using sentinel-1 time series: potential and limitations. *Remote Sens.* 13, 348. <https://doi.org/10.3390/rs13030348>.
- Desai, G., Gaikwad, A., 2021. Deep Learning Techniques for Crop Classification Applied to SAR Imagery: A Survey, in: 2021 Asian Conference on Innovation in Technology (ASIANCON). IEEE, pp. 1–6. Doi: 10.1109/ASIANCON51346.2021.9544707.
- den Besten, N., Dunne, S.S., Mahmud, A., Jackson, D., Aquízerats, B., de Jeu, R., Burger, R., Houborg, R., McGlinchey, M., van der Zaag, P., 2023. Understanding Sentinel-1 backscatter response to sugarcane yield variability and waterlogging. *Remote Sensing of Environment* 290, 113555.
- Deschamps, B., McNairn, H., Shang, J., Jiao, X., 2012. Towards operational radar-only crop type classification: comparison of a traditional decision tree with a random forest classifier. *Can. J. Remote. Sens.* 38, 60–68. <https://doi.org/10.5589/m12-012>.
- Di Martino, T., Guinvarc’h, R., Thirion-Lefevre, L., & Koeniguer, E. C. (2021). Beets or cotton? blind extraction of fine agricultural classes using a convolutional autoencoder applied to temporal sar signatures. *IEEE Transactions on Geoscience and Remote Sensing*, 60, 1–18. Doi: 10.1109/TGRS.2021.3100637.
- Di Martino, T., Guinvarc’h, R., Thirion-Lefevre, L., & Colin, E. (2022). FARMSAR: Fixing AgRicultural Mislabels Using Sentinel-1 Time Series and AutoencodeRs. *Remote Sensing*, 15(1), 35. Doi: 10.3390/rs15010035.
- Dobson, M.C., Ulaby, F.T., Hallikainen, M.T., El-Rayes, M.A., 1985. Microwave dielectric behavior of wet soil-Part II: Dielectric mixing models. *IEEE Trans. Geosci. Remote Sens.* 35–46 <https://doi.org/10.1109/TGRS.1985.289498>.
- Dong, J., Xiao, X., Menarguez, M.A., Zhang, G., Qin, Y., Thau, D., Biradar, C., Moore III, B., 2016. Mapping paddy rice planting area in northeastern Asia with Landsat 8 images, phenology-based algorithm and Google Earth Engine. *Remote Sens. Environ.* 185, 142–154. <https://doi.org/10.1016/j.rse.2016.02.016>.
- Drusch, M., Del Bello, U., Carlier, S., Colin, O., Fernandez, V., Gascon, F., Hoersch, B., Isola, C., Laberinti, P., Martimort, P., 2012. Sentinel-2: ESA’s optical high-resolution mission for GMES operational services. *Remote Sens. Environ.* 120, 25–36. <https://doi.org/10.1016/j.rse.2011.11.026>.
- Dupuis, A., Dadouchi, C., Agard, B., 2023. Methodology for multi-temporal prediction of crop rotations using recurrent neural networks. *Smart Agricult. Technol.* 4, 100152 <https://doi.org/10.1016/j.atech.2022.100152>.
- Erten, E., Lopez-Sánchez, J.M., Yuzugullu, O., Hajnsek, I., 2016. Retrieval of agricultural crop height from space: a comparison of SAR techniques. *Remote Sens. Environ.* 187, 130–144. <https://doi.org/10.1016/j.rse.2016.10.007>.
- Fang, B., Lakshmi, V., 2014. Passive/active microwave soil moisture retrieval disaggregation using SMAPVEX12 data. In: Land Surface Remote Sensing II. SPIE, pp. 83–92. Doi: 10.1117/12.2064441.
- Fernandez-Beltran, R., Baidar, T., Kang, J., Pla, F., 2021. Rice-yield prediction with multi-temporal Sentinel-2 data and 3D CNN: a case study in Nepal. *Remote Sens.* 13, 1391. <https://doi.org/10.3390/rs13071391>.
- Ferrazzoli, P., Paloscia, S., Pampaloni, P., Schiavon, G., Sigismonti, S., Solimini, D., 1997. The potential of multifrequency polarimetric SAR in assessing agricultural and arboreal biomass. *IEEE Trans. Geosci. Remote Sens.* 35, 5–17. <https://doi.org/10.1109/36.551929>.
- Fieuza, R., Sicre, C.M., Baup, F., 2017. Estimation of corn yield using multi-temporal optical and radar satellite data and artificial neural networks. *Int. J. Appl. Earth Obs. Geoinf.* 57, 14–23. <https://doi.org/10.1016/j.jag.2016.12.011>.
- Fontanelli, G., Lapini, A., Santurri, L., Pettinato, S., Santi, E., Ramat, G., Pilia, S., Baroni, F., Tapete, D., Cigna, F., 2022. Early-season crop mapping on an agricultural area in Italy using X-band dual-polarization SAR satellite data and convolutional

- neural networks. *IEEE J Sel Top Appl Earth Obs Remote Sens* 15, 6789–6803. <https://doi.org/10.1109/JSTARS2022.3198475>.
- Freeman, A., Durden, S.L., 1998. A three-component scattering model for polarimetric SAR data. *IEEE Trans. Geosci. Remote Sens.* 36, 963–973. <https://doi.org/10.1109/36.673687>.
- Freudenberg, M., Nölke, N., Agostini, A., Urban, K., Wörgötter, F., Kleinn, C., 2019. Large scale palm tree detection in high resolution satellite images using U-Net. *Remote Sens* 11, 312. <https://doi.org/10.3390/rs11030312>.
- Fuller, A., Millard, K., Green, J.R., 2023. CROMA: Remote Sensing Representations with Contrastive Radar-Optical Masked Autoencoders. Doi: 10.48550/arXiv.2311.00566.
- Gao, F., Anderson, M.C., Zhang, X., Yang, Z., Alfieri, J.G., Kustas, W.P., Mueller, R., Johnson, D.M., Prueger, J.H., 2017. Toward mapping crop progress at field scales through fusion of Landsat and MODIS imagery. *Remote Sens Environ* 188, 9–25. <https://doi.org/10.1016/j.rse.2016.11.004>.
- Gargiulo, M., Dell'Aglio, D.A.G., Iodice, A., Riccio, D., Ruello, G., 2020. Integration of sentinel-1 and sentinel-2 data for land cover mapping using w-net. *Sensors* 20, 2969. <https://doi.org/10.3390/s20102969>.
- Garioud, A., Valero, S., Giordano, S., Mallet, C., 2021. Recurrent-based regression of Sentinel time series for continuous vegetation monitoring. *Remote Sens Environ* 263, 112419. <https://doi.org/10.1016/j.rse.2021.112419>.
- Garnot, V.S.F., Landrieu, L., 2021. Panoptic segmentation of satellite image time series with convolutional temporal attention networks. In: Proceedings of the IEEE/CVF International Conference on Computer Vision. pp. 4872–4881. Doi: 10.48550/arXiv.2107.07933.
- Garnot, V.S.F., Landrieu, L., Giordano, S., Chehata, N., 2020. Satellite image time series classification with pixel-set encoders and temporal self-attention. In: Proceedings of the IEEE/CVF Conference on Computer Vision and Pattern Recognition. pp. 12325–12334. Doi: 10.48550/arXiv.1911.07757.
- Garnot, V.S.F., Landrieu, L., Chehata, N., 2022. Multi-modal temporal attention models for crop mapping from satellite time series. *ISPRS J. Photogramm. Remote Sens.* 187, 294–305. <https://doi.org/10.1016/j.isprsjprs.2022.03.012>.
- Gavahi, K., Abbaszadeh, P., Moradkhani, H., 2021. DeepYield: A combined convolutional neural network with long short-term memory for crop yield forecasting. *Expert Syst Appl* 184, 115511. <https://doi.org/10.1016/j.eswa.2021.115511>.
- Ge, J., Zhang, H., Xu, L., Sun, C., Duan, H., Guo, Z., Wang, C., 2023. A Physically interpretable rice field extraction model for PolSAR imagery. *Remote Sens* 15, 974. <https://doi.org/10.3390/rs15040974>.
- Giordano, S., Bailly, S., Landrieu, L., Chehata, N., 2020. Improved crop classification with rotation knowledge using sentinel-1 and-2 time series. *Photogramm Eng Remote Sensing* 86, 431–441. <https://doi.org/10.14358/PERS.86.7.431>.
- Goodfellow, I., Bengio, Y., Courville, A., 2016. Deep learning. The MIT Press. <http://www.deeplearningbook.org>.
- Graves, A., 2012. Long short-term memory. Supervised sequence labelling with recurrent neural networks, PP. 37–45. Doi: 10.1007/978-3-642-24797-2.
- Gu, L., He, F., Yang, S., 2019. Crop classification based on deep learning in northeast China using SAR and optical imagery, in: 2019 SAR in Big Data Era (BGSARDATA). IEEE, pp. 1–4. Doi: 10.1109/BGSARDATA.2019.8858437.
- Great African Food Company*, 2019. *Great African Food Company Tanzania Ground Reference Crop Type Dataset*.
- Guo, J., Li, H., Ning, J., Han, W., Zhang, W., Zhou, Z.-S., 2020. Feature dimension reduction using stacked sparse auto-encoders for crop classification with multi-temporal, quad-pol SAR Data. *Remote Sens* 12, 321. <https://doi.org/10.3390/rs12020321>.
- Guo, Z., Qi, W., Huang, Y., Zhao, J., Yang, H., Koo, V.-C., Li, N., 2022. Identification of crop type based on C-AENN using time series Sentinel-1A SAR data. *Remote Sens* 14, 1379. <https://doi.org/10.3390/rs14061379>.
- Hajnsek, I., Desnos, Y.-L., 2021. Polarimetric synthetic aperture radar principles and application. Springer Nature. <https://doi.org/10.1007/978-3-030-56504-6>.
- Han, D., Wang, P., Tansey, K., Liu, J., Zhang, Y., Zhang, S., Li, H., 2022. Combining Sentinel-1 and-3 imagery for retrievals of regional multitemporal biophysical parameters under a deep learning framework. *IEEE J Sel Top Appl Earth Obs Remote Sens* 15, 6985–6998. <https://doi.org/10.1109/JSTARS2022.3200735>.
- Han, Z., Zhang, C., Gao, L., Zeng, Z., Zhang, B., Atkinson, P.M., 2023. Spatio-temporal multi-level attention crop mapping method using time-series SAR imagery. *ISPRS J. Photogramm. Remote Sens.* 206, 293–310. <https://doi.org/10.1016/j.isprsjprs.2023.11.016>.
- Hao, P., Di, L., Zhang, C., Guo, L., 2020. Transfer Learning for Crop classification with Cropland Data Layer data (CDL) as training samples. *Sci. Total Environ.* 733, 138869. <https://doi.org/10.1016/j.scitotenv.2020.138869>.
- Haralick, R.M., Shanmugam, K., Dinstein, I.H., 1973. Textural features for image classification. *IEEE Trans Syst Man Cybern* 610–621. <https://doi.org/10.1109/TSMC.1973.4309314>.
- Hashemi, M.G.Z., Abhishek, A., Jalilvand, E., Jayasinghe, S., Andreadis, K.M., Siqueira, P., Das, N.N., 2022. Assessing the impact of Sentinel-1 derived planting dates on rice crop yield modeling. *Int. J. Appl. Earth Obs. Geoinf.* 114, 103047. <https://doi.org/10.1016/j.jag.2022.103047>.
- Hashemi, Mahya G.Z., Tan, Pang-Ning, Jalilvand, Ehsan, Wilke, Brook, Alemohammad, Hamed, Das, Narendra N., 2024. Yield estimation from SAR data using patch-based deep learning and machine learning techniques. *Computers and Electronics in Agriculture* 226, 109340. <https://doi.org/10.1016/j.compag.2024.109340>. ISSN 0168-1699.
- Heupel, K., Spengler, D., Itzrotz, S., 2018. A progressive crop-type classification using multitemporal remote sensing data and phenological information. *PFG – Journal of Photogrammetry Remote Sensing and GeoInformation Science* 86, 53–69. <https://doi.org/10.1007/s41064-018-0050-7>.
- Hinton, G.E., Salakhutdinov, R.R., 2006. Reducing the dimensionality of data with neural networks. *Science* 313, 504–507. <https://doi.org/10.1126/science.1127647>.
- Hoa, P.V., Giang, N.V., Binh, N.A., Hai, L.V.H., Pham, T.-D., Hasanlou, M., Tien Bui, D., 2019. Soil salinity mapping using SAR Sentinel-1 data and advanced machine learning algorithms: a case study at Ben Tre Province of the Mekong River Delta (Vietnam). *Remote Sens* 11, 128. <https://doi.org/10.3390/rs11020128>.
- Holtgrave, A.-K., Lobert, F., Erasmi, S., Röder, N., Kleinschmit, B., 2023. Grassland mowing event detection using combined optical, SAR, and weather time series. *Remote Sens Environ* 295, 113680. <https://doi.org/10.1016/j.rse.2023.113680>.
- Hosseini, M., McNairn, H., Mitchell, S., Dingle Robertson, L., Davidson, A., Homayouni, S., 2019. Synthetic aperture radar and optical satellite data for estimating the biomass of corn. *Int. J. Appl. Earth Obs. Geoinf.* 83, 101933. <https://doi.org/10.1016/j.jag.2019.101933>.
- Hu, Y., Zeng, H., Tian, F., Zhang, M., Wu, B., Gilliams, S., Li, S., Li, Y., Lu, Y., Yang, H., 2022. An interannual transfer learning approach for crop classification in the Hetao Irrigation district, China. *Remote Sens* 14, 1208. <https://doi.org/10.3390/rs14051208>.
- Hu, Z., Zhang, J., Ge, Y., 2021. Handling vanishing gradient problem using artificial derivative. *IEEE Access* 9, 22371–22377. <https://doi.org/10.1109/ACCESS.2021.3054915>.
- Huang, G., Liu, Z., Van Der Maaten, L., Weinberger, K.Q., 2017. Densely connected convolutional networks, in: Proceedings of the IEEE Conference on Computer Vision and Pattern Recognition. pp. 4700–4708. Doi: 10.48550/arXiv.1608.06993.
- Huang, J., Gómez-Dans, J.L., Huang, H., Ma, H., Wu, Q., Lewis, P.E., Liang, S., Chen, Z., Xie, J.-H., Wu, Y., 2019. Assimilation of remote sensing into crop growth models: current status and perspectives. *Agric for Meteorol* 276, 107609. <https://doi.org/10.1016/j.agrmet.2019.06.008>.
- Huang, X., Reba, M., Coffin, A., Runkle, B.R.K., Huang, Y., Chapman, B., Ziniti, B., Skakun, S., Kraatz, S., Siqueira, P., Torbick, N., 2021. Cropland mapping with L-band UAVSAR and development of NISAR products. *Remote Sens Environ* 253, 112180. <https://doi.org/10.1016/j.rse.2020.112180>.
- Ienco, D., Interdonato, R., Gaetano, R., Minh, D.H.T., 2019. Combining Sentinel-1 and Sentinel-2 Satellite Image Time Series for land cover mapping via a multi-source deep learning architecture. *ISPRS J. Photogramm. Remote Sens.* 158, 11–22. <https://doi.org/10.1016/j.isprsjprs.2019.09.016>.
- Inoue, Y., Kurosu, T., Maeno, H., Uratsuka, S., Kozu, T., Dabrowska-Zielinska, K., Qi, J., 2002. Season-long daily measurements of multifrequency (Ka, Ku, X, C, and L) and full-polarization backscatter signatures over paddy rice field and their relationship with biological variables. *Remote Sens Environ* 81, 194–204. [https://doi.org/10.1016/S0034-4257\(01\)00343-1](https://doi.org/10.1016/S0034-4257(01)00343-1).
- Inoue, Y., Sakaiya, E., Wang, C., 2014. Capability of C-band backscattering coefficients from high-resolution satellite SAR sensors to assess biophysical variables in paddy rice. *Remote Sens Environ* 140, 257–266. <https://doi.org/10.1016/j.rse.2013.09.001>.
- Jackson, T., McKee, L., 2007. SMEX03 Vegetation Data: Oklahoma, Version 1. Boulder, Colorado USA. NASA National Snow and Ice Data Center Distributed Active Archive Center. Doi: 10.5067/AIE1EWIHPHAO. [Dataset].
- Jackson, T., Bindlish, R., Van der Velde, R., 2004. SMEX02 Airborne Synthetic Aperture Radar (AIRSAR) Data, Iowa. <https://nsidc.org/data/nsidc-0206/versions/1>.
- Jankowska-Huflejt, H., 2006. The function of permanent grasslands in water resources protection. *J. Water Land Dev.* 55–65. <https://doi.org/10.2478/v10025-007-0005-7>.
- Jentsch, A., Keyling, J., Boettcher-Treschkow, J., Beierkuhnlein, C., 2009. Beyond gradual warming: extreme weather events alter flower phenology of European grassland and heath species. *Glob Chang Biol* 15, 837–849. <https://doi.org/10.1111/j.1365-2486.2008.01690.x>.
- Jin, Y., Liu, X., Chen, Y., Liang, X., 2018. Land-cover mapping using Random Forest classification and incorporating NDVI time-series and texture: a case study of central Shandong. *Int. J. Remote Sens.* 39, 8703–8723. <https://doi.org/10.1080/01431161.2018.1490976>.
- Jo, H.-W., Lee, S., Park, E., Lim, C.-H., Song, C., Lee, H., Ko, Y., Cha, S., Yoon, H., Lee, W.-K., 2020. Deep learning applications on multitemporal SAR (Sentinel-1) image classification using confined labeled data: the case of detecting rice paddy in South Korea. *IEEE Trans. Geosci. Remote Sens.* 58, 7589–7601. <https://doi.org/10.1109/TGRS.2020.2981671>.
- Jo, H.-W., Koukos, A., Sitokstantinou, V., Lee, W.-K., Kontoes, C., 2022. Towards Global Crop Maps with Transfer Learning. <https://doi.org/10.48550/arXiv.2211.04755>.
- Johnson, J.M., Khoshgoftaar, T.M., 2019. Survey on deep learning with class imbalance. *J Big Data* 6, 1–54. <https://doi.org/10.1186/s40537-019-0192-5>.
- Judge, J., Liu, P.-W., Monsiváis-Huertero, A., Bongiovanni, T., Chakrabarti, S., Steele-Dunne, S.C., Preston, D., Allen, S., Bermejo, J.P., Rush, P., DeRoo, R., Colliander, A., Cosh, M., 2021. Impact of vegetation water content information on soil moisture retrievals in agricultural regions: an analysis based on the SMAP/VEG-MicroWEX dataset. *Remote Sens. Environ.* 265, 112623. <https://doi.org/10.1016/j.rse.2021.112623>.
- Jung, J., Maeda, M., Chang, A., Bhandari, M., Ashapure, A., Landivar-Bowles, J., 2021. The potential of remote sensing and artificial intelligence as tools to improve the resilience of agriculture production systems. *Curr. Opin. Biotechnol.* 70, 15–22. <https://doi.org/10.1016/j.copbio.2020.09.003>.
- Kamilaris, A., Prenafeta-Boldú, F.X., 2018. A review of the use of convolutional neural networks in agriculture. *J. Agric. Sci.* 156, 312–322. <https://doi.org/10.1017/S0021859618000436>.
- Kang, B., Li, Y., Xie, S., Yuan, Z., Feng, J., 2020. Exploring balanced feature spaces for representation learning. In: International Conference on Learning Representations.

- Katal, N., Rzanny, M., Mäder, P., Wäldchen, J., 2022. Deep learning in plant phenological research: a systematic literature review. *Front. Plant Sci.* 13, 805738. <https://doi.org/10.3389/fpls.2022.805738>.
- Katharopoulos, A., Vyas, A., Pappas, N. and Fleuret, F., 2020, November. Transformers are RNNs: Fast Autoregressive Transformers with Linear Attention. In International conference on machine learning (pp. 5156–5165). PMLR. Doi: 10.48550/arXiv.2006.16236.
- Kattenborn, T., Leitloff, J., Schiefer, F., Hinz, S., 2021. Review on Convolutional Neural Networks (CNN) in vegetation remote sensing. *ISPRS J. Photogramm. Remote Sens.* 173, 24–49. <https://doi.org/10.1016/j.isprsjprs.2020.12.010>.
- Ke, G., Meng, Q., Finley, T., Wang, T., Chen, W., Ma, W., Ye, Q., Liu, T.-Y., 2017. Lightgbm: A highly efficient gradient boosting decision tree. *Adv Neural Inf Process Syst* 30. <https://proceedings.neurips.cc/paper/2017/file/6449f44a102fde848669bdd9eb6b76fa-Paper.pdf>.
- Kerner, H., Nakalembe, C., Becker-Reshef, I., 2020. Field-level crop type classification with k nearest neighbors: A baseline for a new Kenya smallholder dataset. Doi: 10.48550/arXiv.2004.03023.
- Khan, A., Vibhute, A.D., Mali, S., Patil, C.H., 2022. A systematic review on hyperspectral imaging technology with a machine and deep learning methodology for agricultural applications. *Ecol Inform* 101678. <https://research.mitwpu.edu.in/publication/a-systematic-review-on-hyperspectral-imaging-technology-with>.
- Khan, S.H., Hayat, M., Bennamoun, M., Sohel, F.A., Tognoni, R., 2017. Cost-sensitive learning of deep feature representations from imbalanced data. *IEEE Trans Neural Netw Learn Syst* 29, 3573–3587. <https://doi.org/10.1109/TNNLS.2017.2732482>.
- Kim, S.-B., Huang, H., Liao, T.-H., Colliander, A., 2018. Estimating vegetation water content and soil surface roughness using physical models of L-band radar scattering for soil moisture retrieval. *Remote Sens* 10, 556. <https://doi.org/10.3390/rs10040556>.
- Kim, Y., Jackson, T., Bindlish, R., Lee, H., Hong, S., 2011. Radar vegetation index for estimating the vegetation water content of rice and soybean. *IEEE Geosci. Remote Sens. Lett.* 9, 564–568. <https://doi.org/10.1109/LGRS.2011.2174772>.
- Komisarenko, V., Voormanski, K., Elshawi, R., Sakr, S., 2022. Exploiting time series of Sentinel-1 and Sentinel-2 to detect grassland mowing events using deep learning with reject region. *Sci Rep* 12, 983. <https://doi.org/10.1038/s41598-022-04932-6>.
- Kondmann, L., Toker, A., Rußwurm, M., Camero Unzueta, A., Peressutti, D., Milcinski, G., Longépé, N., Mathieu, P.-P., Davis, T., & Marchisio, G. (2021). DENETHOR: The DynamicEarthNET dataset for Harmonized, inter-Operable, analysis-Ready, daily crop monitoring from space. 35th Conference on Neural Information Processing Systems Datasets and Benchmarks Track, 1–13. <https://openreview.net/pdf?id=uUa4jNMLjlR>.
- Kondmann, L., Boeck, S., Bonifacio, R., Zhu, X.X., 2022. Early Crop Type Classification With Satellite Imagery-An Empirical Analysis. https://pml4dc.github.io/iclr2022/pdf/PML4DC_ICLR2022_3.pdf.
- Krizhevsky, A., Sutskever, I., Hinton, G.E., 2012. Imagenet classification with deep convolutional neural networks. *Adv Neural Inf Process Syst* 25. <https://doi.org/10.1145/3065386>.
- Kussul, N., Lavreniuk, M., Skakun, S., Shelestov, A., 2017. Deep learning classification of land cover and crop types using remote sensing data. *IEEE Geosci. Remote Sens. Lett.* 14, 778–782. <https://doi.org/10.1109/LGRS.2017.2681128>.
- Kussul, N., Mykola, L., Shelestov, A., Skakun, S., 2018. Crop inventory at regional scale in Ukraine: developing in season and end of season crop maps with multi-temporal optical and SAR satellite imagery. *Eur. J. Remote Sens.* 51, 627–636. <https://doi.org/10.1080/22797254.2018.1454265>.
- Lee, J.-S., Pottier, E., 2017. Polarimetric radar imaging: from basics to applications. CRC Press. Doi: 10.1201/9781420054989.
- Le Toan, T., Ribbes, F., Wang, L.-F., Floury, N., Ding, K.-H., Kong, J.A., Fujita, M., Kurosu, T., 1997. Rice crop mapping and monitoring using ERS-1 data based on experiment and modeling results. *IEEE Trans. Geosci. Remote Sens.* 35 (1), 41–56.
- Li, J., Li, C., Xu, W., Feng, H., Zhao, F., Long, H., Meng, Y., Chen, W., Yang, H., Yang, G., 2022b. Fusion of optical and SAR images based on deep learning to reconstruct vegetation NDVI time series in cloud-prone regions. *Int. J. Appl. Earth Obs. Geoinf.* 112, 102818. <https://doi.org/10.1016/j.jag.2022.102818>.
- Li, H., Zhang, C., Zhang, S., Ding, X., Atkinson, P.M., 2021. Iterative Deep Learning (IDL) for agricultural landscape classification using fine spatial resolution remotely sensed imagery. *Int. J. Appl. Earth Obs. Geoinf.* 102, 102437. <https://doi.org/10.1016/j.jag.2021.102437>.
- Li, H., Lu, J., Tian, G., Yang, H., Zhao, J., Li, N., 2022a. Crop classification based on GDSSM-CNN using multi-temporal RADARSAT-2 SAR with limited labeled data. *Remote Sens* 14, 3889. <https://doi.org/10.3390/rs14163889>.
- Li, K., Zhao, W., Peng, R., Ye, T., 2022c. Multi-branch self-learning vision transformer (MSViT) for crop type mapping with optical-SAR time-series. *Comput Electron Agric* 203, 107497. <https://doi.org/10.1016/j.compag.2022.107497>.
- Lin, T.-Y., Dollár, P., Girshick, R., He, K., Hariharan, B., Belongie, S., 2017. Feature pyramid networks for object detection, in: Proceedings of the IEEE Conference on Computer Vision and Pattern Recognition. pp. 2117–2125. Doi: 10.1109/CVPR.2017.106.
- Lin, Z., Zhong, R., Xiong, X., Guo, C., Xu, J., Zhu, Y., Xu, J., Ying, Y., Ting, K.C., Huang, J., 2022. Large-scale rice mapping using multi-task spatiotemporal deep learning and Sentinel-1 SAR time series. *Remote Sens* 14, 699. <https://doi.org/10.3390/rs14030699>.
- Liu, J., Li, M., Wang, X., Feng, X., Zhou, J., Zhang, H., 2023. Early Identification of Tobacco Fields Based on Sentinel-1 SAR Images, in: 2023 11th International Conference on Agro-Geoinformatics. IEEE, pp. 1–5. Doi: 10.1109/Agro-Geoinformatics59224.2023.10233334.
- Liu, Y., Zhao, W., Chen, S., Ye, T., 2021. Mapping crop rotation by using deeply synergistic optical and SAR time series. *Remote Sens* 13, 4160. <https://doi.org/10.3390/rs13204160>.
- Lober, F., Löw, J., Schwieder, M., Gocht, A., Schlund, M., Hostert, P., Erasmi, S., 2023. A deep learning approach for deriving winter wheat phenology from optical and SAR time series at field level. *Remote Sens Environ* 298, 113800. <https://doi.org/10.1016/j.rse.2023.113800>.
- Long, J., Shelhamer, E., Darrell, T., 2015. Fully convolutional networks for semantic segmentation, in: Proceedings of the IEEE Conference on Computer Vision and Pattern Recognition. pp. 3431–3440. Doi: 10.1109/CVPR.2015.7298965.
- Lopez-Sanchez, J.M., Ballester-Berman, J.D., 2009. Potentials of polarimetric SAR interferometry for agriculture monitoring. *Radio Sci* 44, 1–20. <https://doi.org/10.1029/2008RS004078>.
- Luo, J., Lv, Y., Guo, J., 2022. Multi-temporal PolSAR Image Classification Using F-SAE-CNN, in: 2022 3rd China International SAR Symposium (CISS). IEEE, pp. 1–5. Doi: 10.1109/CISST5780.2022.9971318.
- Ma, X., Huang, Z., Zhu, S., Fang, W., Wu, Y., 2022. Rice planting area identification based on multi-temporal sentinel-1 SAR images and an attention U-Net model. *Remote Sens* 14. <https://doi.org/10.3390/rs14184573>.
- Ma, L., Liu, Y., Zhang, X., Ye, Y., Yin, G., Johnson, B.A., 2019. Deep learning in remote sensing applications: A meta-analysis and review. *ISPRS J. Photogramm. Remote Sens.* 152, 166–177. <https://doi.org/10.1016/j.isprsjprs.2019.04.015>.
- Ma, C., Zhang, H.H., Wang, X., 2014. Machine learning for Big Data analytics in plants. *Trends Plant Sci* 19, 798–808. <https://doi.org/10.1016/j.tplants.2014.08.004>.
- Magalhães, I.A.L., de Carvalho Júnior, O.A., de Carvalho, O.L.F., de Albuquerque, A.O., Hermucupe, P.M., Merino, É.R., Gomes, R.A.T., Guimarães, R.F., 2022. Comparing machine and deep learning methods for the phenology-based classification of land cover types in the amazon biome using sentinel-1 time series. *Remote Sens* 14, 4858. <https://doi.org/10.3390/rs14194858>.
- Mandal, D., Kumar, V., Ratha, D., Dey, S., Bhattacharya, A., Lopez-Sanchez, J.M., McNairn, H., Rao, Y.S., 2020. Dual polarimetric radar vegetation index for crop growth monitoring using sentinel-1 SAR data. *Remote Sens Environ* 247, 111954. <https://doi.org/10.1016/j.rse.2020.111954>.
- Mandal, D., Bhattacharya, A., Rao, Y.S., 2021. Radar remote sensing for crop biophysical parameter estimation. Springer. <https://doi.org/10.1007/978-981-16-4424-5>.
- Martinez, J.A.C., La Rosa, L.E.C., Feitosa, R.Q., Sanches, I.D., Happ, P.N., 2021. Fully convolutional recurrent networks for multiday crop recognition from multitemporal image sequences. *ISPRS J. Photogramm. Remote Sens.* 171, 188–201. <https://doi.org/10.1016/j.isprsjprs.2020.11.007>.
- Mas, J.F., Flores, J.J., 2008. The application of artificial neural networks to the analysis of remotely sensed data. *Int J Remote Sens* 29, 617–663. <https://doi.org/10.1080/01431160701352154>.
- Mascolo, L., Lopez-Sánchez, J.M., Vicente-Guijalba, F., Mazzarella, G., Nunziata, F., Migliaccio, M., 2015. Retrieval of phenological stages of onion fields during the first year of growth by means of C-band polarimetric SAR measurements. *Int J Remote Sens* 36, 3077–3096. <https://doi.org/10.1080/01431161.2015.1055608>.
- McDonald, A.J., Bennett, J.C., Cookmartin, G., Crossley, S., Morrison, K., Quegan, S., 2000. The effect of leaf geometry on the microwave backscatter from leaves. *Int J Remote Sens* 21, 395–400. <https://doi.org/10.1080/01431160210911>.
- McNairn, H., Shang, J., Jiao, X., Champagne, C., 2009. The contribution of ALOS PALSAR multipolarization and polarimetric data to crop classification. *IEEE Trans. Geosci. Remote Sens.* 47, 3981–3992. <https://doi.org/10.1109/TGRS.2009.2026052>.
- McNairn, H., Brisco, B., 2004. The application of C-band polarimetric SAR for agriculture: A review. *Can. J. Remote Sens.* 30 (3), 525–542.
- McNairn, H., Kross, A., Lapen, D., Caves, R., Shang, J., 2014. Early season monitoring of corn and soybeans with TerraSAR-X and RADARSAT-2. *Int. J. Appl. Earth Obs. Geoinf.* 28, 252–259. <https://doi.org/10.1016/j.jag.2013.12.015>.
- Mei, X., Nie, W., Liu, J., Huang, K., 2018. PolSAR image crop classification based on deep residual learning network, in: 2018 7th International Conference on Agro-Geoinformatics. IEEE, pp. 1–6. Doi: 10.1109/Agro-Geoinformatics.2018.8476061.
- Meraoumia, I., Dalsasso, E., Denis, L., Abergel, R., Tupin, F., 2023. Multitemporal speckle reduction with self-supervised deep neural networks. *IEEE Trans. Geosci. Remote Sens.* 61, 1–14. <https://doi.org/10.1109/TGRS.2023.3237466>.
- Mercier, A., Betbeder, J., Rapinel, S., Jegou, N., Baudry, J., Hubert-Moy, L., 2020. Evaluation of Sentinel-1 and 2 time series for estimating LAI and biomass of wheat and rapeseed crop types. *J Appl Remote Sens* 14, 24512. <https://doi.org/10.1117/1.JRS.14.024512>.
- Mestre-Quereda, A., Lopez-Sánchez, J.M., Vicente-Guijalba, F., Jacob, A.W., Engdahl, M. E., 2020. Time-series of Sentinel-1 interferometric coherence and backscatter for crop-type mapping. *IEEE J Sel Top Appl Earth Obs Remote Sens* 13, 4070–4084. <https://doi.org/10.1109/JSTARS.2020.3008096>.
- Metternicht, G.I., Zinck, J.A., 2003. Remote sensing of soil salinity: potentials and constraints. *Remote Sens Environ* 85, 1–20. [https://doi.org/10.1016/S0034-4257\(02\)00188-8](https://doi.org/10.1016/S0034-4257(02)00188-8).
- Metzler, C.A., Ikoma, H., Peng, Y., Wetzelstein, G., 2020. Deep optics for single-shot high-dynamic-range imaging, in: Proceedings of the IEEE/CVF Conference on Computer Vision and Pattern Recognition. pp. 1375–1385. Doi: 10.48550/arXiv.1908.00620.
- Mikolajczyk, A., Grochowski, M., 2019. Style transfer-based image synthesis as an efficient regularization technique in deep learning, in: 2019 24th International Conference on Methods and Models in Automation and Robotics (MMAR). IEEE, pp. 42–47. Doi: 10.48550/arXiv.1905.10974.
- Minh, D.H.T., Ienco, D., Gaetano, R., Lalanne, N., Ndikumana, E., Osman, F., Maurel, P., 2018. Deep recurrent neural networks for winter vegetation quality mapping via multitemporal SAR Sentinel-1. *IEEE Geosci. Remote Sens. Lett.* 15, 464–468. <https://doi.org/10.48550/arXiv.1708.03694>.

- Mirzaei, A., Bagheri, H., Khosravi, I., 2023. Enhancing crop classification accuracy through synthetic SAR-optical data generation using deep learning. *ISPRS Int J Geoinf* 12, 450. <https://doi.org/10.3390/ijgi12110450>.
- Mohan, E., Rajesh, A., Sunitha, G., Kondu, R.M., Avanija, J., Ganesh Babu, L., 2021. A deep neural network learning-based speckle noise removal technique for enhancing the quality of synthetic-aperture radar images. *Concurr Comput* 33, e6239.
- Mullissa, A.G., Persello, C., Tolpekin, V., 2018. Fully convolutional networks for multi-temporal SAR image classification. In: *IGARSS 2018–2018 IEEE International Geoscience and Remote Sensing Symposium* (pp. 6635–6638). IEEE. Doi: 10.1109/IGARSS.2018.8518780.
- Muruganantham, P., Wibowo, S., Grandhi, S., Samrat, N.H., Islam, N., 2022. A systematic literature review on crop yield prediction with deep learning and remote sensing. *Remote Sens* 14, 1990. <https://doi.org/10.3390/rs14091990>.
- Najem, S., Baghdadi, N., Bazzi, H., Lalande, N., Bouchet, L., 2023. Detection and mapping of cover crops using sentinel-1 SAR remote sensing data. *IEEE J Sel Top Appl Earth Obs Remote Sens.* <https://doi.org/10.1109/JSTARS.2023.3337989>.
- Nakalembe, C.L., O.H., D.N., & K.B., 2021. 2019 Mali Crop Type Training Data for Machine Learning. Radiant MLHub. Doi: 10.34911/rndt.tgz68o.
- NASA, 2008. Soil Moisture Active Passive Validation Experiment 2008 (SMAPVEX08) In Situ Vegetation Data. Version 1. <https://nsidc.org/data/sm08v/versions/1/>.
- NASA, 2016a. Soil Moisture Active Passive Validation Experiment 2016 (SMAPVEX16) Iowa PALS Brightness Temperature and Soil Moisture Data. Version 1. <https://nsidc.org/data/sm08v/versions/1>. [Dataset].
- NASA, 2016b. Soil Moisture Active Passive Validation Experiment 2016 (SMAPVEX16) Manitoba In Situ Vegetation Data. Version 1. https://nsidc.org/data/sm16m_v/versions/1. [Dataset].
- Nasirzadehdizaji, R., Balik Sanli, F., Abdikan, S., Cakir, Z., Sekertekin, A., Ustuner, M., 2019. Sensitivity analysis of multi-temporal Sentinel-1 SAR parameters to crop height and canopy coverage. *Appl. Sci.* 9, 655. <https://doi.org/10.3390/app9040655>.
- Navaracchia, C., Cao, S., Bauer-Marschallinger, B., Snoeij, P., Small, D., Wagner, W., 2022. Utilising Sentinel-1's orbital stability for efficient pre-processing of sigma nought backscatter. *ISPRS J. Photogramm. Remote Sens.* 192, 130–141. <https://doi.org/10.1016/j.isprsjprs.2022.07.023>.
- Navarro, A., Rolim, J., Miguel, I., Catalão, J., Silva, J., Painho, M., Vekerdy, Z., 2016. Crop monitoring based on SPOT-5 Take-5 and sentinel-1A data for the estimation of crop water requirements. *Remote Sens. (Basel)* 8 (6), 525. <https://doi.org/10.3390/rs8060525>.
- Ndikumana, E., Ho Tong Minh, D., Baghdadi, N., Courault, D., Hossard, L., 2018. Deep recurrent neural network for agricultural classification using multitemporal SAR Sentinel-1 for Camargue, France. *Remote Sens* 10, 1217. Doi: 10.3390/rs10081217.
- Ngo, T.X., Bui, N.B., Phan, H.D.T., Ha, H.M., Nguyen, T.T.N., 2023. Paddy rice mapping in Red River Delta, Vietnam, using Sentinel 1/2 data and machine learning algorithms. *J. Spat Sci* 1–17. <https://doi.org/10.1080/14498596.2023.2174196>.
- Nguyen, D.B., Gruber, A., Wagner, W., 2016. Mapping rice extent and cropping scheme in the Mekong Delta using Sentinel-1A data. *Remote Sensing Letters* 7, 1209–1218. <https://doi.org/10.1080/2150704X.2016.1225172>.
- Ni, J., López-Martínez, C., Hu, Z., Zhang, F., 2022. Multitemporal SAR and polarimetric SAR optimization and classification: reinterpreting temporal coherence. *IEEE Trans. Geosci. Remote Sens.* 60, 1–17. <https://doi.org/10.1109/tgrs.2022.3214097>.
- Nurmement, I., Sagan, V., Ding, J.-L., Halik, Ü., Abliz, A., Yakup, Z., 2018. A WFS-SVM model for soil salinity mapping in keria oasis, northwestern china using polarimetric decomposition and fully PolSAR data. *Remote Sens* 10, 598. <https://doi.org/10.3390/rs10040598>.
- Ofori-Ampofo, S., Pelletier, C., Lang, S., 2021. Crop type mapping from optical and radar time series using attention-based deep learning. *Remote Sens* 13, 4668. <https://doi.org/10.3390/rs13224668>.
- Oktay, O., Schlemper, J., Folgoc, L., Le, Lee, M., Heinrich, M., Misawa, K., Mori, K., McDonagh, S., Hammerla, N.Y., Kainz, B., 2018. Attention u-net: Learning where to look for the pancreas. Doi: 10.48550/arXiv.1804.03999.
- Olimov, B., Subramanian, B., Ugli, R.A.A., Kim, J.-S., Kim, J., 2023. Consecutive multiscale feature-based image classification model. *Sci Rep* 13, 3595. <https://doi.org/10.1038/s41598-023-30480-8>.
- Oquab, M., Bottou, L., Laptev, I., Sivic, J., 2014. Learning and transferring mid-level image representations using convolutional neural networks, in: *Proceedings of the IEEE Conference on Computer Vision and Pattern Recognition*. pp. 1717–1724. Doi: 10.1109/CVPR.2014.222.
- Oveis, A.H., Giusti, E., Ghio, S., Martorella, M., 2022. A survey on the applications of convolutional neural networks for synthetic aperture radar: recent advances. *IEEE Aerosp. Electron. Syst. Mag.* 37, 18–42. <https://doi.org/10.1109/MAES.2021.3117369>.
- Pacheco, A.M., McNairn, H., Merzouki, A., 2010. Evaluating TerraSAR-X for the identification of tillage occurrence over an agricultural area in Canada, in: *Remote Sensing for Agriculture, Ecosystems, and Hydrology XII*. SPIE, pp. 156–162. Doi: 10.1117/12.868218.
- Pandžić, M., Pavlović, D., Matavulj, P., Brdar, S., Marko, O., Crnojević, V., Kilibarda, M., 2024. Interseasonal transfer learning for crop mapping using Sentinel-1 data. *Int. J. Appl. Earth Obs. Geoinf.* 128, 103718. <https://doi.org/10.1016/j.jag.2024.103718>.
- Parikh, H., Patel, S., Patel, V., 2020. Classification of SAR and PolSAR images using deep learning: a review. *Int. J. Image Data Fusion* 11, 1–32. <https://doi.org/10.1080/19479832.2019.1655489>.
- Park, J., Johnson, J.T., Majurec, N., Niamsuwan, N., Piepmeyer, J.R., Mohammed, P.N., Ruf, C.S., Misra, S., Yueh, S.H., Dinardo, S.J., 2011. Airborne L-band radio frequency interference observations from the SMAPVEX08 campaign and associated flights. *IEEE Trans. Geosci. Remote Sens.* 49, 3359–3370. <https://doi.org/10.1109/TGRS.2011.2107560>.
- Paul, S., Kumari, M., Murthy, C.S., Nagesh Kumar, D., 2022. Generating pre-harvest crop maps by applying convolutional neural network on multi-temporal Sentinel-1 data. *Int. J. Remote Sens.* 43, 6078–6101. <https://doi.org/10.1080/01431161.2022.2030072>.
- Periasamy, S., 2018. Significance of dual polarimetric synthetic aperture radar in biomass retrieval: an attempt on Sentinel-1. *Remote Sens. Environ.* 217, 537–549. <https://doi.org/10.1016/j.rse.2018.09.003>.
- Phalke, A.R., Özdogan, M., 2018. Large area cropland extent mapping with Landsat data and a generalized classifier. *Remote Sens. Environ.* 219, 180–195. <https://doi.org/10.1016/j.rse.2018.09.025>.
- Phan, H., Le Toan, T., Bouvet, A., Nguyen, L.D., Pham Duy, T., Zribi, M., 2018. Mapping of rice varieties and sowing date using X-band SAR data. *Sensors* 18, 316. <https://doi.org/10.3390/s18010316>.
- Pires de Lima, R., Marfurt, K., 2019. Convolutional neural network for remote-sensing scene classification: Transfer learning analysis. *Remote Sens* 12, 86. <https://doi.org/10.3390/rs12010086>.
- PlantVillage, 2019. PlantVillage Kenya Ground Reference Crop Type Dataset. Version 1.0. Radiant MLHub. Doi: 10.34911/RDNT.U41J87. [Dataset].
- Prexl, J., Schmitt, M., 2023. Multi-Modal Multi-Objective Contrastive Learning for Sentinel-1/2 Imagery, in: *Proceedings of the IEEE/CVF Conference on Computer Vision and Pattern Recognition*. pp. 2135–2143. Doi: 10.3390/rs15164102.
- Qiao, M., He, X., Cheng, X., Li, P., Luo, H., Tian, Z., Guo, H., 2021. Exploiting hierarchical features for crop yield prediction based on 3-D convolutional neural networks and multikernel Gaussian process. *IEEE J. Sel. Top. Appl. Earth Obs. Remote Sens.* 14, 4476–4489. <https://doi.org/10.1109/JSTARS.2021.3073149>.
- Qu, Y., Zhao, W., Yuan, Z., Chen, J., 2020. Crop mapping from sentinel-1 polarimetric time-series with a deep neural network. *Remote Sens* 12, 2493. <https://doi.org/10.3390/rs12152493>.
- Quast, R., Wagner, W., Bauer-Marschallinger, B., Vreugdenhil, M., 2023. Soil moisture retrieval from Sentinel-1 using a first-order radiative transfer model—a case-study over the Po-Valley. *Remote Sens Environ.* 295, 113651. <https://doi.org/10.1016/j.rse.2023.113651>.
- Radiant Earth Foundation & IDInsight., 2022. AgriFieldNet Competition Dataset, Version 1.0. Radiant MLHub. <https://beta.source.coop/radiantearth/agrifieldnet-competition/>.
- Raney, R.K., Cahill, J.T.S., Patterson, G.W., Bussey, D.B.J., 2012. The m-chi decomposition of hybrid dual-polarimetric radar data with application to lunar craters. *J Geophys Res Planets* 117. Doi: 10.1029/2011JE003986.
- Reicosky, D.C., Forcella, F., 1998. Cover crop and soil quality interactions in agroecosystems. *J Soil Water Conserv* 53(3), pp.224–229. <https://link.gale.com/apps/doc/A21170093/AONE?u=anon~bc52b7&sid=googleScholar&xid=f194559d>.
- Reinermann, S., Gessner, U., Asam, S., Ullmann, T., Schucknecht, A., Kuenzer, C., 2022. Detection of grassland mowing events for Germany by combining Sentinel-1 and Sentinel-2 time series. *Remote Sens* 14, 1647. <https://doi.org/10.3390/rs14071647>.
- Remelgado, R., Zaitov, S., Kenjabaev, S., Stolina, G., Sultanov, M., Ibrakhimov, M., Akhmedov, M., Dukhovny, V., Conrad, C., 2020. A crop type dataset for consistent land cover classification in Central Asia. *Sci Data* 7, 250. <https://doi.org/10.1038/s41597-020-00591-2>.
- Rezaee, M., Mahdianpari, M., Zhang, Y., Salehi, B., 2018. Deep convolutional neural network for complex wetland classification using optical remote sensing imagery. *IEEE J. Sel. Top. Appl. Earth Obs. Remote Sens.* 11, 3030–3039. <https://doi.org/10.1109/JSTARS.2018.2846178>.
- Richardson, A.D., Keenan, T.F., Migliavacca, M., Ryu, Y., Sonnentag, O., Toomey, M., 2013. Climate change, phenology, and phenological control of vegetation feedbacks to the climate system. *Agric. Meteorol.* 169, 156–173. <https://doi.org/10.1016/j.agrmet.2012.09.012>.
- Rineer, J., Beach, R., Lapidus, D., O'Neil, M., Temple, D., Ujeneza, N., Cajka, J., & Chew, R., 2021. Drone imagery classification training dataset for crop types in Rwanda. Version 1. [Dataset]. <https://radiantearth.blob.core.windows.net/mlhub/rti-rwanda-crop-type/documentation.pdf>.
- Rogozinski, M., Martinez, J.A.C., Feitosa, R.Q., 2022. 3D convolution for multiday crop recognition from multitemporal image sequences. *Int. J. Remote Sens.* 43, 6056–6077. <https://doi.org/10.1080/01431161.2021.1976876>.
- Ronneberger, O., Fischer, P., Brox, T., 2015. U-net: Convolutional networks for biomedical image segmentation, in: *Medical Image Computing and Computer-Assisted Intervention—MICCAI 2015: 18th International Conference, Munich, Germany, October 5–9, 2015, Proceedings, Part III* 18. Springer, pp. 234–241. Doi: 10.48550/arXiv.1505.04597.
- Rosen, P.A., Hensley, S., Jouglard, I.R., 2000. F. k. Li, SN Madsen, E. Rodriguez et R. Goldstein: Synthetic aperture radar interferometry. *Proceedings of the IEEE* 88, 333–382. Doi: 10.1109/5.838084.
- Romero-Puig, N., Lopez-Sanchez, J.M., 2021. A review of crop height retrieval using InSAR strategies: Techniques and challenges. *IEEE J. Select. Topics Appl. Earth Observ. Remote Sens.* 14, 7911–7930.
- Roy, D.P., Wuider, M.A., Loveland, T.R., Woodcock, C.E., Allen, R.G., Anderson, M.C., Helder, D., Irons, J.R., Johnson, D.M., Kennedy, R., 2014. Landsat-8: Science and product vision for terrestrial global change research. *Remote Sens Environ.* 145, 154–172. <https://doi.org/10.1016/j.rse.2014.02.001>.
- Russello, H., 2018. Convolutional neural networks for crop yield prediction using satellite images. *IBM Center for Advanced Studies.* <https://api.semanticscholar.org/CorpusID:51786849>.
- Rußwurm, M., County, N., Emonet, R., Lefevre, S., Tuia, D., Tavenard, R., 2023. End-to-end learned early classification of time series for in-season crop type mapping. *ISPRS*

- J. Photogramm. Remote Sens. 196, 445–456. <https://doi.org/10.1016/j.isprsjprs.2022.12.016>.
- Rußwurm, M., Lefèvre, S., Körner, M., 2019. Breizhcrops: A satellite time series dataset for crop type identification, in: Proceedings of the International Conference on Machine Learning Time Series Workshop. Doi: 10.48550/arXiv.1905.11893.
- Rußwurm, M., Körner, M., 2018. Multi-temporal land cover classification with sequential recurrent encoders. ISPRS Int J Geoinf 7, 129. <https://doi.org/10.3390/ijgi7040129>.
- M. Rustowicz, R., Cheong, R., Wang, L., Ermon, S., Burke, M., Lobell, D., 2019. Semantic segmentation of crop type in Africa: A novel dataset and analysis of deep learning methods, in: Proceedings of the IEEE/CVF Conference on Computer Vision and Pattern Recognition Workshops. pp. 75–82. http://openaccess.thecvf.com/content_CVPRW_2019/papers/cv4gc/Rustowicz_Semantic_Segmentation_of_Crop_Type_in_Africa_A_Novel_Dataset_CVPRW_2019_paper.pdf.
- Ryu, D., Lee, S.-G., 2023. Mapping Vegetation Water Content over Agricultural Landscapes Using Satellite C-and X-Band Synthetic Aperture Radar, in: IGARSS 2023–2023 IEEE International Geoscience and Remote Sensing Symposium. IEEE, pp. 399–402. Doi: 10.1109/IGARSS52108.2023.10282451.
- Saadat, M., Seydi, S.T., Hasanolou, M., Homayouni, S., 2022. A convolutional neural network method for rice mapping using time-series of sentinel-1 and sentinel-2 imagery. Agriculture 12, 2083. <https://doi.org/10.3390/agriculture12122083>.
- Saleem, M.H., Potgieter, J., Arif, K.M., 2021. Automation in agriculture by machine and deep learning techniques: A review of recent developments. Precis Agric 22, 2053–2091. <https://link.springer.com/article/10.1007/s11119-021-09806-x>.
- Sanches, I.D., Feitosa, R.Q., Diaz, P.M.A., Soares, M.D., Luiz, A.J.B., Schultz, B., Maurano, L.E.P., 2018. Campo verde database: Seeking to improve agricultural remote sensing of tropical areas. IEEE Geosci. Remote Sens. Lett. 15, 369–373. <https://doi.org/10.1109/LGRS.2017.2789120>.
- Schneider, M., Broszeit, A., Körner, M., 2021. Eurocrops: A pan-european dataset for time series crop type classification. Doi: 10.48550/arXiv.2106.08151.
- Schneider, M., Schelte, T., Schmitz, F., Körner, M., 2023. EuroCrops: All you need to know about the Largest Harmonised Open Crop Dataset Across the European Union. Doi: 10.1038/s41597-023-02517-0.
- Saraiva, M., Protas, É., Salgado, M., Souza Jr., C., 2020. Automatic mapping of center pivot irrigation systems from satellite images using deep learning. Remote Sensing 12 (3), 558.
- Schuster, C., Ali, I., Lohmann, P., Frick, A., Förster, M., Kleinschmit, B., 2011. Towards detecting swath events in TerraSAR-X time series to establish NATURA 2000 grassland habitat swath management as monitoring parameter. Remote Sens 3, 1308–1322. <https://doi.org/10.3390/rs3071308>.
- Shang, J., Liu, J., Poncos, V., Geng, X., Qian, B., Chen, Q., Dong, T., Macdonald, D., Martin, T., Kovacs, J., 2020. Detection of crop seeding and harvest through analysis of time-series Sentinel-1 interferometric SAR data. Remote Sens 12, 1551. <https://doi.org/10.3390/rs12101551>.
- Shang, R., Wang, J., Jiao, L., Yang, X., Li, Y., 2022. Spatial feature-based convolutional neural network for PolSAR image classification. Appl Soft Comput 123, 108922. <https://doi.org/10.1016/j.asoc.2022.108922>.
- Shi, X., Chen, Z., Wang, H., Yeung, D.-Y., Wong, W.-K., Woo, W., 2015. Convolutional LSTM network: A machine learning approach for precipitation nowcasting. Adv Neural Inf Process Syst 28. Doi: 10.48550/arXiv.1506.04214.
- Sharma, P.K., Kumar, P., Srivastava, H.S., Sivasankar, T., 2022. Assessing the potentials of multi-temporal sentinel-1 SAR data for paddy yield forecasting using artificial neural network. Journal of the Indian Society of Remote Sensing 50 (5), 895–907.
- Shi, H., Sheng, Q., Wang, Y., Yue, B., Chen, L., 2022. Dynamic range compression self-adaption method for SAR image based on deep learning. Remote Sens 14, 2338. <https://doi.org/10.3390/rs14102338>.
- Simonyan, K., Zisserman, A., 2014. Very deep convolutional networks for large-scale image recognition. Doi: 10.48550/arXiv.1409.1556.
- Sivasankar, T., Kumar, D., Srivastava, H.S., Patel, P., 2018. Advances in radar remote sensing of agricultural crops: a review. Int. J. Adv. Sci. Eng. Inf. Technol 8, 1126–1137. <https://doi.org/10.18517/ijaseit.8.4.5797>.
- Skakun, S., Kussul, N., Shelestov, A.Y., Lavreniuk, M., Kussul, O., 2015. Efficiency assessment of multitemporal C-band Radarsat-2 intensity and Landsat-8 surface reflectance satellite imagery for crop classification in Ukraine. IEEE J. Sel. Top. Appl. Earth Obs. Remote Sens. 9, 3712–3719. <https://doi.org/10.1109/JSTARS.2015.2454297>.
- Skriver, H., Mattia, F., Satalino, G., Balenzano, A., Pauwels, V.R.N., Verhoest, N.E.C., Davidson, M., 2011. Crop classification using short-revisit multitemporal SAR data. IEEE J. Sel. Top. Appl. Earth Obs. Remote Sens. 4, 423–431. <https://doi.org/10.1109/JSTARS.2011.2106198>.
- Small, D., 2011. Flattening gamma: radiometric terrain correction for SAR imagery. IEEE Trans. Geosci. Remote Sens. 49, 3081–3093. <https://doi.org/10.1109/TGRS.2011.2120616>.
- Sonobe, R., 2019. Parcel-based crop classification using multi-temporal TerraSAR-X dual polarimetric data. Remote Sens 11, 1148. <https://doi.org/10.3390/rs11101148>.
- Sonobe, R., Yamaya, Y., Tani, H., Wang, X., Kobayashi, N., Mochizuki, K., 2017. Assessing the suitability of data from Sentinel-1A and 2A for crop classification. Gisci. Remote Sens. 54, 918–938. <https://doi.org/10.1080/15481603.2017.1351149>.
- Soudani, K., le Maire, G., Dufrêne, E., François, C., Delpierre, N., Ulrich, E., Cecchini, S., 2008. Evaluation of the onset of green-up in temperate deciduous broadleaf forests derived from Moderate Resolution Imaging Spectroradiometer (MODIS) data. Remote Sens. Environ. 112, 2643–2655. <https://doi.org/10.1016/j.rse.2007.12.004>.
- Soussana, J., Loiseau, P., Vuichard, N., Ceschia, E., Balesdent, J., Chevallier, T., Arrouays, D., 2004. Carbon cycling and sequestration opportunities in temperate grasslands. Soil Use Manage. 20, 219–230. <https://doi.org/10.1111/j.1475-2743.2004.tb00362.x>.
- Steele-Dunne, S.C., McNairn, H., Monsvais-Huertero, A., Judge, J., Liu, P.-W., Papathanassiou, K., 2017. Radar remote sensing of agricultural canopies: a review. IEEE J. Sel. Top. Appl. Earth Obs. Remote Sens. 10, 2249–2273. <https://doi.org/10.1109/JSTARS.2016.2639043>.
- Su, Z., Timmermans, W.J., Van Der Tol, C., Dost, R., Bianchi, R., Gómez, J.A., House, A., Hajnsek, I., Menenti, M., Magliulo, V., 2009. EAGLE 2006—Multi-purpose, multi-angle and multi-sensor in-situ and airborne campaigns over grassland and forest. Hydrol Earth Syst. Sci. 13 (833–845), 2009. <https://doi.org/10.5194/hess-13-833-2009>.
- Sun, C., Bian, Y., Zhou, T., Pan, J., 2019a. Using of multi-source and multi-temporal remote sensing data improves crop-type mapping in the subtropical agriculture region. Sensors 19, 2401. <https://doi.org/10.3390/s19102401>.
- Sun, J., Di, L., Sun, Z., Shen, Y., Lai, Z., 2019b. County-level soybean yield prediction using deep CNN-LSTM model. Sensors 19, 4363. <https://doi.org/10.3390/s19204363>.
- Sun, C., Zhang, H., Ge, J., Wang, C., Li, L., Xu, L., 2022. Rice mapping in a subtropical hilly region based on Sentinel-1 time series feature analysis and the dual branch BiLSTM model. Remote Sens 14, 3213. <https://doi.org/10.3390/rs14133213>.
- Szegedy, C., Liu, W., Jia, Y., Sermanet, P., Reed, S., Anguelov, D., Erhan, D., Vanhoucke, V., Rabinovich, A., 2015. Going deeper with convolutions. In: Proceedings of the IEEE Conference on Computer Vision and Pattern Recognition. pp. 1–9. Doi: 10.1109/CVPR.2015.7298594.
- Szegedy, C., Ioffe, S., Vanhoucke, V., Alemi, A., 2017. Inception-v4, inception-resnet and the impact of residual connections on learning. In: Proceedings of the AAAI Conference on Artificial Intelligence. Doi: 10.1609/aaai.v31i1.11231.
- Tamm, T., Zalite, K., Voormansik, K., Talgre, L., 2016. Relating Sentinel-1 interferometric coherence to mowing events on grasslands. Remote Sens 8, 802. <https://doi.org/10.3390/rs8100802>.
- Team, P.F., 2022. Planet Fusion Monitoring Technical Specification, Version 1.0. 0. San Francisco, CA. <https://support.planet.com/hc/en-us/articles/440629528673-Planet-Fusion-Monitoring-Technical-Specification.html>.
- Teimouri, N., Dyrmann, M., Jørgensen, R.N., 2019. A novel spatio-temporal FCN-LSTM network for recognizing various crop types using multi-temporal radar images. Remote Sens 11, 990. <https://doi.org/10.3390/rs11080990>.
- Teimouri, M., Mokhtarzade, M., Baghdadi, N., Heipke, C., 2022. Fusion of time-series optical and SAR images using 3D convolutional neural networks for crop classification. Geocarto Int 37 (27), 15143–15160. <https://doi.org/10.1080/10106049.2022.2095446>.
- Terlikisz, A.S., Altýlar, D.T., 2019. Use of deep neural networks for crop yield prediction: A case study of soybean yield in lauderdale county, alabama, usa, in: 2019 8th International Conference on Agro-Geoinformatics. IEEE, pp. 1–4. Doi: 10.1109/Agro-Geoinformatics.2019.8820257.
- Tesfaye, A.A., Awoke, B.G., Sida, T.S., Osgood, D.E., 2022. Enhancing smallholder wheat yield prediction through sensor fusion and phenology with machine learning and deep learning methods. Agriculture 12, 1352. <https://doi.org/10.3390/agriculture12091352>.
- Thorp, K.R., Drajat, D., 2021. Deep machine learning with Sentinel satellite data to map paddy rice production stages across West Java, Indonesia. Remote Sens. Environ. 265, 112679. <https://doi.org/10.1016/j.rse.2021.112679>.
- Togliatti, K., Lewis-Beck, C., Walker, V.A., Hartman, T., VanLoocke, A., Cosh, M.H., Hornbuckle, B.K., 2022. Quantitative Assessment of satellite L-band vegetation optical depth in the U.S. Corn belt. IEEE Geosci. Remote Sens. Lett. 19, 1–5. <https://doi.org/10.1109/LGRS.2020.3034174>.
- Torres, R., Snoejij, P., Geudtner, D., Bibby, D., Davidson, M., Attema, E., Potin, P., Rommen, B., Flouri, N., Brown, M., Traver, I.N., 2012. GMES Sentinel-1 mission. Remote Sens. Environ. 120, 9–24. <https://doi.org/10.1016/j.rse.2011.05.028>.
- Tripathi, A., Tiwari, R.K., Tiwari, S.P., 2022. A deep learning multi-layer perceptron and remote sensing approach for soil health based crop yield estimation. Int. J. Appl. Earth Obs. Geoinf. 113, 102959. <https://doi.org/10.1016/j.jag.2022.102959>.
- Trudel, M., Charbonneau, F., Leconte, R., 2012. Using RADARSAT-2 polarimetric and ENVISAT-ASAR dual-polarization data for estimating soil moisture over agricultural fields. Can. J. Remote. Sens. 38, 514–527. <https://doi.org/10.5589/m12-043>.
- Tuia, D., Persello, C., Bruzzone, L., 2016. Domain adaptation for the classification of remote sensing data: an overview of recent advances. IEEE Geosci. Remote Sens. Mag. 4, 41–57. <https://doi.org/10.1109/MGRS.2016.2548504>.
- Turkoglu, M.O., D'Arconio, S., Perich, G., Liebsch, F., Streit, C., Schindler, K., Wegner, J. D., 2021. Crop mapping from image time series: deep learning with multi-scale label hierarchies. Remote Sens Environ. 264, 112603. <https://doi.org/10.48550/arXiv.2102.08820>.
- Ulaby, F.T., Dubois, P.C., Van Zyl, J., 1996. Radar mapping of surface soil moisture. J. Hydrol. 184 (1–2), 57–84. [https://doi.org/10.1016/0022-1694\(95\)02968-0](https://doi.org/10.1016/0022-1694(95)02968-0).
- Vali, A., Comai, S., Matteucci, M., 2020. Deep learning for land use and land cover classification based on hyperspectral and multispectral earth observation data: a review. Remote Sens 12, 2495. <https://doi.org/10.3390/rs12152495>.
- Van Tricht, K., Degerickx, J., Gilliams, S., Zanaga, D., Battude, M., Grosu, A., Bomback, J., 2023. WorldCereal: a dynamic open-source system for global-scale, seasonal, and reproducible crop and irrigation mapping. Earth Syst. Sci. Data Discuss. 2023, 1–36. <https://doi.org/10.5194/essd-15-5491-2023>.
- Vanschoren, J., 2018. Meta-learning: A survey. Doi: 10.48550/arXiv.1810.03548.
- Vaswani, A., Shazeer, N., Parmar, N., Uszkoreit, J., Jones, L., Gomez, A.N., Kaiser, L., Polosukhin, I., 2017. Attention is all you need. Adv. Neural Inf. Process. Syst. 30 <https://doi.org/10.48550/arXiv.1706.03762>.
- Veloso, A., Mermoz, S., Bouvet, A., Le Toan, T., Planells, M., Dejoux, J.-F., Ceschia, E., 2017. Understanding the temporal behavior of crops using Sentinel-1 and Sentinel-2.

- like data for agricultural applications. *Remote Sens. Environ.* 199, 415–426. <https://doi.org/10.1016/j.rse.2017.07.015>.
- Vicente-Guijalba, F., Martinez-Marín, T., Lopez-Sanchez, J.M., 2014. Dynamical approach for real-time monitoring of agricultural crops. *IEEE Trans. Geosci. Remote Sens.* 53, 3278–3293. <https://doi.org/10.1109/TGRS.2014.2372897>.
- Victor, B., He, Z., Nibali, A., 2022. A systematic review of the use of Deep Learning in Satellite Imagery for Agriculture. Doi: 10.48550/arXiv.2210.01272.
- Villarroyo-Carpio, A., Lopez-Sanchez, J.M., Engdahl, M.E., 2022. Sentinel-1 interferometric coherence as a vegetation index for agriculture. *Remote Sens. Environ.* 280, 113208 <https://doi.org/10.1016/j.rse.2022.113208>.
- Voormansik, K., Jagdhuber, T., Zalite, K., Noorma, M., Hajnsek, I., 2015. Observations of cutting practices in agricultural grasslands using polarimetric SAR. *IEEE J. Sel. Top. Appl. Earth Obs. Remote Sens.* 9, 1382–1396. <https://doi.org/10.1109/JSTARS.2015.2503773>.
- Waithaka, L., Kramer, B., Hufkens, K., Kivuva, B., & Mansabdar, S., 2022. Eyes on the Ground Image Data, Version 1.0, (Version 1.0) Radiant MLHub. Doi: 10.34911/rndt.1bs2jw.
- Wang, D., Cao, W., Zhang, F., Li, Z., Xu, S., Wu, X., 2022a. A review of deep learning in multiscale agricultural sensing. *Remote Sens.* 14, 559. <https://doi.org/10.3390/rs14030559>.
- Wang, M., Wang, J., Chen, L., 2020. Mapping paddy rice using weakly supervised long short-term memory network with time series Sentinel optical and SAR images. *Agriculture* 10, 483. <https://doi.org/10.3390/agriculture10100483>.
- Wang, M., Wang, J., Cui, Y., Liu, J., Chen, L., 2022c. Agricultural field boundary delineation with satellite image segmentation for high-resolution crop mapping: a case study of rice paddy. *Agronomy* 12. <https://doi.org/10.3390/agronomy12102342>.
- Wang, J., Wang, P., Tian, H., Tansey, K., Liu, J., Quan, W., 2023. A deep learning framework combining CNN and GRU for improving wheat yield estimates using time series remotely sensed multi-variables. *Comput. Electron Agric.* 206, 107705. <https://doi.org/10.1016/j.compag.2023.107705>.
- Wang, Y., Zhang, Z., Feng, L., Ma, Y., Du, Q., 2021. A new attention-based CNN approach for crop mapping using time series Sentinel-2 images. *Comput. Electron. Agric.* 184, 106090 <https://doi.org/10.1016/j.compag.2021.106090>.
- Wang, D., Zhang, Q., Xu, Y., Zhang, J., Du, B., Tao, D., Zhang, L., 2022b. Advancing plain vision transformer toward remote sensing foundation model. *IEEE Trans. Geosci. Remote Sens.* 61, 1–15. <https://doi.org/10.48550/arXiv.2208.03987>.
- Wei, P., Chai, D., Lin, T., Tang, C., Du, M., Huang, J., 2021. Large-scale rice mapping under different years based on time-series Sentinel-1 images using deep semantic segmentation model. *ISPRS J. Photogramm. Remote Sens.* 174, 198–214. <https://doi.org/10.1016/j.isprsjprs.2021.02.011>.
- Wei, S., Zhang, H., Wang, C., Wang, Y., Xu, L., 2019. Multi-temporal SAR data large-scale crop mapping based on U-Net model. *Remote Sens.* 11, 68. <https://doi.org/10.3390/rs11010068>.
- Weikmann, G., Paris, C., Bruzzone, L., 2021. Timesen2crop: a million labeled samples dataset of sentinel 2 image time series for crop-type classification. *IEEE J. Sel. Top. Appl. Earth Obs. Remote Sens.* 14, 4699–4708. <https://doi.org/10.1109/JSTARS.2021.3073965>.
- Weilandt, F., Behling, R., Goncalves, R., Madadi, A., Richter, L., Sanona, T., Spengler, D., Welsch, J., 2023. Early crop classification via multi-modal satellite data fusion and temporal attention. *Remote Sens.* 15, 799. <https://doi.org/10.3390/rs15030799>.
- Weiss, M., Jacob, F., Duveiller, G., 2020. Remote sensing for agricultural applications: a meta-review. *Remote Sens. Environ.* 236, 111402 <https://doi.org/10.1016/j.rse.2019.111402>.
- Wenger, R., Puissant, A., Weber, J., Idoumghar, L., Forestier, G., 2022. Multimodal and multitemporal land use/land cover semantic segmentation on Sentinel-1 and Sentinel-2 imagery: an application on a MultiSenGE dataset. *Remote Sens.* 15, 151. <https://doi.org/10.3390/rs15010151>.
- Whelen, T., Siqueira, P., 2017. Use of time-series L-band UAVSAR data for the classification of agricultural fields in the San Joaquin Valley. *Remote Sens. Environ.* 193, 216–224. <https://doi.org/10.1016/j.rse.2017.03.014>.
- Xu, F., Jin, Y.-Q., 2005. Deorientation theory of polarimetric scattering targets and application to terrain surface classification. *IEEE Trans. Geosci. Remote Sens.* 43, 2351–2364. <https://doi.org/10.1109/TGRS.2005.855064>.
- Xu, Y., Ma, Y., Zhang, Z., 2024. Self-supervised pre-training for large-scale crop mapping using Sentinel-2 time series. *ISPRS J. Photogramm. Remote Sens.* 207, 312–325. <https://doi.org/10.1016/j.isprsjprs.2023.12.005>.
- Xu, L., Zhang, H., Wang, C., Wei, S., Zhang, B., Wu, F., Tang, Y., 2021. Paddy rice mapping in thailand using time-series sentinel-1 data and deep learning model. *Remote Sens.* 13, 3994. <https://doi.org/10.3390/rs13193994>.
- Yahia, M., Ali, T., Mortula, M.M., 2020. Span statistics and their impacts on PolSAR applications. *IEEE Geosci. Remote Sens. Lett.* 19, 1–5. <https://doi.org/10.1109/LGRS.2020.3039109>.
- Yahya, A.A., Liu, K., Hawbani, A., Wang, Y., Hadi, A.N., 2023. A novel image classification method based on residual network, inception, and proposed activation function. *Sensors* 23, 2976. <https://doi.org/10.3390/s23062976>.
- Yamaguchi, Y., Moriyama, T., Ishido, M., Yamada, H., 2005. Four-component scattering model for polarimetric SAR image decomposition. *IEEE Trans. Geosci. Remote Sens.* 43, 1699–1706. <https://doi.org/10.1109/TGRS.2005.852084>.
- Yang, H., Pan, B., Li, N., Wang, W., Zhang, J., Zhang, X., 2021. A systematic method for spatio-temporal phenology estimation of paddy rice using time series Sentinel-1 images. *Remote Sens. Environ.* 259, 112394. <https://doi.org/10.1016/j.rse.2021.112394>.
- Yang, J., Yamaguchi, Y., Yamada, H., Sengoku, M., Lin, S., 1998. Stable decomposition of Mueller matrix. *IEICE Trans. Commun.* 81, 1261–1268. https://search.ieice.org/bin/summary.php?id=e81-b_6_1261.
- Yin, Q., Lin, Z., Hu, W., López-Martínez, C., Ni, J., Zhang, F., 2023. Crop classification of multi-temporal PolSAR based on 3D attention module with ViT. *IEEE Geosci. Remote Sens. Lett.* <https://doi.org/10.1109/LGRS.2023.3270488>.
- Yu, W., Yang, G., Li, D., Zheng, H., Yao, X., Zhu, Y., Cao, W., Qiu, L., Cheng, T., 2023. Improved prediction of rice yield at field and county levels by synergistic use of SAR, optical and meteorological data. *Agric. Meteorol.* 342, 109729. <https://doi.org/10.1016/j.agrmet.2023.109729>.
- Yuan, W., Chen, Y., Xia, J., Dong, W., Maglioli, V., Moors, E., Olesen, J.E., Zhang, H., 2016. Estimating crop yield using a satellite-based light use efficiency model. *Ecol. Indic.* 60, 702–709. <https://doi.org/10.1016/j.ecolind.2015.08.013>.
- Yuan, Y., Lin, L., Zhou, Z.-G., Jiang, H., Liu, Q., 2023. Bridging optical and SAR satellite image time series via contrastive feature extraction for crop classification. *ISPRS J. Photogramm. Remote Sens.* 195, 222–232. <https://doi.org/10.1016/j.isprsjprs.2022.11.020>.
- Zebker, H.A., Villasenor, J., 1992. Decorrelation in interferometric radar echoes. *IEEE Trans. Geosci. Remote Sens.* 30, 950–959. <https://doi.org/10.1109/36.175330>.
- Zeyada, H.H., Ezz, M.M., Nasr, A.H., Shokr, M., Harb, H.M., 2016. Evaluation of the discrimination capability of full polarimetric SAR data for crop classification. *Int. J. Remote Sens.* 37, 2585–2603. <https://doi.org/10.1080/01431161.2016.1182663>.
- Zhang, S., Li, Q., Zhang, X., Wei, K., Chen, L., Liang, W., 2012. Effects of conservation tillage on soil aggregation and aggregate binding agents in black soil of Northeast China. *Soil Tillage Res.* 124, 196–202. <https://doi.org/10.1016/j.still.2012.06.007>.
- Zhang, Q., Li, L., Sun, R., Zhu, D., Zhang, C., Chen, Q., 2020. Retrieval of the soil salinity from Sentinel-1 Dual-Polarized SAR data based on deep neural network regression. *IEEE Geosci. Remote Sens. Lett.* 19, 1–5. <https://doi.org/10.1109/LGRS.2020.3041059>.
- Zhang, W.-T., Liu, L., Bai, Y., Li, Y.-B., Guo, J., 2023. Crop classification based on multi-temporal PolSAR images with a single tensor network. *Pattern Recogn.* 143, 109773. <https://doi.org/10.1016/j.patcog.2023.109773>.
- Zhang, H., Wang, Y., Shang, J., Liu, M., Li, Q., 2021. Investigating the impact of classification features and classifiers on crop mapping performance in heterogeneous agricultural landscapes. *Int. J. Appl. Earth Observ. Geoinform.* 102, 102388. <https://doi.org/10.1016/j.jag.2021.102388>.
- Zhang, W., Yu, Q., Tang, H., Liu, J., Wu, W., 2024. Conservation tillage mapping and monitoring using remote sensing. *Comput. Electron. Agric.* 218, 108705. <https://doi.org/10.1016/j.compag.2024.108705>.
- Zhao, H., Chen, Z., Jiang, H., Jing, W., Sun, L., Feng, M., 2019. Evaluation of three deep learning models for early crop classification using sentinel-1A imagery time series—a case study in Zhanjiang, China. *Remote Sens.* 11, 2673. <https://doi.org/10.3390/rs11222673>.
- Zhao, W., Qu, Y., Chen, J., Yuan, Z., 2020. Deeply synergistic optical and SAR time series for crop dynamic monitoring. *Remote Sens. Environ.* 247, 111952. <https://doi.org/10.1016/j.rse.2020.111952>.
- Zhao, W., Qu, Y., Zhang, L., Li, K., 2022. Spatial-aware SAR-optical time-series deep integration for crop phenology tracking. *Remote Sens. Environ.* 276, 113046. <https://doi.org/10.1016/j.rse.2022.113046>.
- Zheng, A., Casari, A., 2018. Feature Engineering for Machine Learning. O'Reilly Media, Inc., Sebastopol, CA.
- Zheng, B., Campbell, J.B., Serbin, G., Galbraith, J.M., 2014. Remote sensing of crop residue and tillage practices: Present capabilities and future prospects. *Soil Tillage Res.* 138, 26–34. <https://doi.org/10.1016/j.still.2013.12.009>.
- Zhong, L., Hu, L., Zhou, H., 2019. Deep learning based multi-temporal crop classification. *Remote Sens. Environ.* 221, 430–443. <https://doi.org/10.1016/j.rse.2018.11.032>.
- Zhou, Y., Luo, J., Feng, L., Yang, Y., Chen, Y., Wu, W., 2019. Long-short-term-memory-based crop classification using high-resolution optical images and multi-temporal SAR data. *Gisci Remote Sens.* 56, 1170–1191. <https://doi.org/10.1080/15481603.2019.1628412>.
- Zhu, X.X., Montazeri, S., Ali, M., Hua, Y., Wang, Y., Mou, L., Shi, Y., Xu, F., Bamler, R., 2021. Deep learning meets SAR: concepts, models, pitfalls, and perspectives. *IEEE Geosci. Remote Sens. Mag.* 9, 143–172. <https://doi.org/10.48550/arXiv.2006.10027>.